THE ROLE OF UNZIPPED IN AXON GUIDANCE AND TARGETING IN THE OLFACTORY SYSTEM OF DROSOPHILA MELANOGASTER

by

Kaan Mika

B.S., Molecular Biology and Genetics, Istanbul Technical University, 2012

Submitted to the Institute for Graduate Studies in
Science and Engineering in partial fulfilment of
the requirements for the degrees of
Master of Science

Graduate Program in Molecular Biology and Genetics
Boğaziçi University

2014

To my mother…

ACKNOWLEDGEMENTS

First of all, I would like to thank my supervisor Assoc. Prof. Arzu Çelik for her guidance and support during this project. She provided everything needed for this project also giving precious feedback and comments on my data.

Also, I want to thank Assoc. Prof. Stefan Fuss for helping me to shoot troubles and teaching me general cloning tips that I have used during my project.

Additionally, I want to thank to my mother for feeding me and supporting me during this project. Without her delicious food and motivation, I would not be able to finish this thesis.

My sincere thanks go to Xalid Bayramlı who helped me more or less in all experiments that I have done in this laboratory. He is such a great scientist who is spending more time than PCR machines in the laboratory.

I want to thank all former and current members of the Fly laboratory, Stefan Köestler, Bahar Şahin, Çağrı Çevrim, Rıdvan Kıral, Duygu Koldere, Ece Terzioğlu Kara, Gamze Akgün, Selen Zülbahar, Ayşe Candayan, Ayça Yörükoğlu, Mustafa Talay, Güneş Tunçgenç, Çağatay Aydın, and Ece Sönmez. They are all amazing people who made my lab-life fantastic during this project.

I want to thank to Fish lab members as well.

Finally, I want to thank to TUBITAK-TBAG 111T446 and BAP 12B01P5 for financial support.

ABSTRACT

THE ROLE OF UNZIPPED IN AXON GUIDANCE AND TARGETING IN THE OLFACTORY SYSTEM OF *DROSOPHILA MELANOGASTER*

The olfactory system of *Drosophila* is a great model to investigate neural wiring complexity. The fly has two sensory appendages named as antenna and maxillary palp. Hair-like structures called as sensilla cover the appendages and house olfactory sensory neurons (OSN) together with supporting cells. Each OSN expresses one specific type of OR out of a total of 62, and project to a single unit of antennal lobe, called a glomerulus. In each glomerulus, specific synapse formation between the dendrites of projection neurons and OSNs occur. Then, the olfactory stimulus is transmitted to higher brain centers such as the mushroom body and lateral horn, in which olfactory information is converted into a behavioral response. Interaction of neurons and glia is essential for establishment of a proper olfactory system. Glial cells are known to act as guidepost cells in the nervous system, navigating neurons both by secreting molecules and mediating cell-to-cell contacts with cell surface molecules. Several cell surface molecules and transcription factors play an essential role in the establishment of this complex network. Additionally, a subtype of glia in the interhemispheric region of the pupal brain forms a ring-like structure called Transient Interhemispheric Fibrous Ring (TIFR), which is crucial for the formation of the midline commisure. Uzip is a cell adhesion molecule, expressed by glia and neurons (Ding *et al.*, 2011). Uzip mutants show midline crossing and mistargeting phenotypes of OSNs (Zülbahar, 2012). In this study, the endogenous expression of Uzip was analyzed using a mCherry-tagged version of Uzip that was generated by BAC engineering and Uzip enhancer trap line. Additionally, the function of Uzip was analyzed in detail using cell-type specific gain-of-function and loss-of-function analyses. These analyses revealed that Unzip function is required in glial cells and especially in TIFR glia for a proper development of the olfactory commissure.

ÖZET

UNZİPPED'İN *DROSOPHILA MELANOGASTER*'IN KOKU SİSTEMİNDE AKSONLARIN YÖNLENDİRİLMESİ VE HEDEFLENMESİNDEKİ ROLÜ

Drosophila koku alma sistemi karmaşık sinirsel bağlantıları incelemek adına mükemmel bir modeldir. Sinekler anten ve maksilari palp adında iki tür duyusal uzantıya sahiptir. Kıl görünümlü bir yapı olan ve koku reseptör nöronlarını (OSN) ve yardımcı hücrelerini ihtiva eden sensillalar bu uzantıların üstünü örterler. Her bir OSN 62 çeşit koku reseptöründen sadece birini ifade eder ve yumakçık adı verilen anten lobundaki birimlerden sadece birine yönelir. Her bir yumakçıkta santral geçiş nöronları ve koku reseptör nöronlarının dendritleri arasında sinapslar oluşur. Sonrasında koku stimulusları yüksek beyin işlevlerinin gerçekleştiği bölgeler olan mantarımsı yapı ve lateral boynuza gönderilerek buralarda davranışsal tepkilere dönüşmektedirler. Nöronlar ve glia hücreleri arasındaki etkileşim düzgün bir koku sistemi oluşmasında önemlidir. Glia hücreleri moleküller salgılayarak ve hücre yüzeyindeki moleküllerin yardımıyla hücreler arası etkileşimi sağlayarak nöronların yön bulmasına yardımcı olurlar. Bu karmaşık etkileşimlerin oluşmasında önemli birçok hücre yüzeyi molekülü ve transkripsiyon faktörü görev almaktadır. Ayrıca bazı glia hücre türleri tarafından pupa beyninde loblar arası bölgede oluşan loblar arası geçici fibroz halka (TIFR) isimli yapının orta hat birleşme bölgesinin oluşumunda önemli bir göreve sahiptir. Uzip bir hücre yüzeyi molekülüdür ve nöronlar ve glia hücreleri tarafından ifade edilir (Ding *et al*., 2011). Uzip mutantlarının OSN'lerde orta hat geçiş ve yanlış yönelim fenotiplerine neden olduğu gösterilmiştir (Zülbahar, 2012). Bu çalışmada BAC transgenetiği yöntemi kullanılarak mCherry ile işaretli bir Uzip elde edilmiş ve Uzip'in endojen ifade örüntüsünün belirlenmesi için kullanılmıştır.. Bununla birlikte, Uzip ifadesini çeşitli hücre tiplerinde arttırarak ve azaltarak Uzip'in fonksiyonunu detaylarıyla anlamaya çalıştık.

TABLE OF CONTENTS

LIST OF FIGURES

LIST OF TABLES

LIST OF SYMBOLS

g	Gram
kb	Kilobase
L	Liter
ml	Mililiter
mm	Milimeter
M	Molar
ng	Nanogram
nm	Nanometer
rpm	Revolutions per minute
v	Volume
w	Weight
µg	Microgram
µl	Microliter
µm	Micrometer

LIST OF ACRONYMS/ABBREVIATIONS

AL	Antennal Lobe
APF	After Puparium Formation
BAC	Bacterial Artificial Chromosome
Bp	Base Pairs
CNS	Central Nervous System
DNA	Deoxyribonucleic Acid
GFP	Green Fluorescent Protein
Gr	Gustatory Receptor
HRP	Horse Radish Peroxidase
Fmi	Flamingo
IR	Ionotropic receptor
LH	Lateral Horn
MB	Mushroom Body
LN	Local Interneurons
OSN	Olfactory Sensory Neuron
OR	Olfactory Receptor
PBS	Phosphate Buffered Saline
PCR	Polymerase Chain Reaction
PFA	Paraformaldehyde
PN	Projection Neurons
PR	Photoreceptor
RFP	Red Fluorescent Protein
RNA	Ribonucleic Acid
RNAi	RNA Interference
Ser / Thr	Serine / Threonine
SOG	Suboesophageal Ganglion
TIFR	Transient Interhemispheric Fibrous Ring
UAS	Upstream Activating Sequence

Uzip	Unzipped Protein
VNC	Ventral Nerve Cord

1. INTRODUCTION

1.1. The Olfactory System

Each organism is surrounded by chemical stimuli and a proper sensory system to detect external chemicals is essential for survival. In higher organisms, chemical information is turned into a behavioral response such as finding a carbon source, mating, and egg-laying.

In 1991, an article published by Richard Axel and Linda Buck that the identification of olfactory receptors as members of G protein coupled receptors (GPCRs) (Buck and Axel, 1991). In the rat genome around 1000 genes responsible for odor detection have been identified (Mombaerts, 1999). Additionally, it was shown that each olfactory sensory neuron (OSN) exclsively expresses one single olfactory receptor (OR) and targets a single glomerulus in the olfactory bulb (Imai and Sakano, 2007). From flies to mammals, the olfactory system is well conserved and presents a vast variety of receptors. Even though the neural circuits are very similar between olfactory systems of fly and vertebrates, the olfactory system of *Drosophila* appears to be reduced in size containing only 60 OR genes expressing 62 OR proteins (Robertson *et al*., 2003). Neurons expressing the same OR project to a specific glomerulus in the antennal lobe and form a synapse with dendrites of the projection neurons (PNs). Glial cells wraps protoglomeruli and local interneurons regulates the activity of PNs.

1.2. The Olfactory System of *Drosophila*

There are around 1300 OSNs in *Drosophila* whereas this number is drastically higher in mice and zebrafish, which makes *Drosophila* a very useful tool to understand the complexity of the olfactory system. Studies in the olfactory system of *Drosophila* have revealed the localization of the majority of OSN to antennae and maxillary palps, which

are the two olfactory sensory organs; their projections to distinct glomeruli were also mapped (Vosshall *et al*., 1999; Vosshall *et al*., 2000).

Drosophila has two olfactory sensory organs called antenna and maxillary palp. Olfactory sensory neurons are located in hair-like structures, so called sensilla. In the third segment of the antenna three types of sensilla, basiconic, tricoid, and coeloconic can be distinguished according to their morphology. In the maxillary palp only basiconic sensilla are present, which are called palp basiconic sensilla (pb). Sensilla types are determined by the combinatorial expression of transcription factors such as Ato, Lozenge, and Amos (Gupta and Rodrigues 1997; Goulding *et al*., 2000). Every single sensillum contains a sensory organ precursor (SOP) giving rise to 1 to 4 sensory neurons and supporting cells (Endo *et al*., 2007).

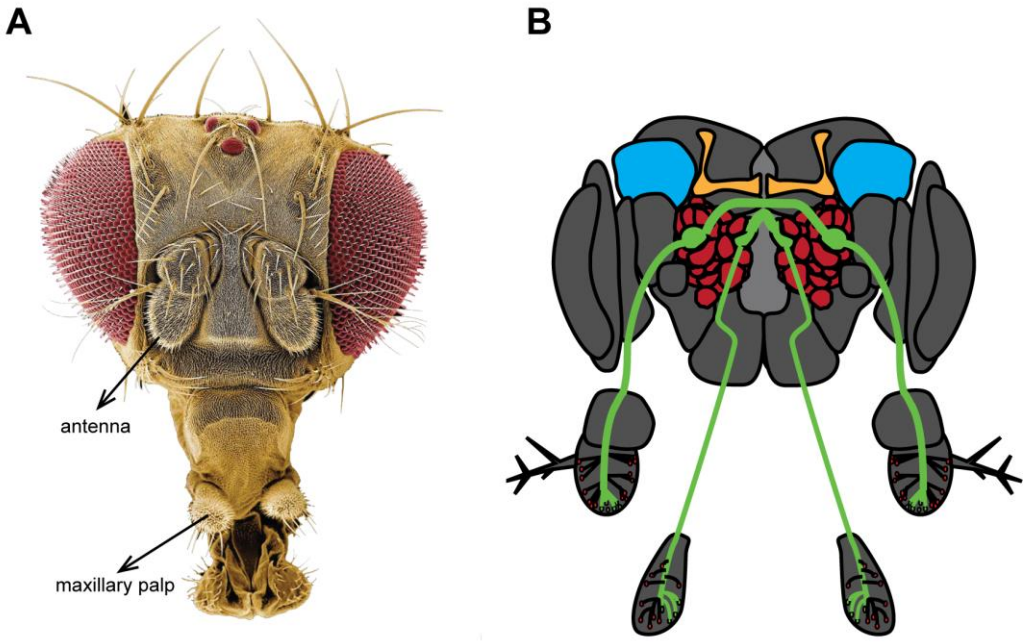

Figure 1.1. Structure of the *Drosophila* olfactory system. (A) Antenna and Maxillary Palp (MP) are shown. (B) This scheme shows the projections of a subset of OSNs from antenna and maxillary palp to their target glomeruli in the antennal lobe (shown in red). After making connections in a glomerulus OSNs cross to the contralateral side and connect to the respective glomerulus (Image was taken by Martin Helmstädter).

Olfactory sensory neurons expressing the same OR project their axons to a single glomerulus in the antennal lobe (AL) (Figure 1), which is functionally similar to the vertebrate olfactory bulb. There are 50 well-defined glomeruli in the AL, which are different targets of sensory neurons located in the antenna and maxillary palp (Laissue *et al*., 1999). During development OSNs located in the 3rd segment of antennae follow the larval antennal nerve and reach the AL earlier then maxillary palp olfactory sensory neurons, which follow the labial nerve and reach the AL around 36h APF. In this region, OSNs transmit the olfactory information to PNs akin to mitral and tufted cells in vertebrates. There are three classes of PNs; anterodorsal (adPNs), lateral (lPNs) and ventral (vPNs). PNs are named according to the location of their cell body around the antennal lobe (Jefferis *et al*., 2001). During the development of the AL, PNs project their dendrites to distinct regions in the AL and they form protoglomeruli before arrival of OSNs. When OSNs reach the AL, they send their axons to contralateral AL and form a commissure. Then a selective targeting event takes place and OSNs expressing the same OR converge on a single PN dendrite and start forming a glomerulus. Then local interneurons invade the developing glomeruli and in the later pupal stages protoglomeruli become surrounded by glial cells, forming the final glomerular structure. From the AL, PNs carry olfactory stimuli to higher olfactory centers in the fly brain such as the mushroom body (MB) calyx and lateral horn (LH). In these higher brain centers, olfactory stimuli are processed and turned into a behavioral response (Liang and Luo, 2010).

In *Drosophila*, ORs are different from vertebrate ORs, which are members of GPCRs. First of all, the *Drosophila* OR topology in the cell membrane is inverted and the majority of *Drosophila* ORs form an ion channel in combination with a broadly expressed OR co-receptor, OR83b (Wicher *et al*., 2008).

1.3. Olfactory Lobe Development

The larval olfactory system resembles the adult olfactory system in terms of the neural circuit organization and the mutually exclusive expression of ORs. Each OSN expresses one single OR and projects to the larval antennal lobe to a specific glomerulus-like structure where it synapses with its target PN. In the larval olfactory system a subset of

the total repertoire, only 21 ORs, are expressed (Python and Stocker, 2002). These OSNs are located in the dorsal organ (DO) and extend their axons to the larval antennal lobe (Heimbeck *et al*., 1999).

During metamorphosis, while most of the larval olfactory structure dies by apoptosis, the larval antennal nerve remains. Between 14 and 18h after puparium formation (APF), some OSNs exit from the antennal disc and target the antennal lobe with help of the antennal nerve (Tissot *et al*., 1997).

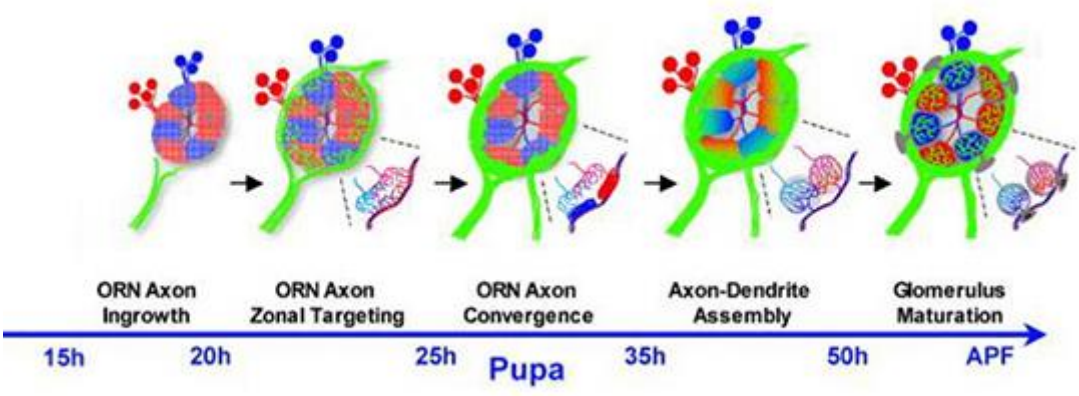

Figure 1.2. Development of the antennal lobe. PNs are the first neurons located around the developing AL and project their dendrites to distinct regions in the AL. OSNs reach the AL around 18h APF, then OSNs target to the prospective zone around the AL. Around 25 h APF, OSNs cross the midline and reach the contralateral AL.

Upon reaching the AL, the axonal bundle of the antenna segregates into fascicles and they surround the proto-antennal lobe. For approximately 15 hours, OSNs stay at the periphery of the AL and converge in the regions of their final target glomerulus. At 25h APF, antennal OSNs axons develop a commissure by reaching the contralateral proto-antennal lobe. Later on, OSNs target to their respective proto-glomeruli, which are initially defined by the dendrite targeting of PNs with the proto-AL. The first glomerulus can be identified at 36h APF (VA1 glomerulus) (Laissue *et al*., 1999). So this one-to-one interaction between OSN and PN subclasses represents a very complex neural wiring problem, which is mainly established by the combination of cell surface molecules expressed by neurons and glia around the AL.

1.4. Axon Guidance and Cell Adhesion Molecules

Axons are attracted or repulsed by local guidance cues, mainly produced by guidepost cells. Growth cones present at the tip of an axon sense and interact with guidance cues thereby navigating and extending towards intermediate targets and finally reaching their final destination.

In earlier phases of axon guidance cell surface and extracellular membrane molecules are crucial for the extension of axons and their expression gradient influences the direction of axon extension. Additionally, when axon tracts surround single axons, they form fascicles generally by cell surface or extracellular martix molecules (Raper and Mason, 2010). Other than contact-dependent attraction or repulsion, chemotropism is important for axon guidance. Intermediate targets or final targets of developing axons secrete chemoattractive or chemorepulsive molecules, thus navigating axonal projections in a long range (Dodd and Jessell, 1988).

1.5. Olfactory Sensory Neurons Targeting and Midline Crossing

OSNs expressing the same OR have the same target in the AL in flys and olfactory bulb in vertebrates, but the mechanisms determining the wiring specificity remains to be elucidated. In mice, it has been shown that OR expression is a key regulator of OSN projection (Mombaerts *et al*., 1996; Wang *et al*., 1998). Also, ORs are localized not only in the dendrites of OSNs, but also to axon termini in mice, which is in line with a role of ORs in axon guidance in addition to odor binding (Barnea *et al*., 2004).

However, in *Drosophila* axon guidance mechanisms of OSNs are independent of OR gene expression (Barnea *et al*., 2004). Rather neuron-neuron and neuron-glia interactions appear to be essential in the organization of the AL and commissure formation. Several cell surface molecules and transcription factors have been shown to be involved in glomerulus formation, correct targeting of OSNs, and midline crossing. Komiyana *et al*.,

(2003) demonstrated that OSNs targeting to specific areas in the developing AL depends cell autonomously and non-cell autonomously on acj6, a POU domain transcription factor. Moreover, within the same sensillum, precursor cell lineages with different Notch activation profiles give rise to two OSN classes: Notch-ON and Notch-OFF. Different Notch levels affect both OR expression choice and OSN targeting (Endo *et al*., 2007).

Additionally, Down Syndrome Cell Adhesion molecule (Dscam) has been shown to regulate axonal targeting of OSNs, providing PNs to occupy their prospective glomerulus and prevent ectopic PN invasions by self-avoidance mechanisms (Hummel *et al*., 2003; Zhu *et al*., 2006). Another important cell surface molecule is N-Cadherin (Ncad), which defines PN dendrite targeting. Mutations in Ncad result in ectopic targeting of PN dendrites (Zhu and Luo, 2004). In addition to that, deletion of Ncad from developing OSNs does not affect arrival of OSNs to the AL, but axons cannot form glomeruli by interacting with PNs (Hummel and Zipursky, 2004).

Furthermore, Semaphorins are important for both OSN-OSN interactions and PN targeting within the AL (Sweeney *et al*., 2007). Semaphorin 1-a (Sema-1a) is a transmembrane protein and its concentration regulates the initial targeting of dorsolateral PN dendrites (Hong and Luo, 2014). On the other hand, two members of the semaphorin family; Sema-2a and Sema-2b are secreted putative ligands of Sema1a and are important for ventromedial targeting of PN dendrites (Sweeney *et al*., 2011).

1.6. Glia

In vertebrates neurons are outnumbered by glia. Glia are closely associated with neurons to provide support and maintenance of the nervous system. Four main types of glia can be distinguished in mammals; astrocytes, oligodendrocytes, Schwann cells and microglia.

In *Drosophila*, glial cell types are characterized as cortex, neuropil, peripheral, and surface glia (Freeman and Doherty, 2005). Cortex glia surround neuron cell bodies and are responsible for supplying oxygen and nutrients to neurons; in this sense they are

functionally related with astrocytes in vertebrates. Neuropil glia ensheaths axons and their axonal targets, which relates them functionally to vertebrate oligodendrocytes. Thus, they insulate axons and enable axons to fascicle properly (Klämbt *et al*., 1991). Peripheral glia wrap sensory and motor neurons in the peripheral nervous system (PNS), just like Schwann cells in vertebrates. Peripheral glia isolate PNS neurons from the high potassium concentration in the hemolymph, thereby keeping sensory and motor neurons excitable (Auld *et al*., 1995).

In the nervous system of vertebrates, glia ensheathment is very important for isolation, proper fasciculation and velocity of signal transmission in the case of myelination of neurons. Similar interactions between neurons and glia are well conserved in insects as well. In *Drosophila*, loco, wrapper, and gliotactin genes regulate glial ensheathment of neurons (Freeman and Doherty, 2005).

1.7. The Role of Glia in Axon Guidance

In order to have a functional nervous system, a proper axon guidance mechanism must be established. It has been a fundamental question how axons find their ways and reach their final targets. According to Bate (1976), axons use guidepost cells on their way to their targets and follow them from one to another. These guidepost cells are mostly glial cells, which are located on the crossroads of axon trajectories and they can mediate repulsive or attractive interactions with the growing axons. Genetic ablations of both Central nervous system (CNS) and peripheral nervous system (PNS) glial cells result in severe axonal guidance defects, indicating the active role of glia as guidepost cells in development (Hidalgo and Booth, 2000; Sepp *et al*., 2001).

To develop a functional nervous system, communication between the right and left side of the body is crucial. PNS neurons, such as motor neurons and sensory neurons contact the CNS through interneurons located in the ventral nerve cord (VNC) in flies, and in the spinal cord in mammals. During embryogenesis, initially pioneering neurons form three fascicles at both sides of the VNC. These fascicles and longitudinal glia together assemble a platform called longitudinal tract that interneurons use to reach their final

targets. In the VNC, midline glia are present at the commissures and act as guidepost cells for extending axons. By secreting attractive cues, *Drosophila* midline glia regulate the connections of commissural axons within the right and left side of the VNC. Additionally, midline glia repel longitudinal axons from crossing the midline via secreting repellent molecules. In this context midline glia in *Drosophila* have a very similar function to floorplate cells in vertebrates.

During olfactory system development of *Drosophila*, glial cells surround the synapses between PNs and OSNs, thereby helping to sustain glomerulus formation in the AL.

It has been shown that *atonal* (*ato*) lineage peripheral glial cells enwrap and defasciculate OSNs into three main fascicles in the 3rd segment of antenna (Jhaveri and Rodrigues, 2002). In *ato* mutants, OSNs can reach the AL but their entrance to the AL is interrupted and glomeruli cannot be formed (Jhaveri and Rodrigues, 2002). Furthermore, by using a perineural glia enhancer, Mz317-Gal4, and a PN enhancer line, GH146-Gal4, two glia subtypes were identified in the antenna of *Drosophila*, named as Mz317 glia and GH146 glia, respectively (Jhaveri and Rodrigues, 2002).

1.8. Transient Interhemispheric Fibrous Ring (TIFR)

Glial cells play a very active role during the development of *Drosophila*. Especially during pupal stages, some glial cells die by apoptosis after they have performed their function.

For example, during the 3rd instar larval stage, at the interhemispheric junction of the larval brain, a distinct subset of glial cells was identified by Simon *et al*., (1998), which are present only transiently. At early stages of pupal development, these cells form a ring-like structure, which is referred to as transient interhemispheric fibrous ring (TIFR). Derailed (Drl), a receptor tyrosine kinase found to be involved in central complex formation and Wnt5, the ligand of Drl are expressed by TIFR glia (Yao *et al*., 2007; Sakurai *et al*., 2009).

Interestingly, between 25h APF and 48h APF, TIFR glia are present at the midline of the *Drosophila* brain and its interaction with OSN axon bundles is essential for AL commissure formation (Simon *et al*., 1998). A Gal4 insertion in the first intron of *drl*, *C442*, has been identified as a specific enhancer of the TIFR structure (Hitier *et al*., 2000). Using this driver (*c442*-Gal4) a selective ablation of TIFR glia can be achieved, which leads to a complete disruption of the AL commissure (Chen and Hing, 2008). TIFR has a donut-like shape where glial protrusions form 4 distinct canals. It is reported that OSNs cross the midline between two AL through the 3rd canal (Chen and Hing, 2008). The same study also showed that, *Neuroglian* (*Nrg)*, a cell adhesion molecule mediating homophilic binding, is fundamental for TIFR formation and AL commissure. In Neuroglian mutants OSNs cannot cross the midline because the TIFR structure is disturbed dramatically (Chen and Hing, 2008).

1.9. Unzipped is a Novel Cell Adhesion Molecule

Uzip encodes a 488 amino acid cell adhesion molecule without any obvious homology to other cell adhesion molecules (Figure 1.3). According to a published analysis of Uzip function in the fly embryo, Uzip is mainly expressed by glial cells with a low level of expression detected in neurons (Ding *et al*., 2011). Overexpression of Uzip in neurons was shown to result in an axon clustering phenotype, which is in line with a function of Uzip as a cell adhesion molecule. Aggregation assays performed by the same group show that Uzip mediates adhesion by homophilic binding (Ding *et al*., 2011).

Analysis of Uzip protein structure revealed that it has two isoforms; a membrane-attached and a cleaved form, which have an estimated molecular mass of 80kDa and 65kDa, respectively. Phosphoinositide phospholipase C (PI-PLC) cleavage assays performed by Ding *et al*., (2011), revealed that Uzip is indeed a GPI-anchored protein. Additionally, there are also 5 N-glycoslation sites of Uzip and there might be other post-translational modifications of Uzip, which have not been studied yet. Moreover, there is also Serine / Threonine rich domain of Uzip, shown in yellow in Figure 1.3, is a good candidate region for O-glycosylation (Gonzalez *et al*., 2012).

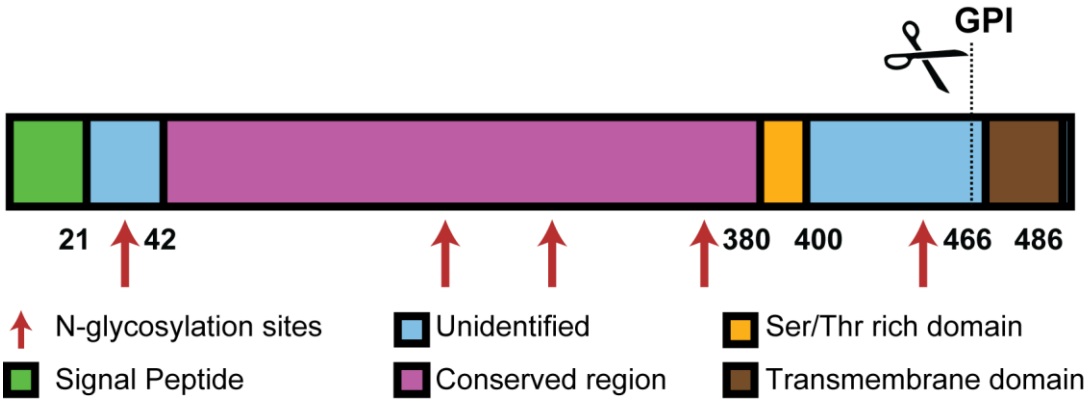

Figure 1.3. Uzip protein structure. Unzipped encodes a protein of 488 amino acids. Unzipped has 5 N-glycosylation sites and a GPI anchored site at Asn^{465}. From this region, Unzipped can be cleaved by PI-PLC enzyme. Uzip has a Serine and Threonine rich domain between amino acids 380 and 400, and between amino acids 42 and 380 Unzipped is highly conserved among arthropoda (Adapted from Ding *et al*., 2011).

When the sequence of Uzip was compared between insects, no homology could be found between amino acids 401 and 450 and aggregation assays demonstrate that deletion of this region does not affect the homophilic binding ability of Uzip (Ding *et al*., 2011). In contrast, the region between amino acids 42 and 380 (pink region in Figure 1.3) is highly conserved among insects and deletions made in this region disrupt the homophilic binding ability of Uzip.

In embryonic stage 15-16, Uzip antibody stainings revealed that Uzip is mainly expressed by longitudinal glia and a weaker expression pattern is observed in the axons of VNC. Uzip mutants give no detectable phenotypes in the development of the ventral nerve cord, but double mutants of Uzip together with either Ncad or Wnt5 mutants enhanced the severity of the axonal phenotypes in the VNC. These data suggest that Uzip genetically interacts with these two molecules (Ding *et al*., 2011).

Uzip was discovered in an enhancer trap screen for photoreceptor R8 cell-specific expression. The expression pattern displayed by this enhancer trap line (AC783-Gal4) likely corresponds to that of Uzip and was thus further analyzed. Since there is a very

strong expression level around the AL and olfactory sensory organs, we further investigated the role of Uzip in the development of the olfactory system of *Drosophila*.

1.10. Binary Expression Systems in *Drosophila*

Drosophila melanogaster is one of the leading model organisms to reveal the function of genes. Simplicity to drive expression of transgenes by using binary expression systems have paved the way for to control the expression level of genes only by bringing two components of the binary systems in a simple genetic cross. There are three well-known binary expression systems in drosophila which are namely Gal4-UAS, LexA-LexAop, and QF-QUAS systems. Gal4-UAS system is the most commonly used binary system which has two components: the yeast Gal4 transcriptional activator which is expressed in a tissue-specific manner and a transgene whose expression is controlled by upstream activation sequence (UAS) that is bound and activated by Gal4 (Brand and Perrimon, 1993). These two components of the system can be easily combined by a simple genetic cross and in the next generation the transgene is only expressed in cells which express Gal4. Over the past two decades after the discovery of Gal4-UAS system, several enhancements have been made on the system. One of the important refinements is the addition of Gal80 to the system which binds the transactivation domain of Gal4 preventing it to bind to UAS sequence to drive the expression of the transgene (Lue *et al*, 1987). One of the important consequences of repressing activity of Gal4 by Gal80 in certain cells was the development of MARCM technique which is used to generate marked mutant clones (Lee and Luo, 1999).

The other two binary systems in drosophila, LexA-LexAop and QF-QUAS, have the same working principle as Gal4-UAS system. In LexA-LexAop system LexA binds and activates the LexA operator (Lai and Lee, 2006). LexA is a DNA-binding domain of a bacterial transcription factor which is linked to the activation domain of Gal4. In this way, Gal4 cannot bind to UAS sequence but it can still be repressed by Gal80. Therefore, LexA-LexAop system is generally used in combination with Gal4-UAS system when one needs a stronger expression of a transgene in a given tissue or they can be used in combination to simultaneously perform two manipulations of gene expression in vivo. The QF-QUAS, which is the newest binary system in drosophila, based on a cluster of regulatory genes

from *Neurospora crassa* (Potter *et al*., 2010). This system also contains a repressor element which is called QS. Like Gal80 in Gal4-UAS system, it inhibits the activity of QF. Additionally, QF-QUAS system can be regulated by quinic acid which inhibits the activity of QS relieving its suppression on QF. Like LexA-LexAop system, QF-QUAS system can be used in combination with Gal4-UAS system.

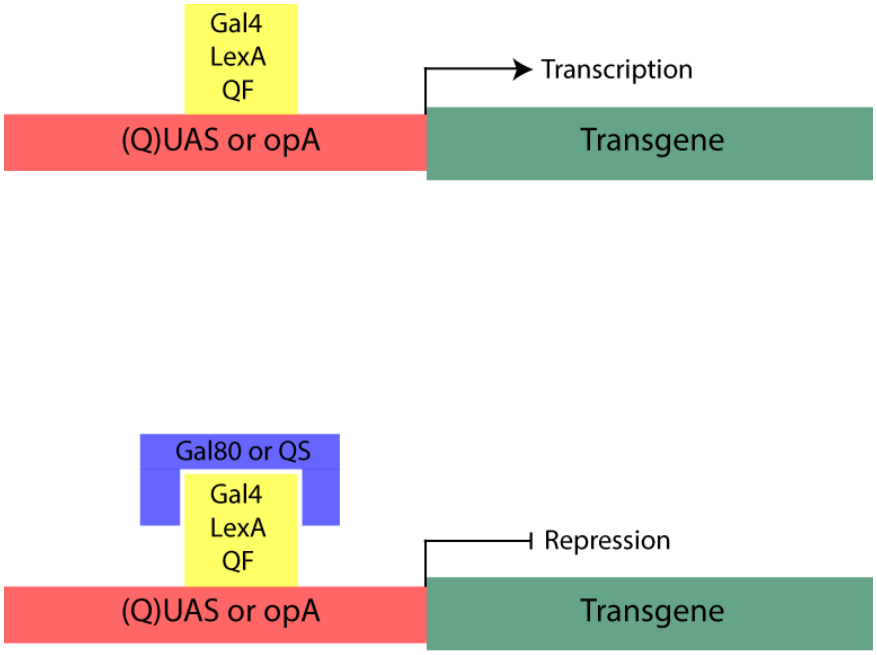

Figure 1.4. Binary expression systems in *Drosophila melanogaster*. Three binary systems are shown in the figure. Gal4 transcription activator of the yeast binds to upstream activation sequence (UAS) to drive the expression of the transgene. LexA-LexAop and QF-QUAS systems work by the same mechanism as Gal4-UAS system. In all binary systems there are repressor elements to inhibit the activity of transcription activators.

2. AIM OF THE STUDY

A functional nervous system requires proper neural circuit formation during development. The olfactory system of *Drosophila*, is an intriguing and complex example of wiring specificity of neurons.

The olfactory sensory system is highly conserved from flies to mammals with some minor differences. However as it is less complex in its organization *Drosophila* is a good model to study neural circuit formation. One of the most intriguiging questions in neurobiology is how different classes of olfactory sensory neurons segregate and later converge into different glomeruli in the antennal lobe.

Glia are essential for mediating axon guidance by expressing secreted and membrane bound cell surface molecules and glial ablation causes severe developmental defects. Cell surface molecules of glia guide extending axons to their targets, thereby helping to establish proper neural circuits.

Unzipped is a cell adhesion molecule present in both neurons and glia. Earlier studies show that, loss of Unzip causes targeting defects of olfactory sensory neurons and inability in forming a commissure between the antennal lobes.

The aim of this project is to reveal the role of Unzipped in axon guidance and midline crossing of olfactory sensory neurons and identify the underlying mechanism. To do so, we generated tools to visualize the endogenous expression pattern of Unzipped and investigated its role in a special subset of glia that are important for commissure formation of olfactory sensory neurons.

3. MATERIALS AND METHODS

3.1. Biological Material

Flies were grown at 25 ºC with 70-80% humidity and a 12:12 day and night cycle in incubators. Applied Scientific (USA) fly food was prepared by dissolving 180g fly food in 1 liter of distilled water. Fly food of the fly stocks were refreshed once in three weeks. Fly stocks used in this study are shown in Table 3.1.

Table 3.1. Fly strains used in this study.

Name of line	Chr. No.	Description
Gal4 Drivers		
AC783-Gal4	2	Enhancer trap line with Gal4 insertion in the second intron of *uzip*
Elav-Gal4	3	Expresses Gal4 in post-mitotic neurons under the control of *elav*
Repo-Gal4	3	Expresses Gal4 in all glial cells, except the midline glia, under the control of *repo*
Repo-Gal4	2	Expresses Gal4 in all glial cells, except the midline glia, under the control of *repo*
Sg18.1-Gal4	2	Expresses Gal4 in a large subset of olfactory sensory neurons
GH146-Gal4	3	Expresses Gal4 in subsets of projection neurons
OR59c-Gal4	3	Expresses membrane bound GFP in the control of *OR59c* promoter
OR47b-Gal4	3	Expresses membrane bound GFP in the control of *OR47b* promoter
OR47a-Gal4	3	Expresses membrane bound GFP in the control of *OR47a* promoter
UAS Constructs		
UAS-*Dicer2*	2	Expresses *Dicer2* under the control of UAS
UAS-*uzip*-RNAi	3	Expresses double stranded RNAi of *uzip* under the control of UAS (TRIP)
UAS-CD8::GFP	3	Expresses mCD8-tagged GFP under the control of UAS sequences

Table 3.1. Fly strains used in this study (cont).

UAS-syt::RFP	3	Labels synaptic vesicles with RFP
UAS-nGFP	1	Labels nucleus with GFP
UAS-*uzip*$^{237-488}$	3	Expresses truncated Uzip
UAS-*uzip*$^{130-488}$	3	Expresses truncated Uzip
UAS-*uzip*$^{1-237}$	3	Expresses truncated Uzip
General Stocks		
y w	1	Yellow body color and white eye phenotype
w^{1118}	1	White eye phenotype
Uzip^{D43}	2	Null Uzip allele
Uzip^{23}	2	Hypomorphic Uzip allele
Uzip (BAC)	3	Expresses Uzip
Uzip::mCherry	3	Expresses mCherry tagged Uzip
Nrg^{849}	1	Nrg mutant
Drl^{exc21}	2	*Drl* mutant
OR46a-mCD8::GFP	3	Expresses cell surface GFP under the control of *OR46a* promoter
OR42b-mCD8::GFP	2	Expresses cell surface GFP under the control of *OR42b* promoter
OR42b-mCD8::GFP	3	Expresses cell surface GFP under the control of *OR42b* promoter
Balancers and Markers		
CyO	2	Balancer chromosome with curly wings
Sp	2	Supernumerary bristles marker
MKRS	3	Balancer chromosome with stubble bristle phenotype
CyO::GFP	2	Balancer chromosome with curly wings and GFP expression
TM3	3	Balancer chromosome with haltere phenotype
TM2	3	Balancer chromosome with large halteres and/or with bristles on halteres
TM6B	3	Balancer chromosome with humeral and tubby markers
Bl	2	Phenotypic marker
yw^{67}; QB		Sp/CyO; TM2/TM6B

3.2. Chemicals and Supplies

All chemicals used in this study were supplied from Sigma, Fisher Scientific, Roche or Molecular Probes.

3.2.1. Enzymes

Restriction enzymes and buffers were supplied from New England Biolabs or Fermentas. T4 ligase and T4 ligase buffer were used from New England Biolabs. Phusion Polymerase and polymerase buffer were used from New England Biolabs and GoTaq polymerase and polymerase buffer were from Promega.

3.2.2. Antibodies

Antibodies used in this study are shown in Table 3.2.

Table 3.2. The list of antibodies used in this study.

Name	Antigen	Species	Dilution	Source
Primary Antibodies				
Anti-Brp	Bruchpilot	Mouse	1:100	DSHB (nc82)
Anti-Elav	Elav	Mouse	1:20	DSHB (9F8A9)
Anti-Elav	Elav	Rat	1:20	DSHB (7E8A10)
Anti-FasII	Fasciclin II	Mouse	1:300	DSHB (1D4)
Anti-Fmi	Flamingo/Starry night	Mouse	1:20	DSHB (#74)
Anti-Futsch	Futsch	Mouse	1:50	DSHB (22C10)
Anti-GFP	GFP	Chicken	1:1000	Abcam (ab13970)

Table 3.2. The list of antibodies used in this study (cont).

Anti-GFP	GFP	Rabbit	1:500	Torrey Biolabs (TP401)
Anti-GFP	GFP	Mouse	1:1000	Unknown
Anti-Ncad	N-Cadherin	Rat	1:20	DSHB (MNCD2)
Anti-Nrg^{180}	Neuroglian	Mouse	1:20	DSHB (BP104)
Anti-Repo	Repo	Mouse	1:50	DSHB (8D12)
Secondary Antibodies				
Alexa 488	Chicken	Goat	1:200	Invitrogen
Alexa 488	Rabbit	Goat	1:800	Invitrogen
Alexa 488	Rabbit	Donkey	1:800	Invitrogen
Alexa 555	Mouse	Donkey	1:800	Invitrogen
Alexa 555	Rabbit	Goat	1:800	Invitrogen
Alexa 633	Rat	Goat	1:800	Invitrogen
Alexa 647	Rat	Donkey	1:800	Invitrogen
Alexa 647	Rabbit	Goat	1:800	Invitrogen
Cy5	Mouse	Goat	1:800	Invitrogen

3.2.3. Chemical Supplies

Table 3.3. Chemicals with their respective manufacturers are shown.

Chemical	Manufacturer
1 kb Marker	NEB; USA (N3232L)
6X Loading Buffer	Fermentas
Bovine Serum Albumin	Sigma-Aldrich, USA (A9647)
Ethidium Bromide	Sigma Life Sciences, USA (E1510)
$MgCl_2$	Riedel-de Haen, Germany (13152)
NaCl	Sigma-Aldrich, USA (S7653)
Normal Donkey Serum (NDS)	Millipore

Table 3.3. Chemicals with their respective manufacturers are shown (cont).

Normal Goat Serum (NGS)	Millipore (S26-100ML)
NuSieve® GTG® Agarose	Lonza, USA
Paraformaldehyde	Sigma-Aldrich, USA (P6148)
SeaKem LE Agarose	Biomax(104514PR)
Sodium Deoxycholate	Sigma-Aldrich, USA (30970)
Tris	Sigma-Aldrich, USA (T6066)
Triton X-100	AppliChem, USA (A4975)
Trypsin-EDTA 0.05%	Sigma-Aldrich, USA (59417C)
Tween 20	Roche, USA (11332465001)

3.2.4. Buffers and Solutions

Buffers and solutions used in this study are shown in Table 3.3.

Table 3.4. List of buffers and chemicals used in this study.

Buffer/Solution	Content
Binding Buffer	Confidential / Commercial
EB (Elution Buffer)	10 mM Tris Cl, pH 8.5
Formaldehyde Solution (16%)	8 g paraformaldehyde in 50 ml dH_2O 1M NaOH until solution becomes transparent pH 7.4
LB Agar	5 g/l NaCl 10 g/l Tryptone 5 g/l Yeast extract 14 g/l Agar
LB Broth	5 g/l NaCl 10 g/l Tryptone 5 g/l Yeast extract
P1(Resuspension Buffer)	50 mM Tris-Cl, pH 8.0 10 mM EDTA 100 µg/ml RNase A
P2 (Lysis Buffer)	200 mM NaOH 1% SDS (w/v)

Table 3.4. List of buffers and chemicals used in this study (cont).

P3 (Neutralization Buffer)	3.0 M Potassium acetate, pH 5.5
PaxDD	10 g BSA 3 g Sodium Deoxycholate 3 ml Triton X-100 50 ml Normal Donkey Serum 100 ml 10X PBS dH_2O to 1 L
PBS (1X)	137 mM NaCl 2.7 mM KCl 10 mM Na_2HPO_4 1.8 mM KH_2PO_4
PBX3	0.3% Triton X-100 in 1X PBS
PBX30	3% Triton X-100 in 1X PBS
QF (Elution Buffer)	1.25 M NaCl 50 mM Tris-Cl, pH 8.5 15% Isopropanol (v/v)
TAE Buffer (1x)	40 mM Tris-Cl 1 mM EDTA 0.1% Acetic acid

3.2.5. Oligonucleotide Primers

Uzip-mCherry and Uzip galk primers were designed with 50 bp homology arms to BAC construct containing Uzip sequence. Seq (sequencing) primers were designed to check for the presence and orientation of cloned inserts. The other primers in Table 3.4. were used to generate the truncated Uzip constructs. All primers were ordered from Macrogen Inc. (Korea). Primers are kept in –20ºC with 100 pmol/ µl final concentration.

Table 3.5. List of primers used in this study.

Primer Name	**Primer Sequence (5' to 3')**	**Tm (ºC)**
Uzip-mCherry-F	TTGCGGGGTCGGCTTTATTAACTCTACTTTTAACAATTTTTTTGAGTCTGGGCAGCGGCATGGTGAGCAAGGGCGAGG	88.4
Uzip-mCherry-R	CAACAACAACAATTAAACTCTATACTGAGTCCACAGCTCAATTTCATCTAGCCGCTGCCCTTGTACAGCTCGTCCATGC	87.2
Uzip-galk-F	TTGCGGGGTCGGCTTTATTAACTCTACTTTTAACAATTTTTTTGAGTCTGCCTGTTGACAATTAATCATCGGCA	83.4

Table 3.5. List of primers used in this study (cont).

Uzip-galk-R	CAACAACAACAATTAAACTCTATACTGAGTCCACAGC TCAATTTCATCTATCAGCACTGTCCTGCTCCTT	83.6
SeqF1	CACGAGGCTCCAGAGAACAT	63.3
SeqF2	AAGCAGAGGCTGAAGCTGAAG	61.3
SeqR	CGTGTTAAAGAAGAAGCCTTGGGA	63.5
galkF	TGCGTTGGCAAACAGAGATTGTGTT	64.1
Uzip-F	ATGACATCAAATAGTTGTTTAATC	55
Uzip-R	CAATTTTTTTGAGTCTGTAG	50.2
Uzip-130-F	GTTGGCTGGCGTCATTGG	58.4
Uzip-237-F	GTTACTAGGAAGCTTGAAAATCTG	60.3
Uzip-237-R	CAAGAGAATATGACTGAACTG	55.4
SP-130-R	CGCCAATGACGCCAGCCAACAGCTAGAATTTGAATAA GGAC	78.9
SP-237-R	GATTTTCAAGCTTCCTAGTAACAGCTAGAATTTGAATA AGGAC	74.2
TM-237-F	CAAGAGAATATGACTGAACTGGCAGCGGGGTCAACAT TTATTG	78

3.2.6. Embedding Media

Tissue samples were embedded in Vectashield Embedding Medium (Vector Laboratories, Inc) after immunohistochemistry.

3.2.7. Disposable Labware

Disposable Labware used in this study are shown in Table 3.6.

Table 3.6. List of disposable labwares used in this study.

Material	Manufacturer
Filter Tips	Greiner Bio-One, Belgium

Table 3.6. List of disposable labwares used in this study (cont).

Microscope cover glass	Fisher Scientific, UK
Microscope slides	Fisher Scientific, UK
Petri Dishes, 60 x 15 mm	TPP Techno Plastic Products AG, Switzerland
Pipette Tips	VWR, USA
Test Tubes, 0.5 ml	Citotest Labware Manufacturing, China
Test Tubes, 1.5 ml	Citotest Labware Manufacturing, China
Test Tubes, 2 ml	Citotest Labware Manufacturing, China
Test Tubes, 15 ml	Becton, Dickinson and Company, USA
Test Tubes, 50 ml	Becton, Dickinson and Company, USA
Syringe (1 cc)	Becton, Dickinson and Company, USA

3.2.8. Equipment

The list of equipments used in this study is shown in Table 3.7.

Table 3.7. List of equipment used in this study.

Equipment	**Manufacturer**
Autoclave	Astell Scientific Ltd., UK
Centrifuges	Eppendorf, Germany (Centrifuge 5424, 5417R)
Confocal Microscope	Leica Microsystems, Germany (TCS SP5-II)
Fluorescence Stereomicroscope	Leica Microsystems, USA (MZ16FA)
Freezers	Arçelik, Turkey
Incubator	Weiss Gallenkamp, USA (Incubator Plus Series)
Inverted Microscope	Zeiss, USA (Axio Observer, Z1)
Laboratory Bottles	Isolab, Germany
Micropipettes	Eppendorf, Germany
Microwave oven	Vestel, Turkey

Table 3.7. List of equipment used in this study (cont).

pH meter	WTW, Germany (Ph330i)
Refrigerators	Arçelik, Turkey
Stereo Microscope	Olympus, USA (SZ61)
Vortex Mixer	Scientific Industries, USA (Vortex Genie2)

3.3. Histological Techniques

3.3.1. Immunohistochemistry

3.3.1.1. Adult Brain Staining. Adult flies were dissected in PBS and fixed in 4% PFA in PBS for 20 minutes. Samples were washed 3 times for 15 minutes in PBX (0.3% Triton-X in PBS) and 1 hour blocking was performed in PAXDD. Primary antibodies were diluted in PAXDD and samples were incubated on a shaker overnight at 4ºC. The next day, samples were washed in PBX 3 times for 15 minutes each. Secondary antibodies were diluted in PAXDD and samples were incubated on a shaker at room temperature in the dark. After 2 hours of incubation, samples were washed in PBX 3 times for 15 minutes. Finally, adult brains were mounted in Vectashield.

3.3.1.2. Staining of Uzip::mCherry lines. The Uzip::mCherry line was stained using the adult brain staining protocol with following minor modifications. The antibody staining was optimized using different dilutions of the primary antibody from 1:1000 to 1:500 and performing the secondary antibody incubation either for 2 h at RT or overnight (at 4º C).

3.3.1.3. Antenna Staining. Before dissections, fly heads were removed using forceps and incubated in 4% PFA in PBS for 15 minutes. Then antennae were cut and damaged from the proximal part and collected into a 500µl tubes containing 4% PFA solution for 10 minutes. Antennae were washed 4 times for 15 minutes in 3% PBX. Then 1 hour blocking was performed in PAXDD. Primary antibodies were diluted in PAXDD and samples were

incubated on a shaker overnight at 4ºC. The next day, samples were washed with 3% PBX 2 times 10 minutes each and a third wash for 30 minutes. Secondary antibodies were diluted in PAXDD and samples were incubated (this step was performed in dark) overnight at 4ºC on a shaker. The following day, samples were washed with 0.3% PBX 3 times for 15 minutes. Then antennae were mounted in Vectashield.

3.4. Molecular Biological Techniques

3.4.1. Plasmid Isolation

Plasmid MiniGeneJet Isolation kit (Thermo Scientific) was used according to the manufacturer's instructions to isolate plasmids in small scale from bacterial cultures.

3.4.1.1. MidiPrep. In order to get large scales of DNA, QIAGEN plasmid Midi Kit (QIAGEN) was used following the manufacturer's instructions. For BAC DNA, instead of elution buffer, dH_2O was used to minimize the salt concentration for subsequent microinjections into fly embryos.

3.4.1.2. BAC DNA isolation. Since obtaining BAC DNA is more difficult because of its huge size, maxiprep was done using QIAGEN Plasmid Midi Kit (QIAGEN). A single BAC containing colony was picked and inoculated in 25 ml LB containing chloramphenicol (12.5 mg/ml) at 32 ºC for 8 hours. Then 5 ml of inoculated culture was diluted in 500 ml LB containing chloramphenicol at 32 ºC overnight. The volume of the buffers was determined according to the initial medium amount and the protocol was done according to the manufacturer's suggestions. At the final step, after centrifuging with ethanol, the supernatant was discarded. Then, the pellet was air-dried to get rid of ethanol totally and samples were resuspended in 50 µl dH_2O.

3.4.2. Restriction Digestion of DNA

Restriction enzymes and buffers were used from Fermentas and Invitrogen. All incubations were done at 37ºC and 3 hours. The amount of the enzyme was determined according to the concentration of DNA sample and total volume of the reaction. For the digestion of 1 µg of DNA, ~3-4 Unit (U) restriction enzyme was used.

3.4.3. Alkaline Phosphatase Treatment

In cases of cloning fragments using a single restriction cutting sites the recircularization and religation of the vector is prevented by a dephosphorylation reaction. Alkaline phosphatase treatment was performed following vector digestion using CIAP enzyme. The enzyme was added directly to the digestion reaction and the reaction was incubated with CIAP for 30 minutes at 37º C. Later CIAP was inactivated by increasing the temperature to 75º C for 15 minutes. To get rid of the enzymes, the digestion reaction was loaded on 0.8% agarose gel and the linearized vector was purified from the gel with help of a DNA gel extraction kit.

3.4.4. Ligation

3.4.4.1. Ligation into pGEM- T-Easy vector. pGEM-T-Easy ligation reactions were set as follows: 2X ligase buffer, 1 unit of Promega Ligase, Promega 50 ng pGEM-T-Easy vector and 3,5 µl insert in 10 µl total volume. Ligation reactions were incubated at 16º C overnight.

3.4.4.2. Ligation into P-element vectors. The vector concentration and insert concentrations were measured using a nanodrop spectrophotometer and a 1:3 molar ratio of vector:insert was used. Ligation reactions were prepared in a total volume of 20 ul as follows: 1 X T4 DNA ligase buffer, 1 unit of T4 DNA ligase, total DNA amount of less

than 200 ng. Ligation reactions were initially incubated at 25ºC for 2 hours, and then incubated at 16º C overnight.

3.4.5. Preparation of Competent Cells

A single colony from TOP10 MRF' strain was inoculated in 5 ml LB at 37ºC overnight. 500µl of overnight culture was diluted in 500 ml LB and incubated again at 37ºC until the OD_{550} read was reached to 0.6. After this step, bacterial culture was incubated on ice for 15 minutes and then centrifuged at 3000 rpm at 4ºC for 10 minutes. Then, the supernatant was discarded and the pellet was dissolved in the residual supernatant. After this resuspension step, 500µl of CT1 solution was added and the sample was incubated on ice for 30 minutes. Then, the sample was centrifuged at 3000 rpm for 10 minutes at 4ºC. Again, the supernatant was discarded and this time 20 µl CT2 solution was added and the pellet was resuspended. 50µl of aliquots were prepared and frozen quickly in liquid nitrogen. Aliquots were kept -80 ºC until use.

3.4.6. Transformation

For transformation, 50 µl of competent TOP10 cells were taken from - 80ºC and thawed on ice for 5 minutes. 5 µl ligation reaction was added to the bacteria and mixed by pipetting well. Then transformation reaction was incubated on ice for 30 minutes. After the incubation, heat shock was given by incubating the transformation reaction at 42ºC for 90 seconds. After 90 seconds, the reaction was incubated on ice for 5 minutes. 1 ml LB was added to transformed cells for recovery and cells were incubated at 37ºC for 1 hour. After recovery, transformed cells were spread on LB agar plates containing the necessary antibiotic and incubated over night at 37 ºC.

3.4.7. Polymerase Chain Reaction (PCR)

3.4.7.1. Conventional PCR. For amplification of galK and mCherry constructs master mixes were prepared in nuclease free water as: 10µM forward primer, 10µM reverse primer, ~10ng template DNA, 10 mM dNTP, 1X Phusion high-fidelity buffer, 1-3 units of

Phusion high fidelity DNA polymerase. Standard PCR cycling conditions were followed with adjusted extension time according to the size of the desired product. 2 minutes of initial denaturation step at 95º C followed by 25 cycles of 30 seconds denaturation at 95º C, 15 seconds of annealing with salt adjusted TMs of primer pairs and 60 seconds/kb of extension at 72º C. After 10 minutes final extension at 72º C, reaction was terminated by keeping it at 4º C until further use.

3.4.7.2. Colony PCR. To validate positive colonies after a transformation, colony PCRs were performed. Single colonies were picked with micropipette tips and first plated on a replica plate and then dipped in 20 µl dH_2O in an eppendorf tube to be used as template in a PCR reaction. Replica plates were incubated over night at the optimal temperature. 10 µl of Master Mix was prepared for each reaction, containing 10 mM desired primer pairs, 0.2 mM dNTP, 1X Fermentas KCl buffer, 1.5 mM $MgCl_2$ and 1-3 units of Taq polymerase which has been produced by our lab. 20 µl of templates were vortexed rigorously to damage cell membranes and incubated at 95ºC for 10 minutes. Afterwards templates were added to PCR tubes containing 10 µl of master mix. Before starting the PCR reaction, samples were mixed well by pipetting and spinned down. PCR conditions for the colony PCR are as follows: 5 minutes of initial denaturation at 95ºC which was followed by 30 cycles of 30 seconds of denaturation at 95ºC, 15 seconds of annealing at the temperature which has been adjusted according to the TMs of primer pairs, and 60 seconds/kb of extension at 72ºC. After 10 minutes of final extension at 72ºC, the reaction was kept at 4ºC until further use

3.4.8. Agarose Gel Electrophoresis

1% agarose gel was prepared in 1X TAE and (0.5µg/ml) EtBr was added when agarose gel solution was colled down to ~55ºC. Prior to loading DNA samples to the agarose gel, all samples were mixed with 6X Fermentas Loading Buffer. 1 kb and 100bp DNA ladders were used from Fermentas. All samples were run between 80-120 V according to expected band sizes. Agarose gels were visualized under UV using a Bio-RAD Transilluminator.

3.4.9. DNA Gel Extraction

Desired DNA bands were cut from the gel by a razor blade and transferred into 1,5 ml eppendorf tubes. QIAquick Gel Extraction Kit (QIAGEN) was used according to the manufacturer's instructions. Instead of TE buffer, samples were eluted with distilled water for BAC recombineering experiments.

3.4.10. *DpnI* digestion

DpnI digestion was performed for the elimination of template DNA. 1 µl of *DpnI* enzyme was added to PCR reaction when the reaction is completed and 1 hour incubation was done at 37 ºC.

3.4.11. Sequencing Analysis

In order to verify DNA sequences, purified DNA samples were sent to Macrogen Inc. (Korea) for sequencing. Sequence results were analyzed using Vector NTI software.

3.4.12. PCR Purification

PCR products were purified by using High Pure PCR Purification Kit (Roche, USA) according to manufacturer's instructions.

3.4.13. Creating 3' A Overhangs for TA Cloning

Since high fidelity DNA polymerases like Phusion DNA polymerase do not add 3' overhangs, following reaction mixture was prepared to generate 3' overhangs for TA cloning: 10 mM dATP, 1 Unit of DNA polymerase, 1X PCR buffer with $MgCl_2$ added to the reaction. The reaction was incubated at 72º C for 30 minutes.

3.4.14. Generating Transgenic Lines with BAC transgenesis

3.4.14.1. Transformation of galk cassette into BAC. For generating Uzip::mCherry transgenic line, CH322-174H16 BAC clone containing whole uzip sequence was chosen from versatile P[acman] BAC library. This BAC clone was already inserted into P[acman] vector from BamHI site of the vector and successfully transformed into SW102 cells by Zülbahar *et al*., (2012).

Freeze stock of SW102 cells containing desired P[acman] vector inside was inoculated in 5 ml (12.5 mg/ml) overnight at 32 ºC. The next day, 1 ml from inoculated culture was transferred into 25 ml (12.5 mg/ml) until OD_{600} was reach to 0.55 (approximalely 5-6 hours). 11 ml was transferred to another flask and moved to 42 ºC for heat shock induction and the rest was stayed at 32 ºC incubator (15 minutes incubation). Then both induced and uninduced culture was chilled on ice for 10 minutes and centrifuged (0 ºC) at 45000 rpm for 5 minutes (0 ºC). All supernatant was discarded and pellet was dissolved in 1 ml ice cold dH_2O by gently shaking samples in ice. Then, 9 ml ice cold dH_2O was added to the samples and centrifugation step was repeated. Supernant discarded and pellet was dissolved in 1 ml ice cold dH_2O. Until the electroporation samples were always kept on ice. Same centrifugation step was followed, but samples were inverted on a paper towel and pellet was dissolved in remaining water (~50-100 µl). 25 µl of induced and 25 µl of uninduced cells were mixed with 30ng (2-3 µl) *DpnI* digested, gel purified galk cassete containing homology arms to the BAC construct. Then, both induced and uninduced cells were transformed in 0.1 cm BioRad Cuvette with 1,75 kV and t:4 settings of the electroporation device. Then, 1 ml LB with no antibiotics was added into cuvette and transferred to 15 ml Falcon tubes. Transformed cells were incubated in water bath at 32 ºC for an hour. After the recovery, cells were centrifuged at 13.200 rpm for a minute and supernatant was discarded. Then, pellet was dissolved in 1xM9 salts and centrifuged at maximum speed again. This washing step was repeated once more. Finally pellet was resuspended in 1 ml 1xM9 salts and three dilutions were prepared following as 1:10, 1:100 and 1:1000. 200 µl of undiluted and dilution series were plated on M63 minimal plates. These plates were incubated at 32 ºC for 3-4 days.

3.4.14.2. *GalK* selection by using MacConkey Plates. After 3-4 days of incubation at 32 ºC, 8 single colonies were picked with pipette tip and streak onto MacConkey agar plates. After one day incubation at 32 ºC, *GalK* positive colonies turned into bright red colonies. These colonies were tested by colony PCR to prove *Galk* transformation.

3.4.14.3. Transformation of mCherry. After validating *GalK* positive colonies, one single colony was picked and inoculated in 5 ml LB containing chloramphenicol. By using the same protocol with transformation of *GalK* cassette, SW102 cells were made electro competent. This time, 25 µl induced and uninduced cells were mixed with 200ng (3,5 µl) of (*DpnI* digested, gel purified and eluted in dH_2O) mCherry PCR product with homology arms similar to *GalK* cassette. Same settings were used as in electroporation of Galk cassette but this time recovery was done with 10 ml LB in 50 ml falcon tube for 4 hours at 32 ºC. After the long recovery, same washing steps were followed as in *Galk* Transformation, and 1:10, 1:100 and 1:1000 serial dilutions of the induced cells were prepared with 1xM9 salts. 200 µl of induced and dilution series and also uninduced cells were plated on M63 minimal plates containing DOG (2-deoxy-galactose) and chloramphenicol. All plates were incubated at 32 ºC for 3-4 days. Single colonies were observed after 3 days, were picked and colony PCR was performed to prove that *mCherry* is replaced with *GalK* cassette. mCherry positive cells were chosen and MaxiPrep was performed to isolate BAC DNA. Isolated BAC DNA was sequence at Macrogen Inc, Korea. One of the mutation-free colonies was sent to Genetivision Inc, USA for injection. Uzip::mCherry construct was injected into VK31 (3L) 62E1 docking site of the transgenic flies.

3.5. Experiments for Expression Profile Analysis of Unzipped

3.5.1. Expression Analysis of Unzipped Enhancer Trap Line

In order to analyse the expression pattern of Uzip in adult brain and sensory organs, fly stocks which were generated by Selen Zülbahar (master thesis, 2012) were used (Figure 3.1 A - C) Additionally, AC783-Gal4 enhancer trap line was crossed with UAS-syt::RFP,

to visualize synaptic targeting of Uzip. To address, which glomerulus is targeted by Uzip expressing cells, a second cross was set with OR2a-CD8::GFP expressing flies as in Figure 3.1 D.

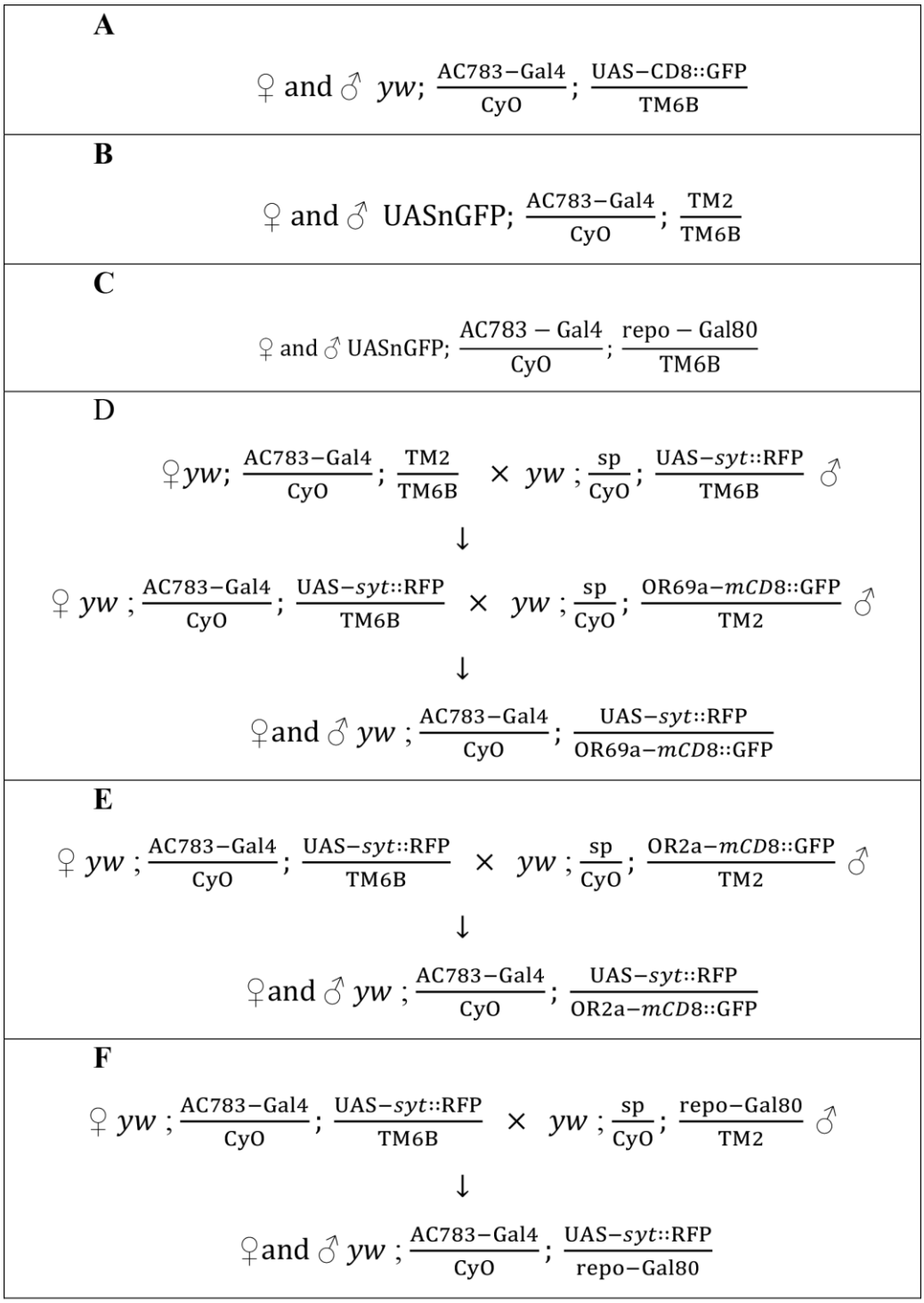

Figure 3.1. Uzip expression experiments using AC783-Gal4.

3.5.2. Expression Analysis of Uzip::mCherry Transgesinc Line

mCherry tagged Uzip expressing transgenic flies were used to understand the endogenous expression pattern of Uzip in larvae, pupae and adult brains. Moreover, to analyze the endogenous expression pattern of Uzip in antenna and maxillary palp, Uzip::mCherry expressing flies were crossed with transgenic flies with different glia subtypes expressing membrane bound GFP.

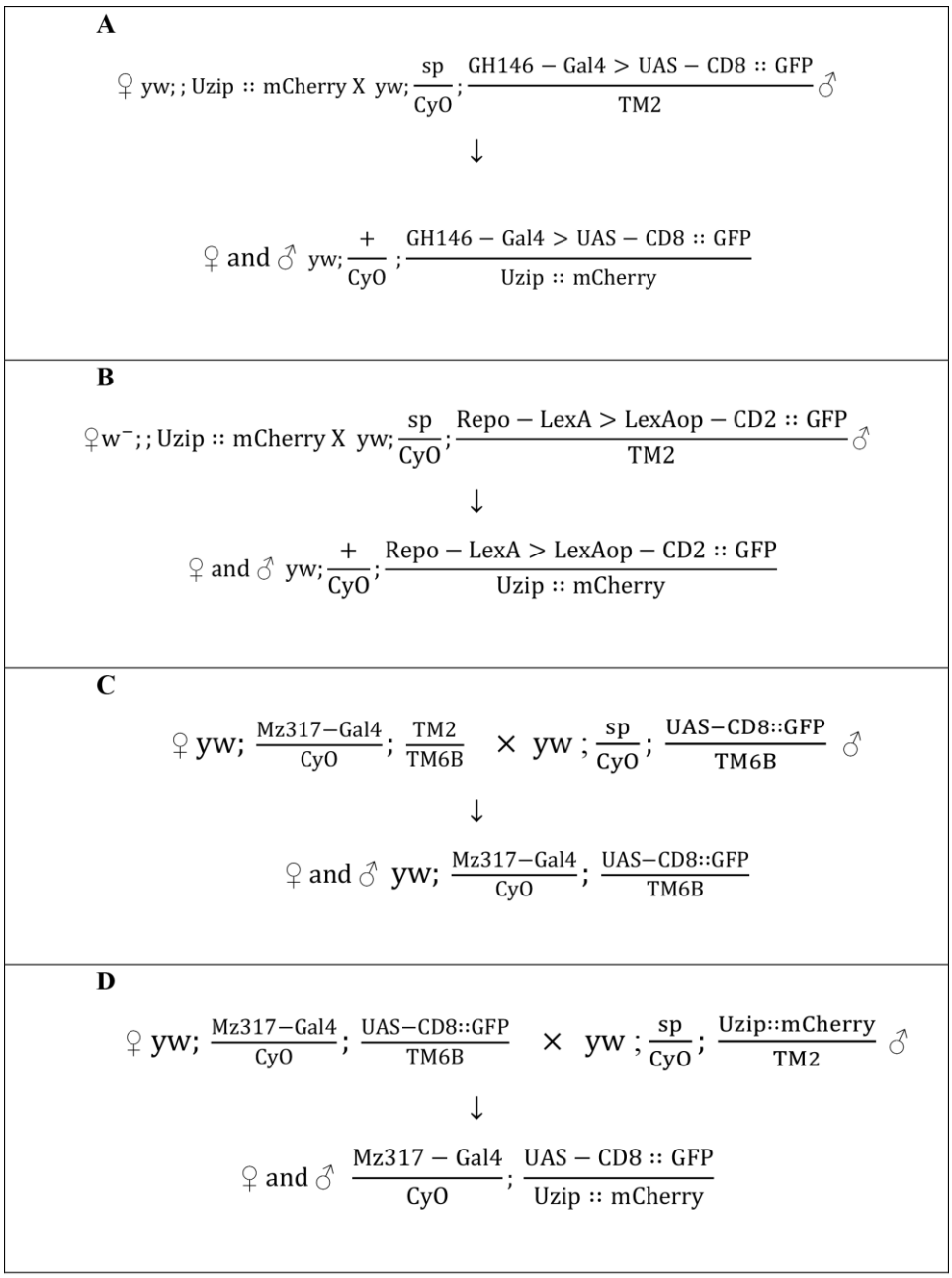

Figure 3.2. Expression pattern analysis of Uzip with glia-specific drivers.

3.6. Mutant Analysis

In order to analyze the effect of transheterozygous Uzip mutants, Crosses were set shown in Figure3.3. By using different OR-Gal4 drivers and membrane bound GFP reporters, OSNs projections were detected. Heterozygous *Uzip*^{D43} mutant flies were used as controls.

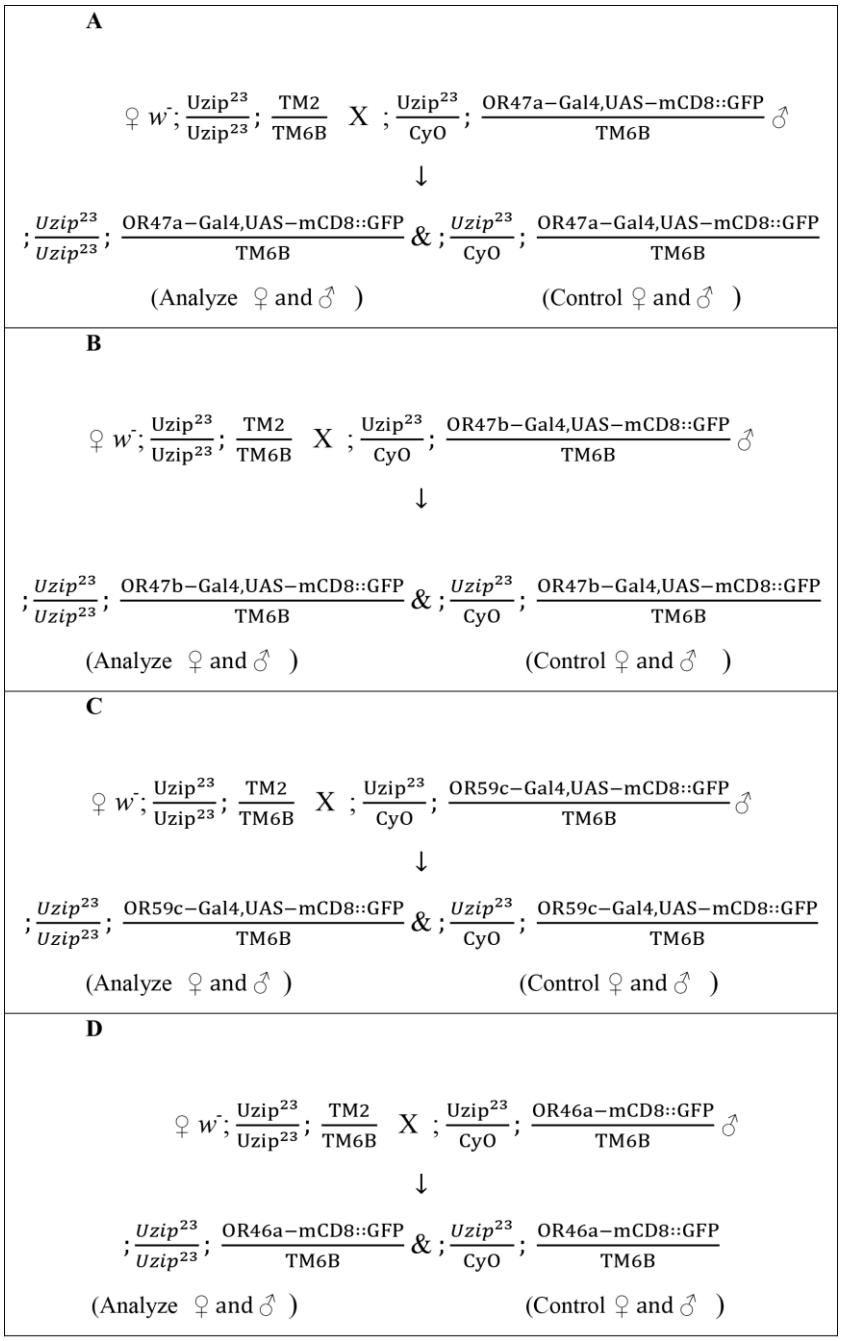

Figure 3.3. Crosses set to analyze transheterozygous Uzip mutants.

3.7. Functional Analysis of Uzip

Functional analysis of Uzip is done by using a UAS-RNAi line from Transgenic RNAi Project (TRiP) for downregulation. Also, overexpression of Uzip is done by crossing several driver lines to UAS-Uzip line which was generated in our laboratory and also UAS-Uzip::CFP (Ding *et al*., 2011).

3.7.1. Ubiquitously downregulating or overexpressing Uzip

Ubi-Gal4 line was used to downregulate or overexpress Uzip ubiquitously. Crosses were set for functional analysis of Uzip is shown at Figure3.4. In order to enhance Gal4 activity and UzipRi penetrance, Flies were grown at 29 ºC.

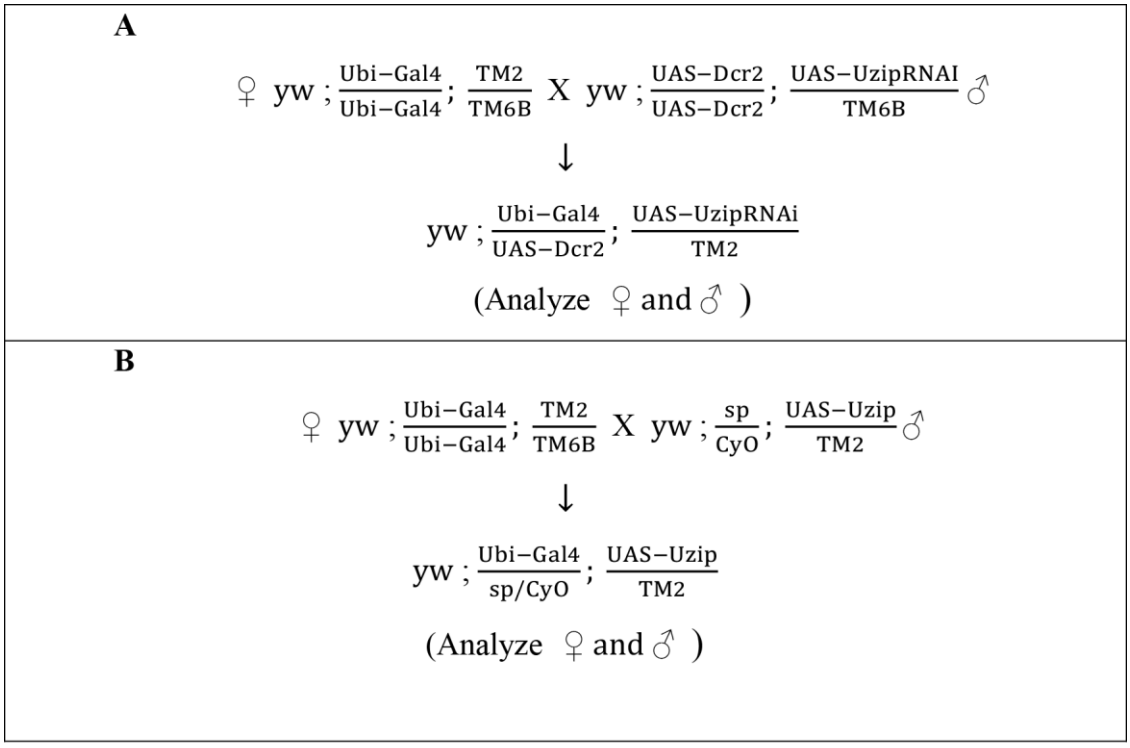

Figure 3.4. Overexpression and downregulation of Uzip in all cells.

3.7.2. Misexpression of Uzip in TIFR glia

For TIFR glia specific loss- of- function and gain-of-function experiments, *c442*-Gal4 driver line was crossed with UAS-UzipRi and UAS-Uzip lines, respectively. Since all of the OR-CD8::GFP lines in our hands were in 3rd chromosome, we had to recombine c442-gal4 driver with both of UAS-UzipRi and UAS-Uzip. To enhance the effect of UzipRi, Flies were also crossed with UAS-Dicer lines. In order to increase Gal4 Activity, flies were grown at 29 ºC.

A

$$\text{♀ yw};\frac{\text{sp}}{\text{CyO}};\frac{\text{C442-Gal4}}{\text{TM2}}\ \text{X}\ \text{yw};\frac{\text{sp}}{\text{CyO}};\frac{\text{UAS-UzipRNAi}}{\text{TM2}}\text{♂}$$

$$\downarrow$$

$$\text{♀ yw};\frac{\text{sp}}{\text{CyO}};\frac{\text{C442-Gal4}}{\text{UAS-UzipRNAi}}\ \text{X}\ \text{yw};\frac{\text{sp}}{\text{CyO}};\frac{\text{TM2}}{\text{TM6B}}\text{♂}$$

$$\downarrow$$

$$\text{♀ and ♂ yw};\frac{\text{sp}}{\text{CyO}};\frac{\text{C442-Gal4,UAS-UzipRNAi}}{\text{TM6B}}$$

B

$$\text{♀ yw};\frac{\text{sp}}{\text{CyO}};\frac{\text{C442-Gal4}}{\text{TM2}}\ \text{X}\ \text{yw};\frac{\text{sp}}{\text{CyO}};\frac{\text{UAS-Uzip}}{\text{TM2}}\text{♂}$$

$$\downarrow$$

$$\text{♀ yw};\frac{\text{sp}}{\text{CyO}};\frac{\text{C442-Gal4}}{\text{UAS-Uzip}}\ \text{X}\ \text{yw};\frac{\text{sp}}{\text{CyO}};\frac{\text{TM2}}{\text{TM6B}}\text{♂}$$

$$\downarrow$$

$$\text{♀ and ♂ yw};\frac{\text{sp}}{\text{CyO}};\frac{\text{C442-Gal4, UAS-Uzip}}{\text{TM6B}}$$

C

$$\text{♀ yw};\frac{\text{sp}}{\text{CyO}};\frac{\text{C442-Gal4, UAS-UzipRNAi}}{\text{TM6B}}\ \text{X}\ \text{yw};\frac{\text{UAS-Dcr2}}{\text{CyO}};\frac{\text{TM2}}{\text{TM6B}}\text{♂}$$

$$\downarrow$$

$$\text{♀ and ♂ yw};\frac{\text{UAS-Dcr2}}{\text{CyO}};\frac{\text{C442-Gal4, UAS-UzipRNAi}}{\text{TM6B}}$$

Figure 3.5. Recombinations for Uzip misexpression with TIFR glia driver are shown.

3.7.3. Downregulation and Overexpression of *Uzip* in Glia

In order to downregulate Uzip in glia, crosses were set as in Figure 3.6.

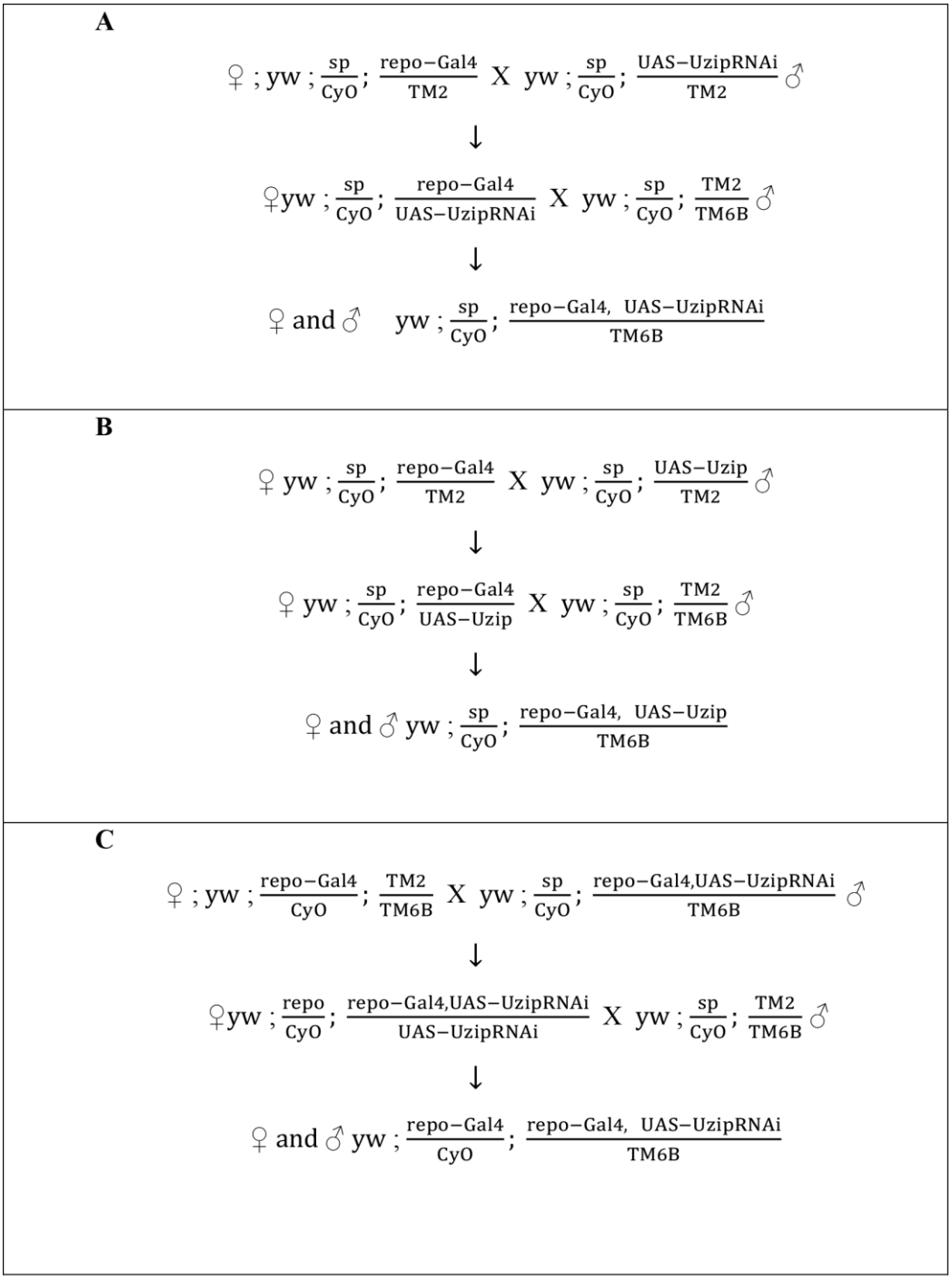

Figure 3.6. Uzip overexpression and downregulation with repo driver Rescue Experiments.

To reveal the role of Uzip in axon guidance, homozygous mutants flies were crossed with BAC constructs generated in this study. Moreover, cell type specific drivers and UAS-Uzip to check in which cells Uzip expression can recover crucial for axon guidance.

3.7.4. Rescue Experiment with BAC Constructs

Rescue experiments with BAC constructs were used in this study are shown in Figure 3.7.

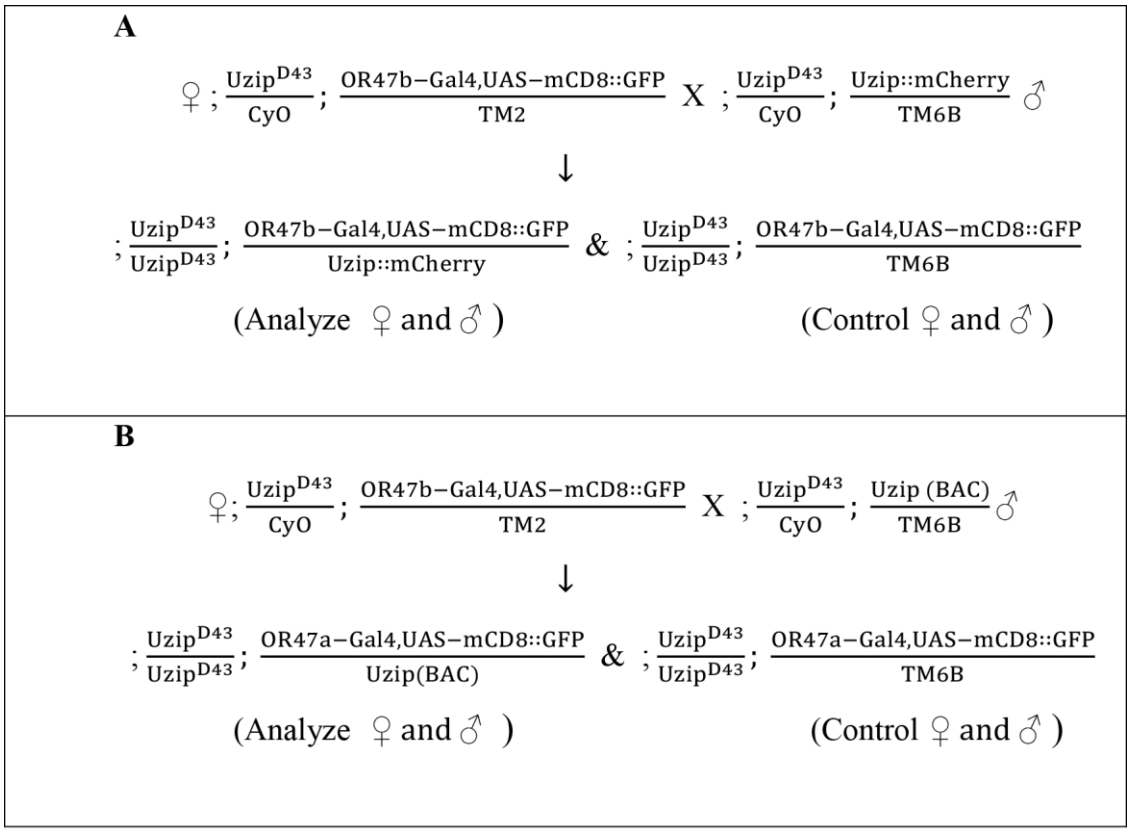

Figure 3.7. Rescue experiments with Uzip BAC and Uzip::mCherry.

3.7.5. Molecular Rescue Experiments

Figure 3.8 shows the crossing strategy for moleculer rescue experiments.

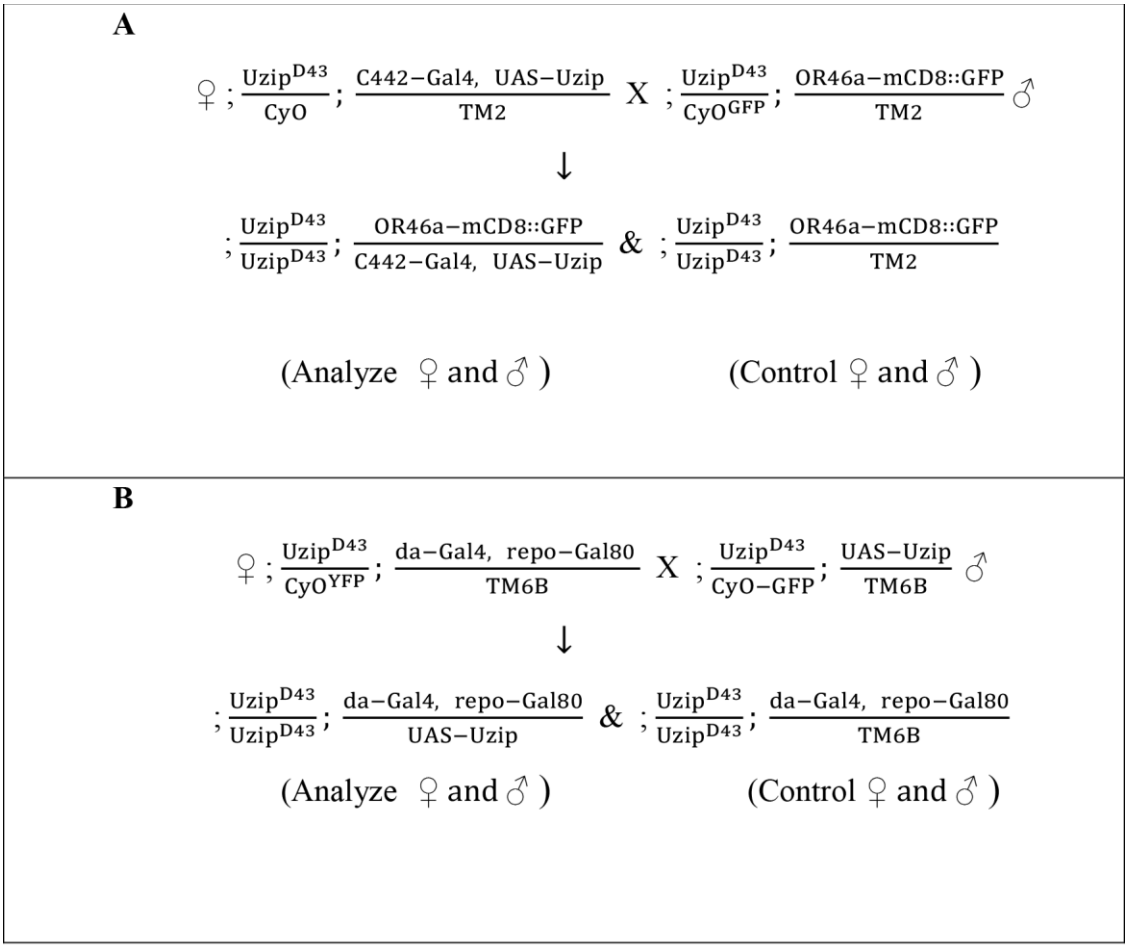

Figure 3.8. Molecular rescue experiments with UAS-Uzip overexpression line.

3.8. Uzip Genetic Interaction Experiments

Interaction of Uzip and different mutants were checked. Crossing strategy was designed as in Figure 3.9.

For Nrg and Uzip transheterozygous mutants, females flies were analyzed, whereas for Drl and Uzip transheterozygous null mutants, both genders were examined.

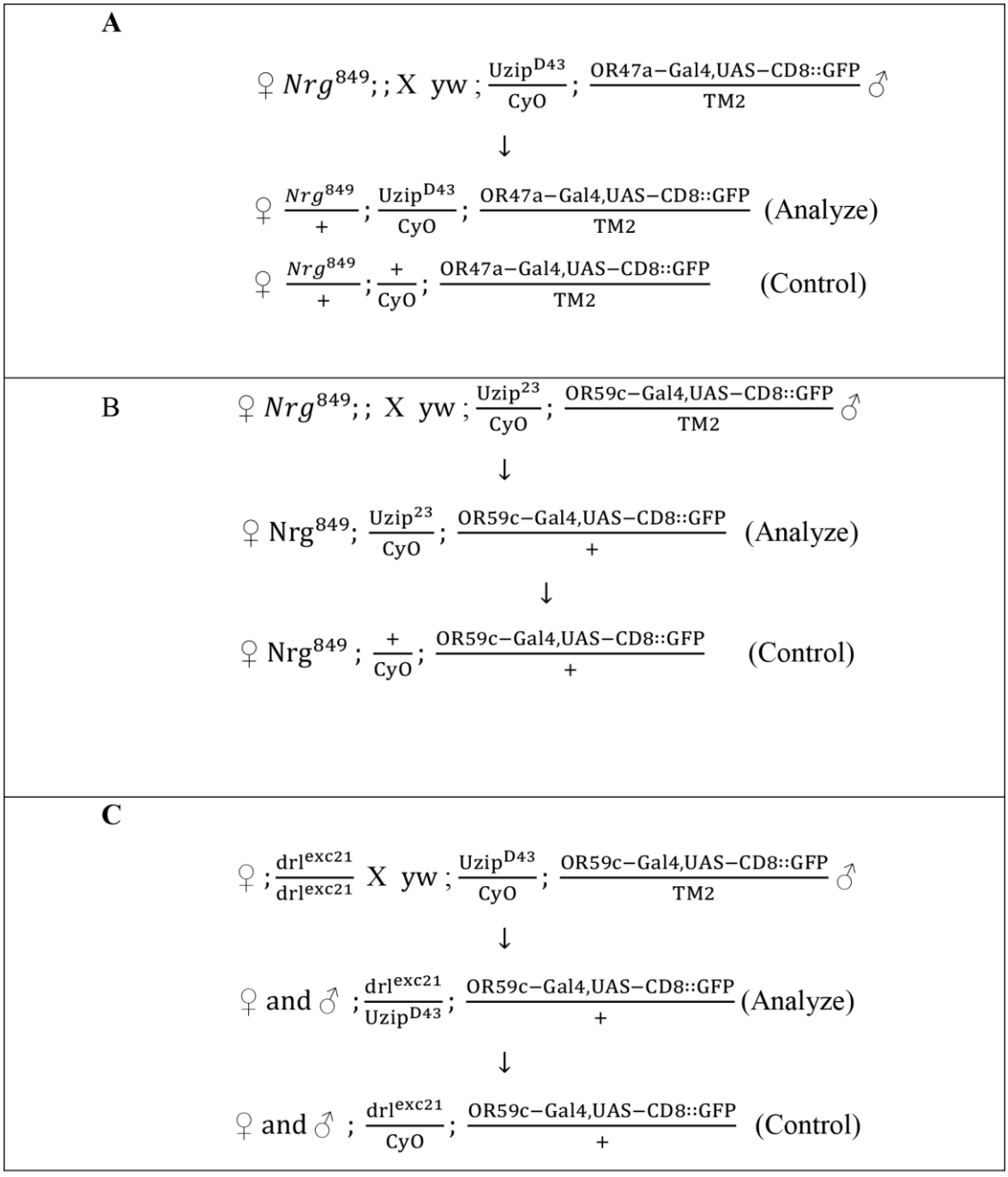

Figure 3.9. Genetic interaction crosses of Uzip.

4. RESULTS

Uzip is a cell adhesion molecule and has an important role in axon guidance. In embryonic stages, longitudinal glia and some neurons express Uzip. Uzip genetically interacts with Ncad and Wnt5, yet the interaction mechanism remains to be elucidated (Ding *et al*., 2011).

In a previous study performed in our lab by Selen Zülbahar (2012), the role of Uzip during olfactory system development of *Drosophila* was investigated. In Uzip mutants, OSNs were shown to have mistargeting and midline crossing phenotypes indicating a role of Uzip in axon guidance of OSNs. In order to understand the function of Uzip, gain-of-function and loss-of-function experiments were done using UAS-Uzip and UAS-UzipRi, which were generated in a previous study (Ding *et al*., 2011). Unfortunately, functional studies of Uzip gave inconclusive results since UAS-Uzip and UAS-UzipRi lines were not working properly.

In this study, we generated UAS-Uzip transgenic flies to assess gain-of-function phenotypes. Moreover, an UAS-UzipRNAi transgenic line generated by the Transgenic RNAi Project (TRiP) was used for loss-of-function experiments. Additionally, a more detailed expression pattern analysis of the Uzip enhancer trap was performed. Also, Uzip protein was tagged with mCherry reporter protein using the BAC recombineering technique and expressed under the endogenous regulatory region. This line was used for protein localization analysis. Moreover, cell type-specific gain-of-function and loss-of-function studies were done to understand the function of Uzip. Finally, the genetic interaction of Uzip was investigated with candidate cell surface molecules, which have similar roles to Uzip during olfactory sensory system development.

4.1. Analysis of the Expression Pattern of Uzip using an Enhancer Trap Line

In a previous study by Zülbahar (2012), Uzip expression pattern was analyzed in adult brain by using the AC783 - Gal4 enhancer trap line. This line was crossed with several reporter lines in order to find the location and synaptic interactions of Uzip expressing cells. The results of expression analysis showed that Uzip has a very broad expression pattern in the adult brain. In Figure 4.1, AC783-Gal4 > UAS-CD8::GFP line was analyzed in which GFP is targeted to the membranes of Uzip-expressing cells. This clearly indicates that Uzip is expressed around the AL, MB, and SOG region.

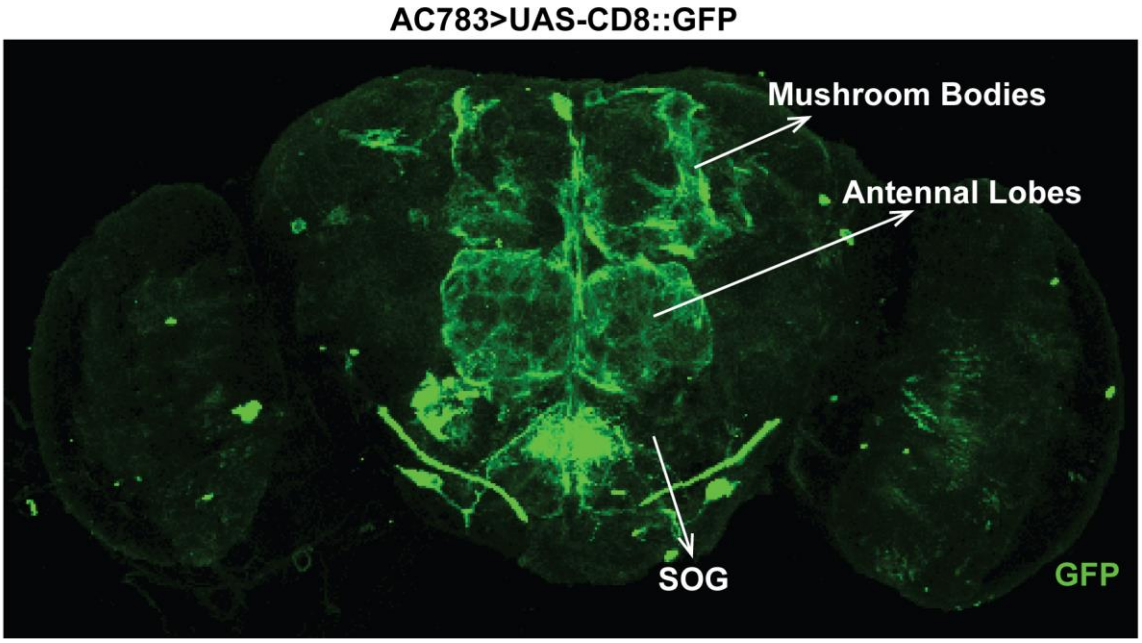

Figure 4.1. Uzip expression pattern using the AC783-Gal4 > UAS-CD::GFP enhancer-reporter line in adult brain. Uzip is mainly expressed around ALs, MBs, SOG region.

Additionally, Uzip expression has been shown by driving a pre-synaptic GFP reporter line under the control of AC783 – Gal4 line. It was observed that Uzip-expressing cells made a synapse with a single glomerulus in the antennal lobe of the adult fly brain (Zülbahar *et al*.,, 2012). By looking at the antennal lobe map of *Drosophila* (Fishilevich and Vosshall, 2005), a few candidates such as OR19a, OR56a, OR43a, and OR2a were chosen based on their position to look at the identity of the Uzip-expressing neurons.

Among them, it was shown that OR19a and OR56a neurons are not projecting to the *uzip* expressing glomerulus (Zülbahar *et al*., 2012).

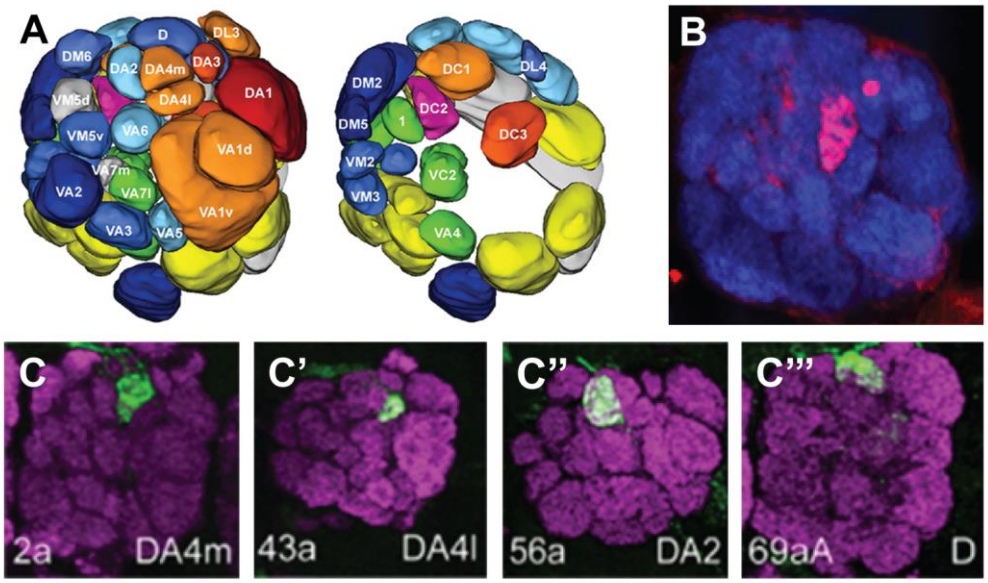

Figure 4.2. Identification of the Uzip-positive target glomerulus in the AL. (A) 3D map of Antennal lobe, which is composed of different glomeruli is shown. (B) The AC783-Gal4 > UAS-syt::RFP line was used to show the Uzip-positive glomerulus. (C, C', C'', C''') The positions of possible candidate glomeruli and their corresponding ORs (Figures were taken from Cauto *et al*., 2005).

In this study, we also investigated the target of Uzip-positive cells in the AL by trying other OR candidates. To determine the glomerular target, Uzip expression was visualized by a pre-synaptic RFP reporter line (AC783-Gal4 > UAS-syt::RFP) and this fly line was crossed with some candidate transgenic OR lines which have CD8::GFP sequence downstream of the OR promoter. Anti-Dsred antibody was used to detect the Uzip-positive glomerulus and Anti-GFP antibody was used to detect the projection of candidate OR neurons.

Initially, OR69a-positive glomerulus called D was labeled together with the Uzip-positive glomerulus. In order to show a possible co-localization the *OR69a*-CD8::GFP line, which expresses membrane-bound GFP under the control of the *OR69a* promoter was

used. As shown in Figure 4.3, Uzip-positive neurons do not project to the D glomerulus, but to an adjacent glomerulus.

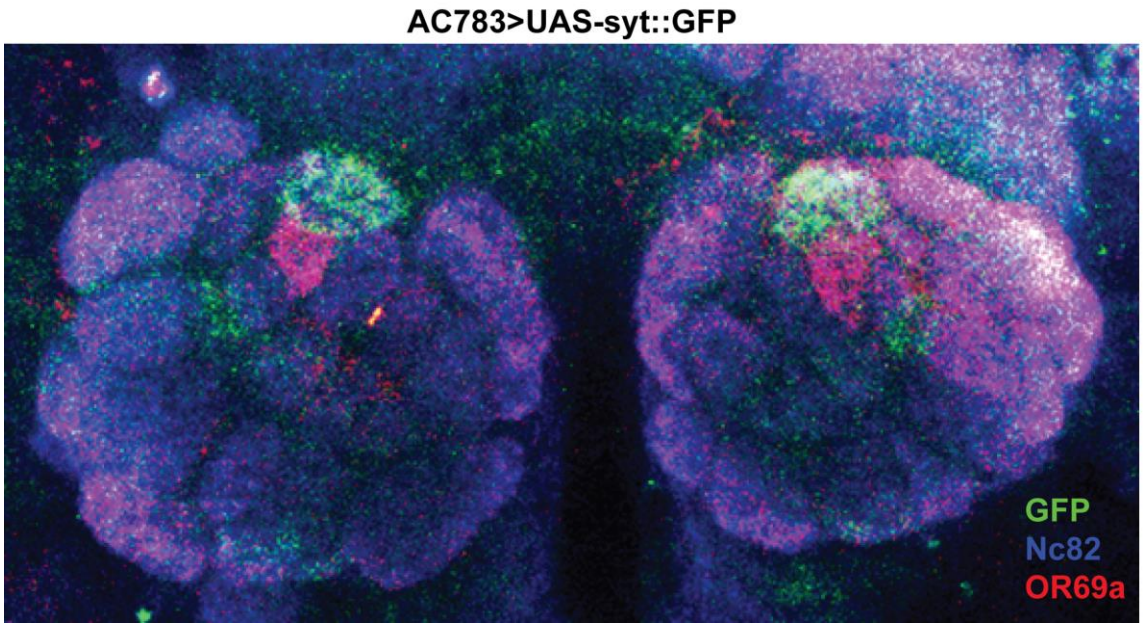

Figure 4.3. Uzip-positive neurons do not project to the D glomerulus. AC783 – Gal4 > UAS-*syt*::RFP adult brains were examined to check whether Uzip-positive neurons project to the D glomerulus targeted by OR69a neurons. As can be observed, Uzip-projections and OR69a-projections do not co-localize and project to distinct, but adjacent glomeruli.

Before choosing the next candidate, glomeruli close to D glomerulus were examined carefully and localization of the target glomerulus was predicted as DA4m to which OR2a neurons project. To validate this prediction, AC783 – Gal4 > UAS-syt::RFP flies were crossed with OR2a-CD8::GFP transgenic flies. Figure 4.4A, shows that Uzip-positive neurons project to the DA4m glomerulus.

In order to evaluate whether glia or neurons project to the DA4m glomerulus, repo-Gal80 expressing lines were crossed with AC783-Gal4 > UAS-syt::RFP. Repo-Gal80 suppresses Gal4 expression specifically in glia. Interestingly, an additional Uzip-positive glomerulus was identified as the VL1 glomerulus, which is targeted by ionotropic receptor 75d (IR75d) neurons. (Figure 4.4B)

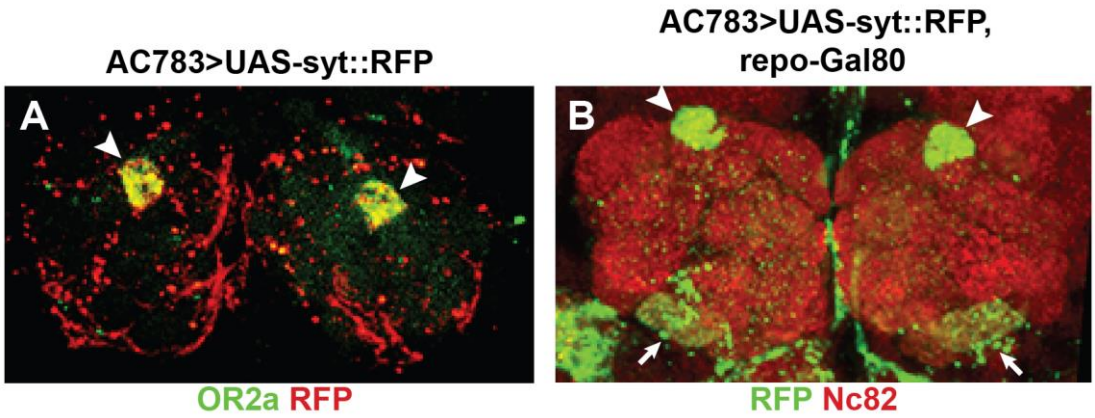

Figure 4.4. Uzip-positive cells target to DA4m and VL1 glomerulus. (A) OR2a-CD8::GFP, AC783 – Gal4 > UAS-syt::RFP transgenic flies were analyzed. Arrowheads indicate the co-localization of Uzip-positive neurons and OR2a neurons. Anti-Dsred (red) antibody recognizes RFP and shows the synaptic target of uzip-positive cells. (B) AC783 – Gal4 > UAS-syt::RFP flies, repo-Gal80 were analyzed.

4.1.1. Expression Pattern in the Maxillary Palp

In order to investigate which type of cells express uzip in the antenna and the maxillary palp, the *AC783*-Gal4 line was crossed with the UAS-*nGFP* nuclear reporter line. Maxillary palps of these flies were dissected and stained with anti-GFP, anti-Elav, and anti-Repo antibodies (Figure 4.5). This experiment clearly shows that, some non-neuronal cells inside the maxillary palp and some glia cells express Uzip. Additionally, co-localization of Uzip was observed in a few OSNs, although a more careful analysis is required to prove this observation.

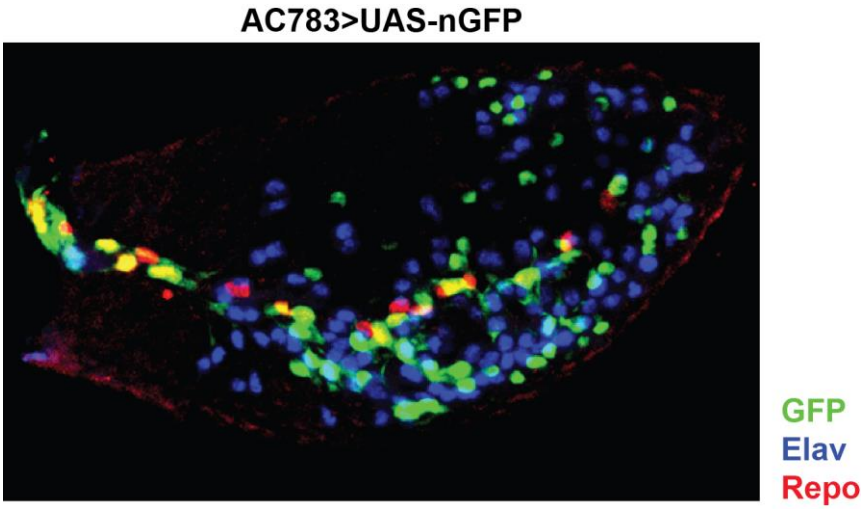

Figure 4.5. Uzip is expressed in several glia, a few neurons and non-neuronal cells in the maxillary palp. *AC783*-Gal4 > UAS-*nGFP* flies are analyzed. In the maxillary palp, nuclei of Uzip-positive cells were visualized by anti-GFP staining. Uzip expression was observed mostly in non-neuronal cells. Additionally, Uzip-positive cells colocolize with several glia and a few OSNs. Anti-Repo (red) stains glial nuclei and anti-Elav stains neuronal nuclei.

In order to evaluate if Uzip is expressed in neurons, a glial-specific Gal4 repressor, *repo*-Gal80 was used and the resulting Uzip expression pattern was re-evaluated. Figure 4.6 shows maxillary palps of flies of the following genotype: AC783 > UASnGFP, *repo*-Gal80. Antibody stainings with repo and elav showed no colocalization of repo and Uzip positive cells, indicating that *repo-Gal80* worked efficiently. Additionally, the total number of cells detected by GFP staining decreased. Under these experimental conditions no co-localization between neurons and Uzip-positive cells was observed. Thus, in the maxillary palp the expression reported by the Uzip enhancer-trap line is restricted to non-neuronal and glial cells. The location of non-neuronal cells is adjacent to neurons and they thus the non-glial, non-neuronal cells might correspond to supporting cells of the sensilla. Further experiments are needed to identify the identity of these cells.

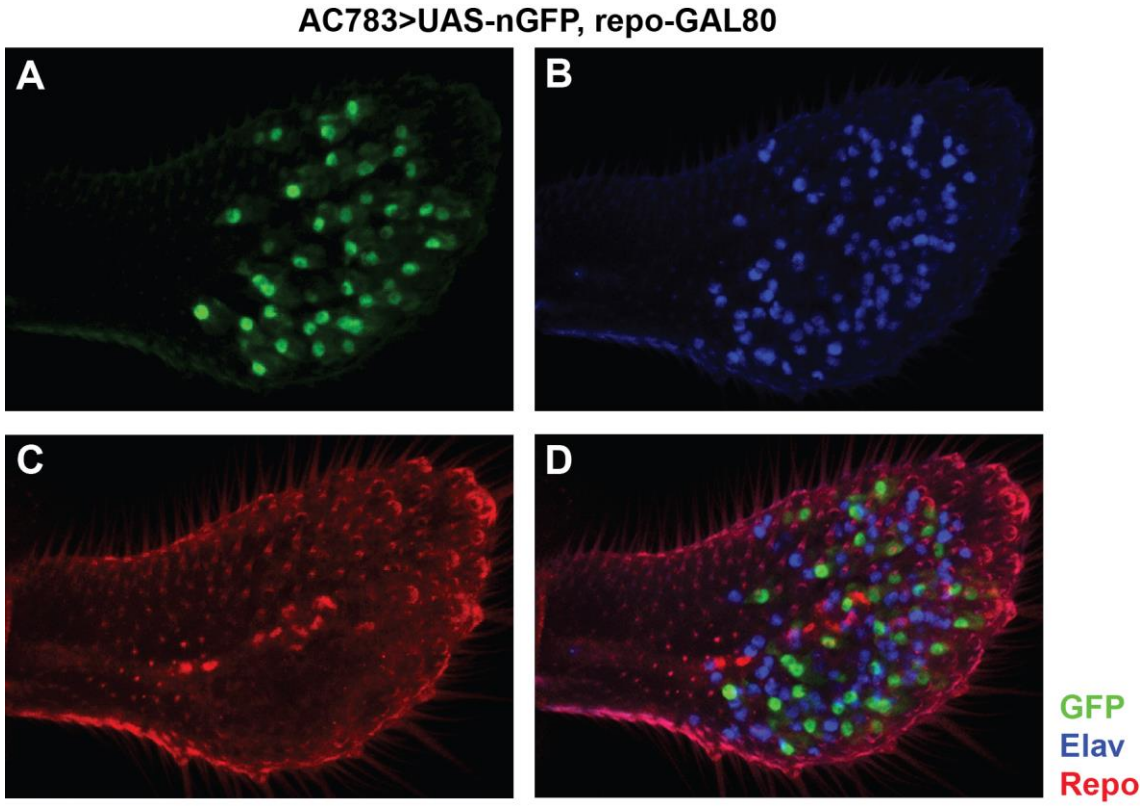

Figure 4.6. Uzip-positive cells are mainly non-neuronal cells in the maxillary palp. The maxillary palps of AC783-Gal4>UASnGFP; *repo-Gal80* flies were examined. Repo-Gal80 suppresses the activity of AC783-Gal4 in glial cells, which enables one to investigate if Uzip expression in the maxillary palp originates from cells other than the glial cells.

4.1.2. Expression pattern of Uzip enhancer in antenna

Drosophila antennae are made of three segments and OSNs are housed in the 3rd segment. In order to investigate the role of Uzip in the olfactory system, the 3rd segment of antenna were stained. Enhancer trap expression analysis showed that Uzip is expressed widely in the 3rd antennal segment. To define which cell types express Uzip, anti-elav and anti-repo antibodies were used to label neurons and glia, respectively.

Unfortunately, the stainings appeared problematic due to the presence of a thick cuticle surrounding the antenna, reflected by poor antibody penetration. To increase the efficieny of antibody penetration, some modifications to the protocol were made, including increasing the antibody concentration as well as varying the Triton-X concentration during

the washing steps. Stainings with the most optimal protocol revealed a broad Uzip expression in the 3rd antennal segment. Uzip-positive cells appeared to colocalize with non-neuronal cells similar to the expression in the maxillary palp (Figure 4.7.). As the anti-Repo antibody did not work we cannot comment on if the identity of the non-neuronal cells is glial. Further studies will be needed may be by crossing in transgenic reporter constructs for glial cells and/or supporting cells, if available.

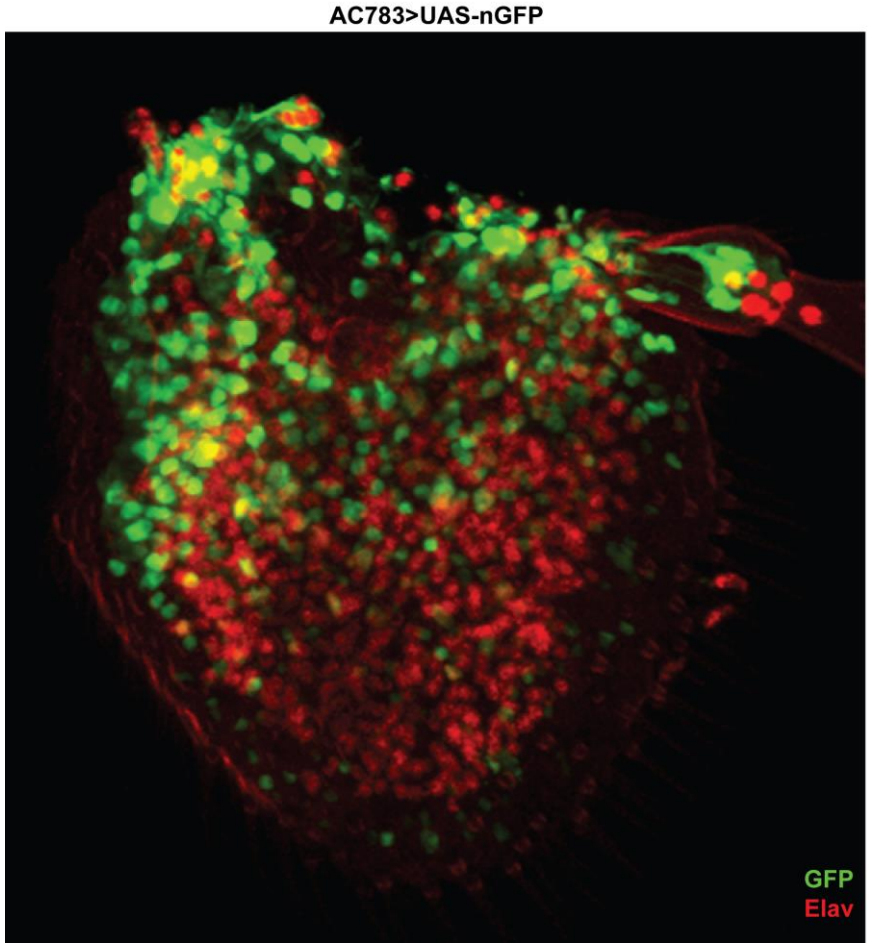

Figure 4.7. Uzip is mainly expressed by non-neuronal cells in the 3rd antennal segment. AC783 > UAS-nGFP fly antennae were dissected and stained with anti-Elav (red), anti-Repo (blue), and anti-GFP (green) antibodies. Co-localization of Uzip-positive cells and a few neurons was observed. This is difficult to evaluate because of the dense packing of the cells and the strong GFP signal. Uzip expression was observed throughout the antenna.

4.2. Generation of mCherry tagged Uzip and Uzip (BAC) lines by using BAC Recombineering

The expression of Uzip expression was examined using the enhancer-trap line generated in our lab AC783. However, while this line is inserted into the Uzip locus, it cannot be excluded that the observed expression refelects the activity of a distant enhancer. The available antibody generated by Ding *et al*., did not work in our hands. Thus, to visualize endogenous Uzip expression a transgenic line in which endogenous Uzip protein was expressed under its putative regulatory region and was tagged with the reporter protein mCherry to be able to follow its localization. To achive this goal, we benefited from BAC recombineering technique.

BAC recombineering, is a very useful tool for tagging proteins with fluorescent reporters, creating deletions or mutations in a desired DNA sequence. We used P[acman] BAC library and the P[acman]-CM^R BW vector, containing a attB site, a conditionally amplifiable origin of replication, 3' and 5' P-element transposable ends, and a multiple cloning site. From the Pacman-Fly website (Figure 4.8) (Venken *et al*., 2006) a BAC clone containing the Uzip genomic region with upstream and downstream sequences was chosen. The clone CH322 – 174H16 is 22048 bp long and does not contain any other genes in the upstream or downstream regions of Uzip. This constrtuct was ligated to P[acman] vector from BamHI cleavage site (Figure 4.8.) and transformed into SW102 cells, in which *galk* operon was deleted. We planned to create a Uzip (BAC) constrtuct without any modification to use as a control to the mCherry tagged version of Uzip construct.

To generate mCherry tagged Uzip protein, we used a two step recombination procedure. In the first step *galk* cassette, which contains 50 bp homology sequences on both sides was integrated before the last stop codon of uzip in the BAC construct by homologous recombination. Only *galk* recombined bacteria were able to grow on minimal media only containing galactose (positive selection). In the next step, double stranded mCherry construct, which have the same homology arms as in *galk* insertion was replaced with *galk* sequence. In the next step, were grown on the media containing glycerol and 2-

deoxygalactose (DOG) plates. DOG is toxic when it is phosphorylated by *galk* and galk cassette containing cells cannot survive on this plate (negative selection).

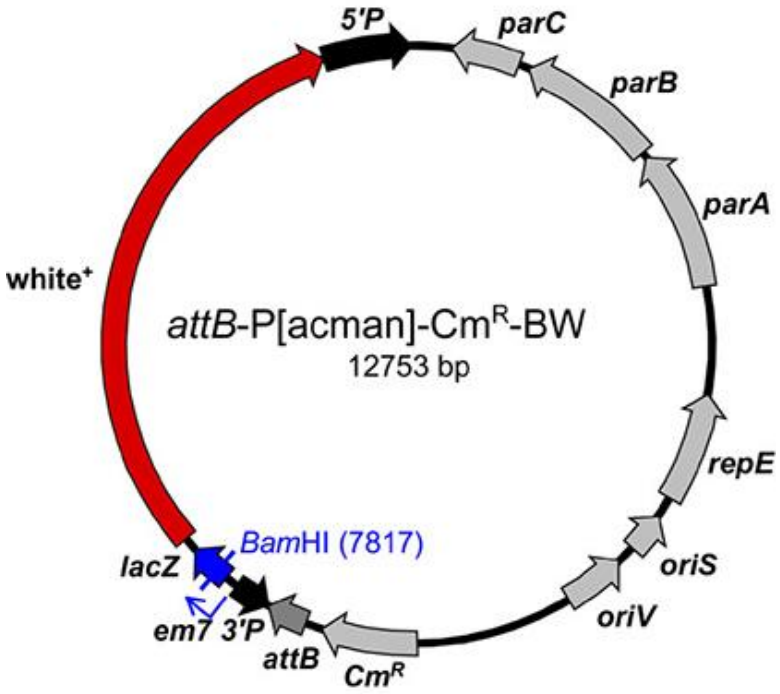

Figure 4.8. *attB*-P[acman]- Cm^R – BW vector map. This vector contains a low copy replication origin namely ori*S* and a high copy replication origin namely ori*V*. It also contains 3', 5' P-element transposable ends and an attB attachment site. The *Bam*HI restriction site was used to ligate genomic BAC constructs into the vector (Venken *et al*., 2006).

Two primer pairs were designed to amplify *galk* and mCherry coding sequences containing 50bp homology arms homologous to 50 bp upstream of the last stop codon of Uzip and 50bp downstream of the last stop codon sequence of Uzip. To prevent any misfolding of Uzip protein which might be caused by the mCherry tag, 9 bp linker sequences were included into the mCherry primer pair (Figure 4.9).

First, a *galk* containing vector was used as a template to amplify a targeting sequence with the primers Galk F1 and Galk R1, which contain 50 bp overhang sequences homologous to the left and right homology arms of the Uzip region, to generate a double-stranded amplicon. The double-stranded galk fragment was transformed into competent SW102 cells by electroporation. A homologous recombination event took place between

the homology arms of the BAC DNA and double stranded galk amplicon. Transformed cells were incubated on MacConkey indicator plates where only *galK* containing colonies turn into a reddish color due to decreased pH caused by *galK* activity. A colony PCR experiment was performed to check if these reddish colonies contain the *galK* cassette by testing them with GalK F1 and GalK R1 and GalK F1 GalK R2 primers. Figure 4.10 shows that with both of the primers pairs colony 1 has a successfully integrated the *galk* sequence before the last stop codon of *uzip*.

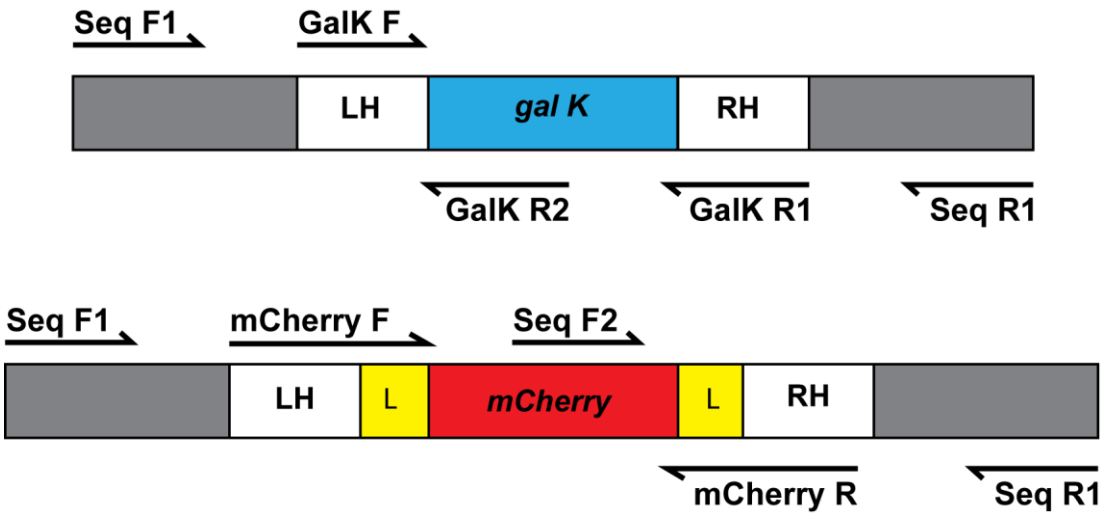

Figure 4.9. *galk* and mCherry sequences were amplified with specific primer pairs containing the same homology arms. GalK F and GalkR1 primers were used to amplify functional *galk* containing homology arms on both sides.

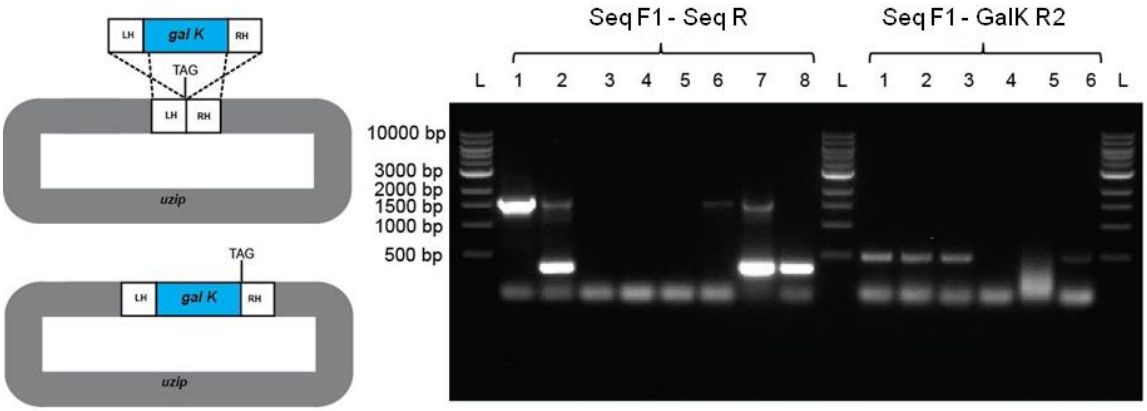

Figure 4.1. Homologous recombination of galK cassete before the last stop codon of Uzip. A BAC construct containing the Uzip genomic region and left homology (LH) and right

homology (RH) arms is shown. A Galk cassette containing LH and RH homology was generated and inserted before the last stop codon of Uzip by homologous recombination.

The *gal K*-positive colony 1 was picked and these cells (containing *galk* cassette) were made competent. This time, the double stranded mCherry cassette was transformed. In this second round of homologous recombination the replacement of the *galk* cassette by the *mCherry* cassette was expected (Figure 4.11). Transformed cells were grown on DOG plates where *galK* containing cells die and only successfully recombined cells can survive. A colony PCR was performed to confirm the faithful insertion of mCherry in its correct orientation. SeqF1 and SeqR were used to confirm the mCherry insertion and the SeqF2 and SeqR primer pair was used to confirm the correct orientation of the insert (Figure 4.11).

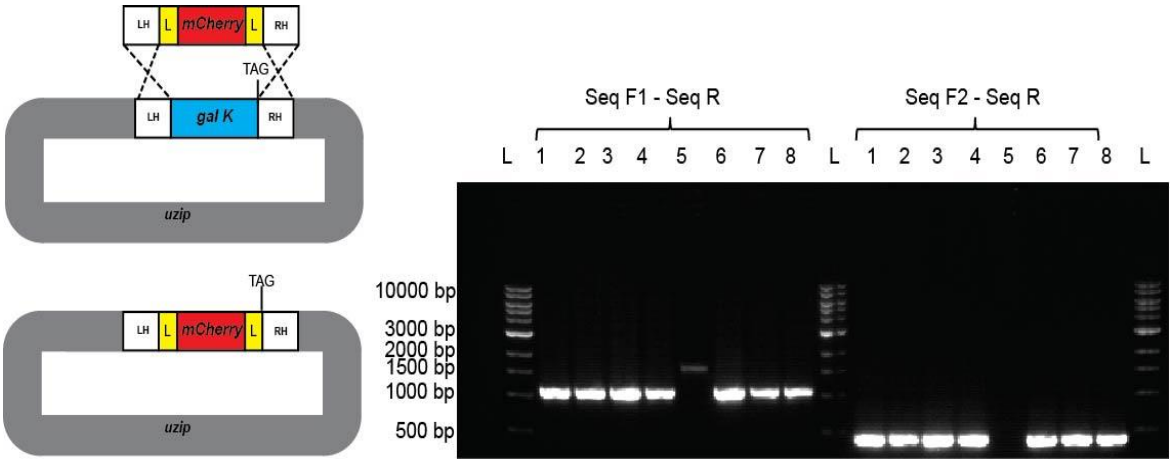

Figure 4.11. Replacement of the galK cassette with the mCherry cassette. In this step, the homologous recombination event took place and mcherry was inserted before the last stop codon of uzip. In the gel photo, 8 single colonies were checked for the insertion and orientation, respectively. All of the colonies except colony 5 were mCherry positive.

mCherry positive cells were grown in LB medium containing Chl and the BAC DNA was extracted using a Maxi Prep protocol for low copy plasmids (QIAGEN). These BAC constructs were sent for sequencing. After confirmation of the the BAC sequences, one mutation-free clone was selected. Both Uzip::mCherry and unmodified BAC line, which was ligated into P[acman] vector, sent for injection into flies with an attachment site on the third chromosome (VK31) by using (ϕ)c31 integration The successfully generated

transgenic fly lines were selected for two markers, white and yellow, which are eye-color and body-color markers, respectively (see Figure 4.12). Finally, Uzip::mCherry and Uzip (BAC) lines were obtained.

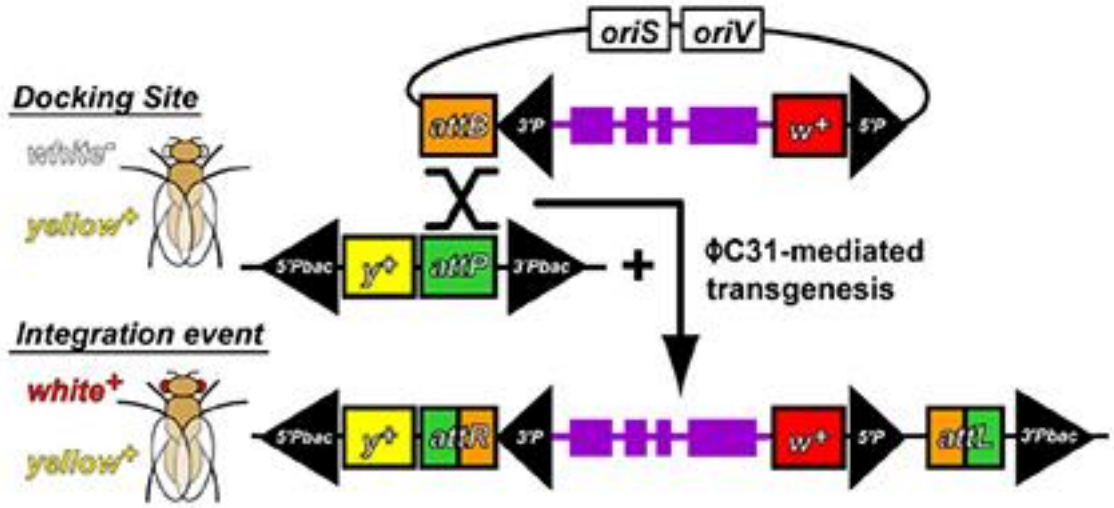

Figure 4.12. Injection of Uzip::mCherry into flies bearing *attP* and ΦC31-mediated transgenesis event. Uzip::mCherry containing BAC construct was injected into *Drosophila* embryos which contain yellow marker, 3' and 5' transposase sites and *attP* site. Uzip::mCherry-containing BAC construct was integrated into the 3rd chromosome of *Drosophila* by recombination between attachment sites(Taken from Venken *et al*., 2007).

4.3. Analysis of the Expression Pattern of Uzip::mCherry Transgenic Flies

In the framework of this study, a detailed analysis of Uzip localization was undertaken using the Uzip::mCherry transgenic line generated under 4.2. Previously, Uzip was tagged with Flag and HA from the N-terminal which resulted to detect both form of this protein. Unfortunately, detection of the secreted form of Uzip resulted too much background which made detection of endogenous uzip expression harder (Zülbahar, 2012). In order to get rid of the secreted form of Uzip, mCherry was tagged to the C-terminal end of the Uzip protein, which should report the localization of only the membrane-attached form, but not the secreted form. Adult brain stainings with an antibody against mcherry showed that Uzip is mainly localized to glia. Additionally, Uzip localization in the

peripheral olfactory structures, the 3rd segment of antenna and the maxillary palp, were also investigated both in pupal and adult stages.

4.3.1. Uzip Expression Resembles The Distribution of Ensheating Glia in The Adult Brain

Adult brains of flies carrying the mCherry tagged version of Uzip were examined with anti-Dsred staining. Strong Uzip expression was detected around the ALs, MBs, optic lobes, and in all components of the central complex, the elipsoid body, protocerebral bridge, fan-shaped body, and the nodula (Figure 4.13). Interestingly, Uzip appeared to cover these structures similar to ensheathing glia in the adult brain. This pattern of expression also correlates with the results obtained by looking at the enhancer trap. Stainings with an anti-repo antibody showed specific localization of Uzip::mcherry around the glial nuclei (data not shown).

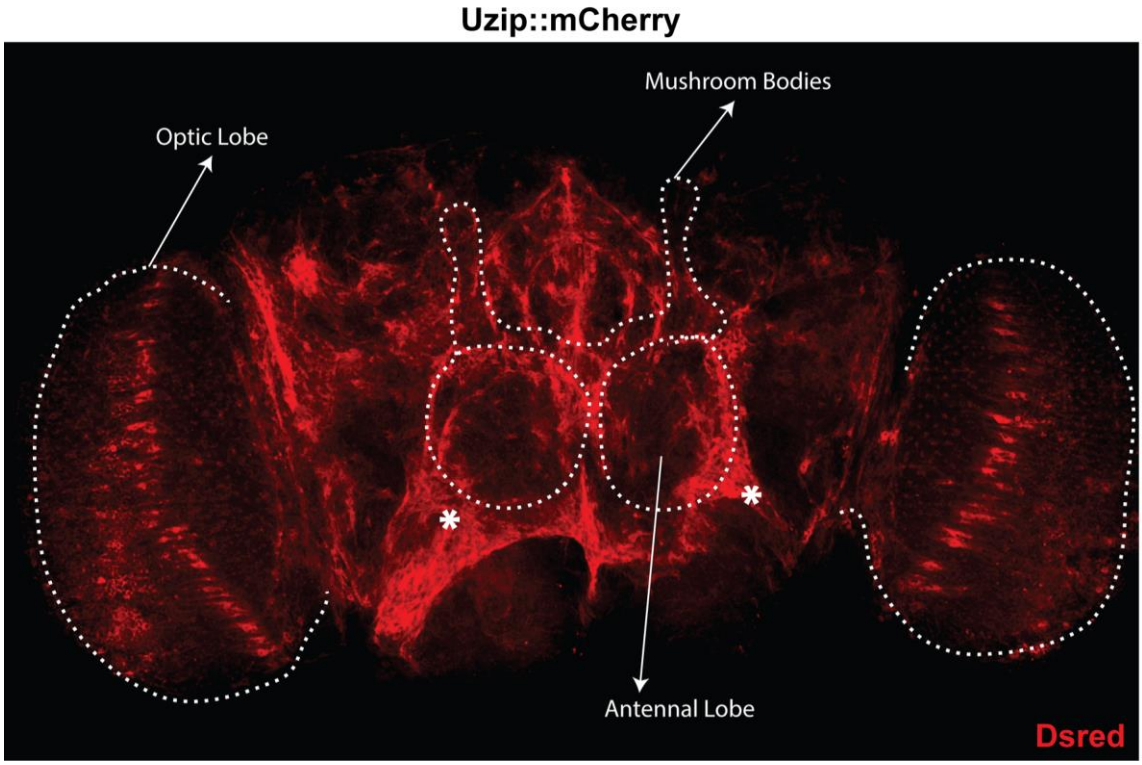

Figure 4.13. Uzip is expressed around the ALs, mushroom bodies, central complex, antennal nerve, and the optic lobes. Adult brains of Uzip::mCherry transgenic flies were

analyzed using anti-Dsred antibody to detect mCherry. Mushroom bodies, antennal nerve (Shown with asterisk), and ALs surrounded by Uzip. Additionally, a glial-specific expression pattern was observed in the optic lobes.

4.3.2. Localization of Uzip::mcherry to Antenna and Maxillary Palps

Uzip expression in antenna and maxillary palp was examined using the modified protocol to overcome antibody penetration problems. Antennae and maxillary palps complete their maturation before the mid-pupal stage. Staining of pupal maxillary palp and antennae is easier as the surrounding cuticle is not as thick as in the adult. Thus, maxillary palp and antenna stainings were performed at 96h APF. Anti-Elav and anti-Repo antibodies were used in conjunction with an anti-Dsred antibody to visualize neurons, glia, and Uzip::mcherry, respectively.

In the maxillary palp, Uzip was localized to the labial nerve, where OSNs projections fasciculate with the help of glia and are directed to the ALs. Anti-Elav staining showed the positions of the sensory neurons in the maxillary palp and anti-Repo staining revealed the location of glia nuclei on the labial nerve.

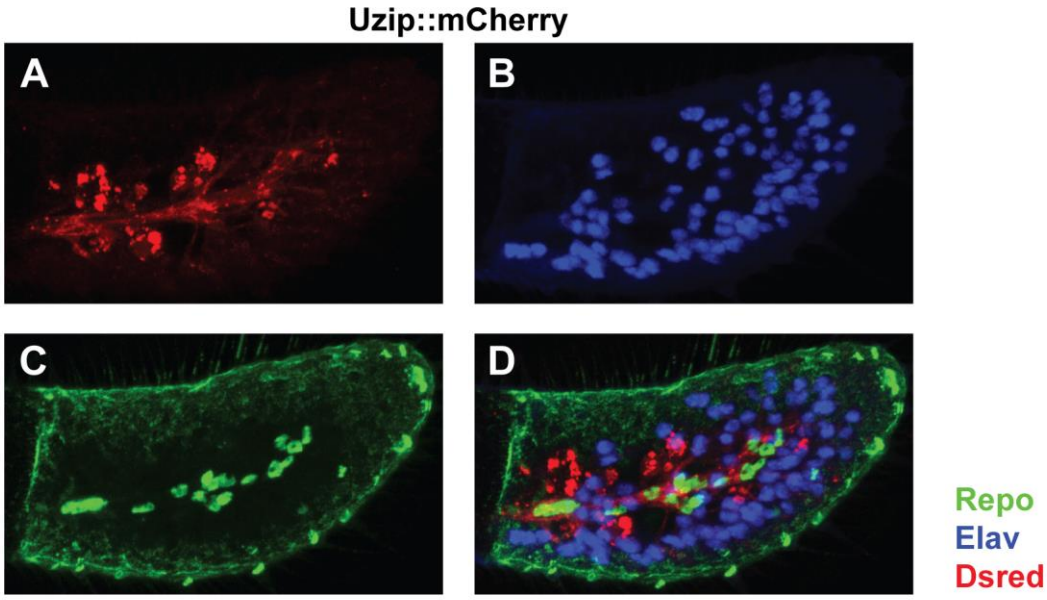

Figure 4.14. Uzip protein localizes to glial processes in 96h APF maxillary palps. (A) Anti-Dsred (red) visualizes mCherry-tagged Uzip protein. (B and C) Anti-Elav (blue) and anti-Repo (green) antibodies were used to detect neuronal nuclei and glia, respectively. (D) Uzip appears to localize to tiny branches that surround each individual neuron and the labial nerve.

In antenna, a similar localization of Uzip protein was observed, where it mainly accumulates in the center where glia nuclei are densely located. In contrast, sensory neurons are distributed throughout the antenna. As shown in Figure 4.15, Uzip expression was observed around each sensory neuron and main axonal trajectories of the antenna.

These stainings indicate that, uzip is widely expressed in the antenna and maxillary palp and Uzip protein surrounds glia and neuron nuclei. In order to identify which cells express Uzip, different glial subtypes in the antenna and maxillary palp were examined. Additionally, anti-Futsch antibody was used to show if Uzip localizes to OSN membranes.

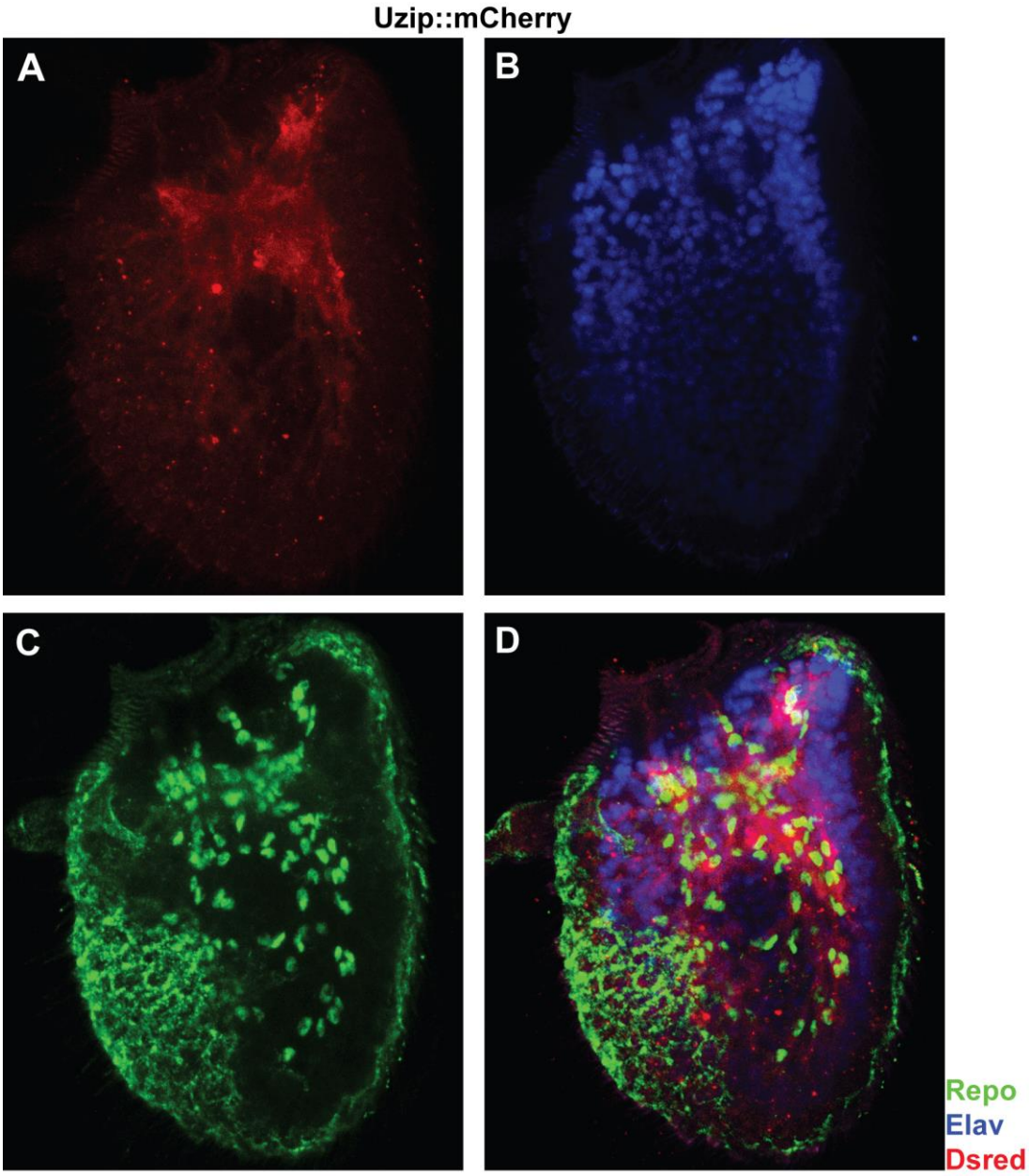

Figure 4.15. Uzip protein shows a broad distribution in 96h APF antenna, and an association with glia. Anti-Elav (blue), anti-Repo (green), and anti-Dsred (red) antibodies were used. Uzip expression was mostly observed in central region of the antenna where glial cell bodies are localized. From the center of the antenna, Uzip-expressing cells project protrusions to surround antennal neurons.

4.3.2.1. Uzip expression in glial sub-populations. Uzip is a cell-surface molecule and Uzip::mCherry transgenic flies only show the membrane-attached form of Uzip with a mCherry tag. Here, we investigated if Uzip localizes on the membrane of glia by crossing the Uzip::mcherry line with the Repo-LexA > LexAop-CD2::GFP line, in which *repo* drives expression of membrane bound GFP and enables the visualization of glial membranes with anti-GFP staining. Anti-Repo antibody was used to detect nuclei of glial cells.

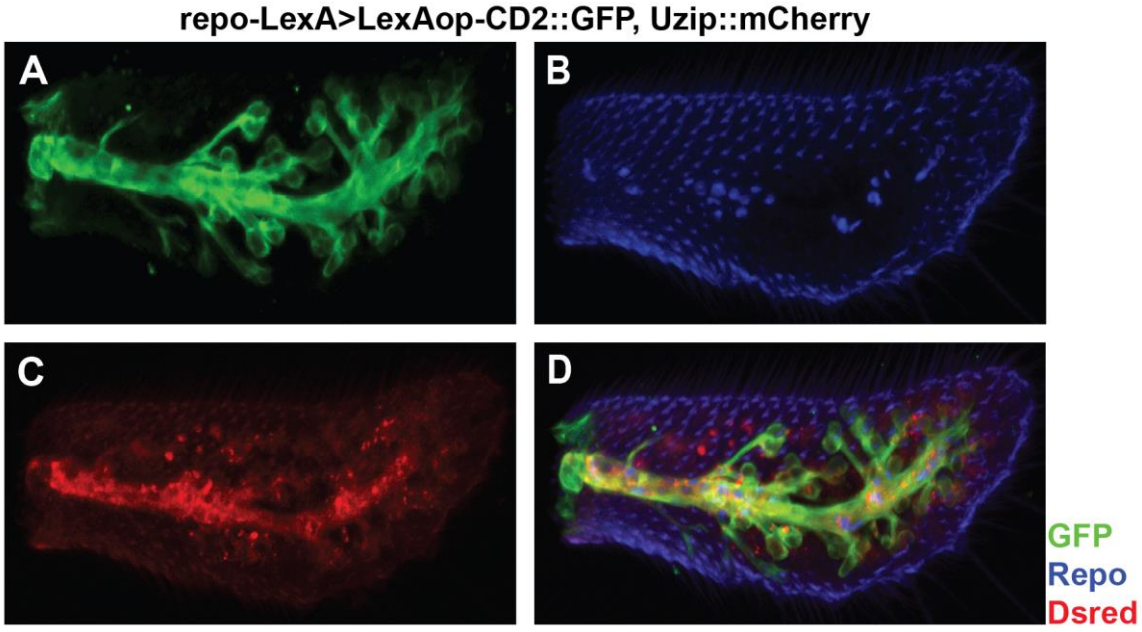

Figure 4.16. Evaluation of Uzip localization to glial membranes in the maxillary palp using Repo-LexA > LexAop-CD2::GFP, Uzip::mCherry flies. Membranes and nuclei of glia are shown in (A) and (B). (C) shows the expression pattern of Uzip::mCherry. (D) is the merged image showing that, Uzip has a glia-like expression pattern in the maxillary palp.

In Figure 4.16 shows adult maxillary palp stainings. Anti-Repo antibodies label the nuclei of glia on the labial nerve and anti-GFP displays the protrusions of glial cells, which surround sensory neurons of the maxillary palp. Anti-Dsred detects a specific pattern of Uzip on the membranes of glial cells and also non-glial patterns in distinct regions of the maxillary palp where no glia are observed. Additionally, two subtypes of glial cells, namely GH146-glia and Mz317-glia cand be distinguished in the antenna and maxillary palp of *Drosophila*. Among these subtypes, there are also glia, which cannot be labeled

with anti-Repo antibody. Since the GFP signal is too strong in comparison with the mCherry signal in the ALs, Uzip seems to localize on glial membranes and a more detailed analysis of the maxillary palp is required to conclude in which type of glia Uzip is expressed in the maxillary palp.

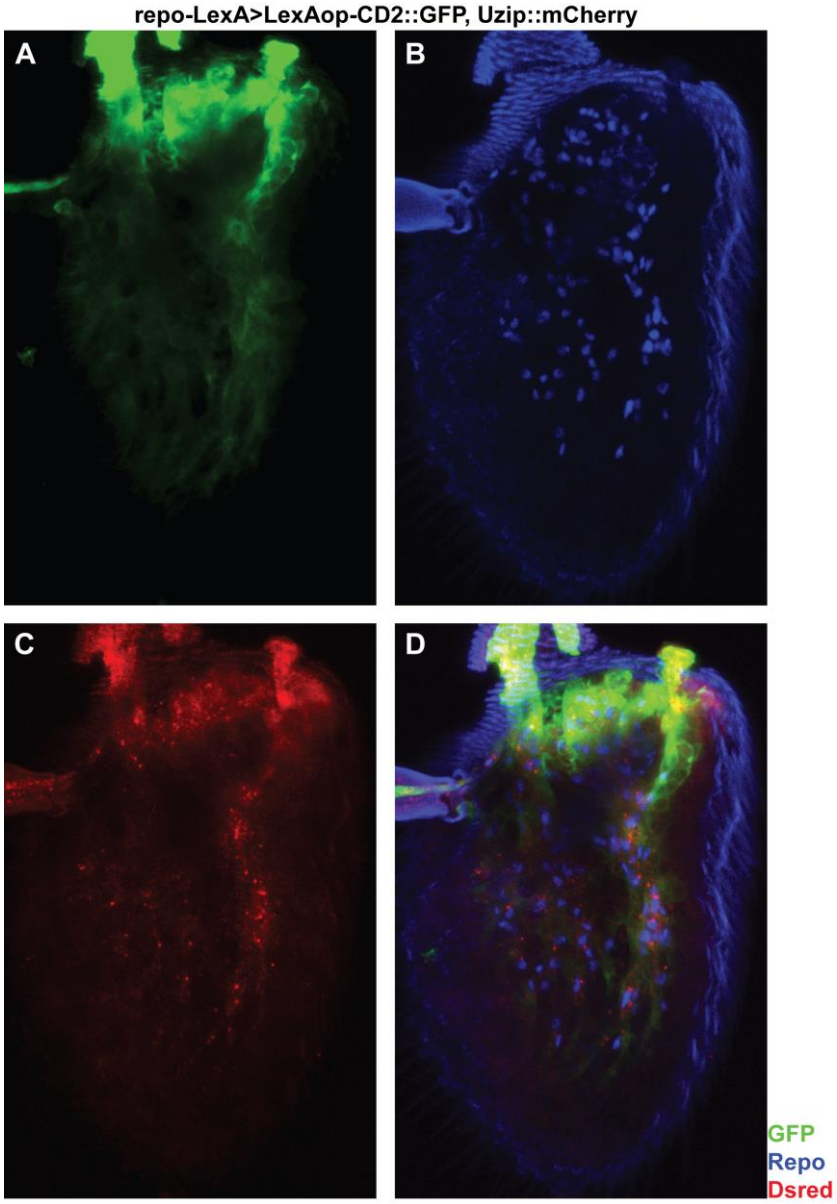

Figure 4.17. Uzip expression pattern is analyzed in *repo* > CD2::GFP, Uzip::mCherry flies. (A) GFP antibody detects the membranes of glial cells and (B) Repo was used as a nuclear marker for glia. (C) Dsred detects mCherry bound Uzip. (D) shows the merged image.

In addition, adult antenna of the Repo-LexA > LexAop-CD2::GFP, Uzip::mCherry transgenic flies were investigated. Interestingly, Uzip is localized at the borders of glial nuclei and on glia membranes, which were tagged with GFP (see Figure 4.17). Two layers of Glia surround OSNs in the antenna, which makes it very difficult to distinguish which cells have Uzip on their cell surface. In order to overcome this problem, expression analysis was done by using Uzip::mcherry line together with the MZ317-specific glial driver and the GH146-specific glial driver, respectively. Additionally, neuron-specific Futsch antibody was used to visualize axons of OSNs.

4.3.2.2. GH146 glia and Uzip expression. GH146 glia are a subtype of glia that migrates to the antenna from the ALs during pupal development and directly ensheaths OSNs (Sen *et al*., 2005). The antenna and maxillary palps of GH146-Gal4 > UAS-CD8::GFP, Uzip::mcherry flies were examined to see if GH146 glia express Uzip. While the GFP staining did not work properly for antenna, in maxillary palps a partial overlap in the localization of Uzip and GH146 glia was observed (See Figure 4.18).

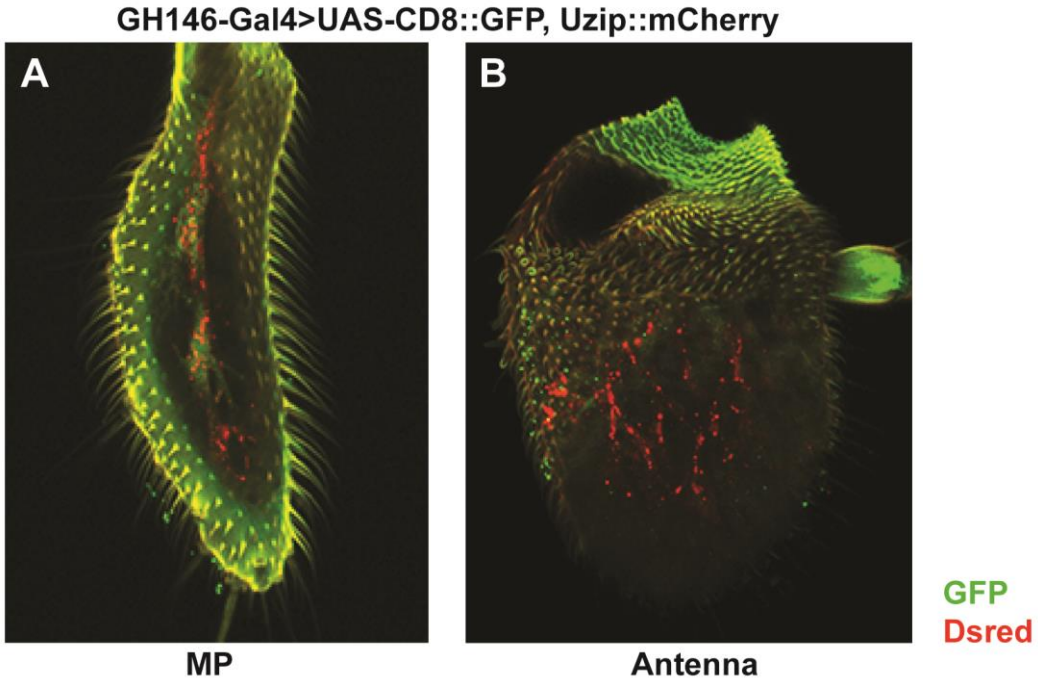

Figure 4.18. Localization of Uzip in relation to GH146 glia in maxillary palp and antenna. Anti-GFP and Anti-Dsred antibodies were used to detect membranes of GH146

glia and mCherry-tagged Uzip, respectively. (A) Uzip expression is partially overlapping with GH146 glia in the maxillary palp. (B) In the antenna, evaluation is not possible since the GFP staining did not work properly.

4.3.2.3. Mz317 glia and Uzip expression. Mz317 glia, located around the ALs and in the antenna, are a subtype of glia that ensheath the cell bodies of sensory organs in the antenna (Sen *et al*., 2005).

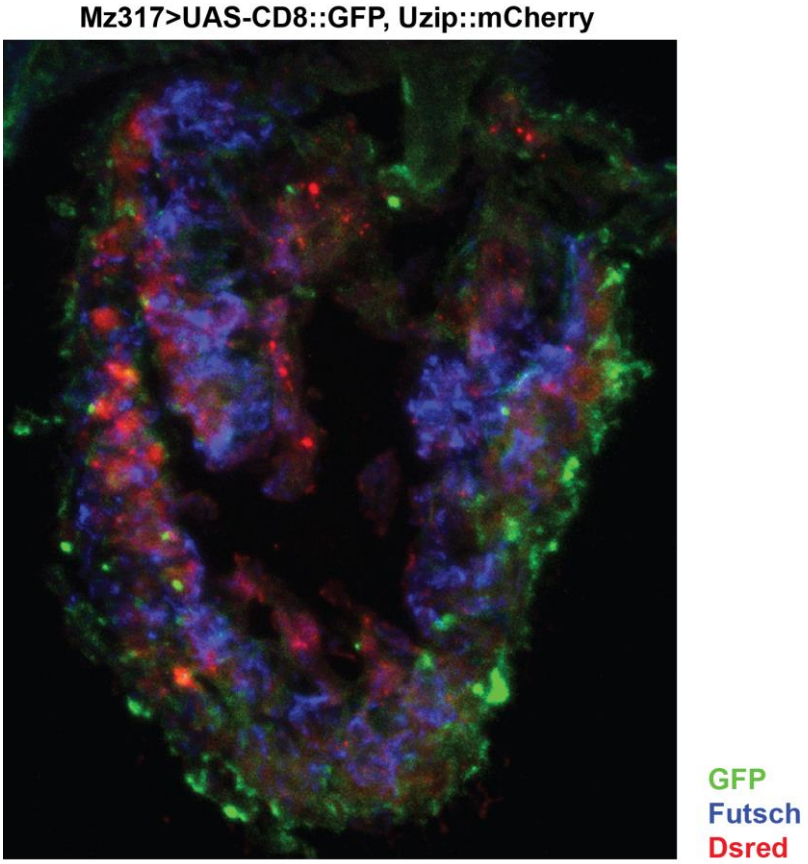

Figure 4.19. Cryosections of an antenna reveal associations between Mz317 glia and Uzip::mCherry. Membranes of Mz317 glia were detected by anti-GFP and Futsch antibody was used to detect OSNs in the antenna. Uzip::mCherry expression was observed between Mz317 glia, which ensheath sensory organs and sensory neurons.

Mz317 glia and Uzip::mCherry interaction was observed by crossing Uzip::mcherry transgenic line to Mz317-Gal4 > UAS-CD8::GFP line. To solve the antibody penetration problem, 14 µm sections of adult antenna were taken and stained with

anti-Dsred, anti-GFP and the neuron-specific anti-Futsch antibody, which labels intracellular axonal compartments of sensory neurons (Estes *et al*., 1996) (Figure 4.19).

In Figure 4.19, Futsch antibody stains the membranes of the sensory neurons in the antenna, whereas Mz317 glia ensheath these neurons by forming a peripheral layer. Uzip expression, which was detected with a Dsred antibody was observed between Mz317 glia and neurons. These results indicate that Uzip might be localizing to the extracellular matrix surrounding sensory neurons or on the membranes of GH146 glia. For a better understanding of Uzip expression, co-localization of Uzip and sensory neurons should be performed using an anti-HRP antibody, which will label the plasma membrane of sensory neurons.

4.4. Uzip Mutant Analysis

Two mutants of Uzip have been generated previously and used to analyse olfactory system development. The first mutant $Uzip^{D43}$ is a null allele that has been generated by the deletion of the Uzip coding region using the FLP/FRT system (Ding *et al.*, 2011) (Figure 4.17). The second mutant $Uzip^{23}$ is a hypomorph that has been created by imprecise excision and expresses reduced levels of Uzip (Ding *et al*., 2011).

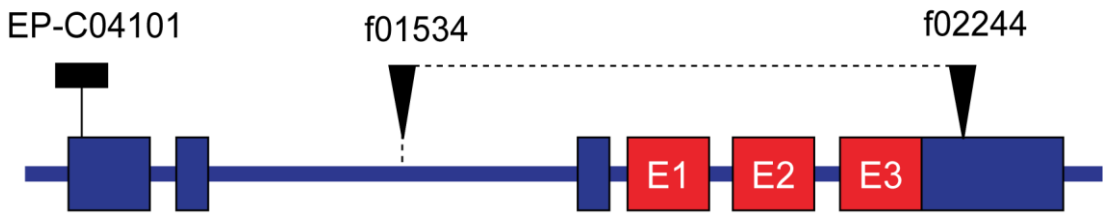

Figure 4.20. The Uzip genomic locus and description of $Uzip^{D43}$ and $Uzip^{23}$ mutants. *EP-C04101* is a piggyBac vector inserted into the first exon of *uzip* that has been mobilized by transposase. A 300 bp sequence of the vector was left behind resulting in the hypomorphic

allele called *Uzip*^{23}. *f01534* and *f02244* are two piggyBac elements that have integrated into the first and sixth exon of *uzip*, respectively (Adapted from Ding *et al*., 2011).

In a previous study performed in our group Selen Zülbahar showed that OSNs have severe projection defects in an *Uzip*^{D43} mutant background. Analysis of the projection pattern of five different ORNs subtypes showed that in all cases OSNs are not able to cross the midline and reach the contralateral glomerulus. Similar targeting defects were also observed in ALs of *Uzip*^{23} / *Uzip*^{D43} transheterozygous flies. In *Uzip*^{D43} null mutants, maxillary palp OSNs displayed additional axon stalling and mistargeting defects (Zülbahar, 2012).

In the framework of this study the previous experiments were repeated and the number of analyzed brains per subtype of OSNs was increased in both *Uzip*^{D43} and *Uzip*^{23} mutant backgrounds to reach significance levels. Interestingly, in *Uzip*^{23} mutants the antennal OSNs subtypes display the same loss of commissure phenotype (see Figure 4.18). Moreover, in a few adult brains the commissure could still be formed but was observed to be much weaker compared to wild type flies (data not shown).

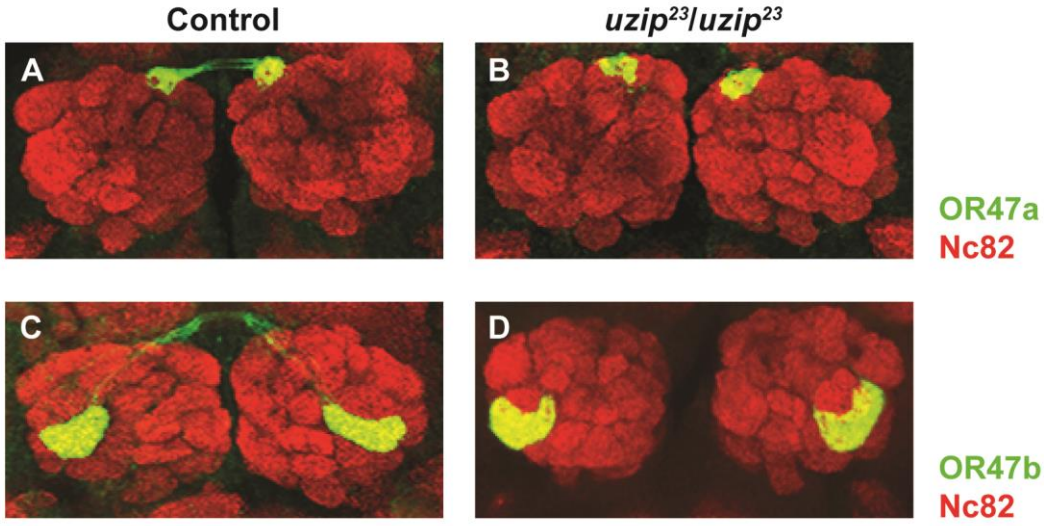

Figure 4.21. Homozygous Uzip hypomorphs antennal OSNs has midline crossing defect. Projection patterns of OR47a and OR47b neurons were examined in *Uzip*^{23} heterozygous (A and C) and homozygous mutants. (B and D) In homozygous mutant background, OSNs

cannot form the commissure between two ALs. Nc82 antibody labels ALs (red) and GFP antibody detects plasma membranes of OSN subtypes (green).

Additionally, in *Uzip*^{23} mutant background axonal projections of two subtypes of OSNs were tested by using *OR59c*-Gal4 > UAS-CD8::GFP and *OR46a*-CD8::GFP transgenic flies. As expected, these neurons exhibit severe mistargeting and axon stalling phenotypes (see Figure 4.19). In OR59c expressing neurons, axon-stalling phenotypes in SOG were detected in almost all samples. In contrast to the axon-stalling phenotype of OR59c neurons, *OR46a*-expressing neurons in Uzip mutants displayed mistargeting phenotypes. In the adult brain, OR46a neurons project to an additional glomerulus, which seems to be chosen by a random process.

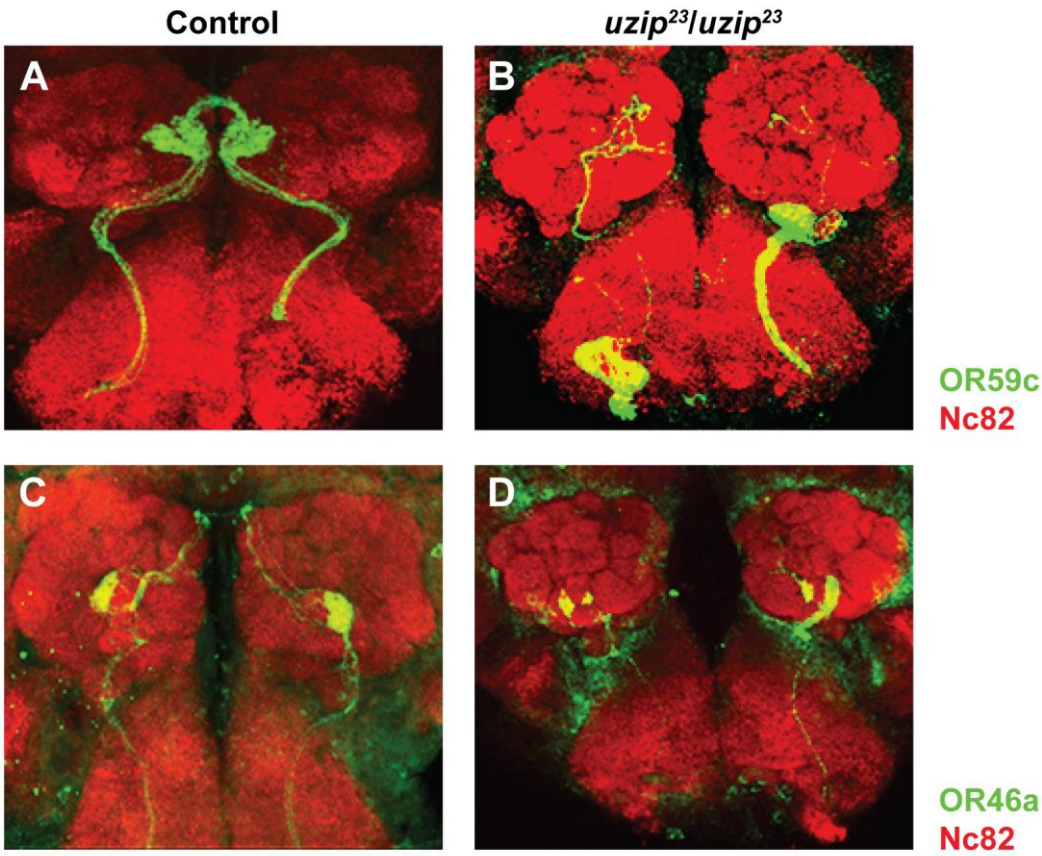

Figure 4.22. The maxillary palp OSNs display severe axon projection defects in Uzip hypomorph mutants. OR59c and OR46a neuron projections were investigated in heterozygous (A and C) and homozygous *Uzip*^{23} mutants (B and D). None of the OSNs can

cross the midline between the two ALs. Additionally, OR59c neurons displayed a severe axon stalling phenotype, whereas this phenotype was not observed in OR46a neurons.

To get some insight into the mechanism that leads to the phenotype Uzip mutants were analyzed during developmental stages. 36h APF brains were dissected to show that none of the ORNs can cross the midline. In wild type flies, specifically at this developmental stage ORN commissure can be visualized by using the Flamingo (Fmi) antibody (Figure 4.20). In the mutant it can be seen clearly that no commisure can be formed as none of the ORNs crosses the midline. All OSNs seem to get stuck in the antennal lobe. In Uzip null mutants, a gap between the two hemispheres was observed at the central complex as well. Here we speculate that, Uzip might have a dynamic role in forming the connections between the right and left hemispheres of the *Drosophila* brain.

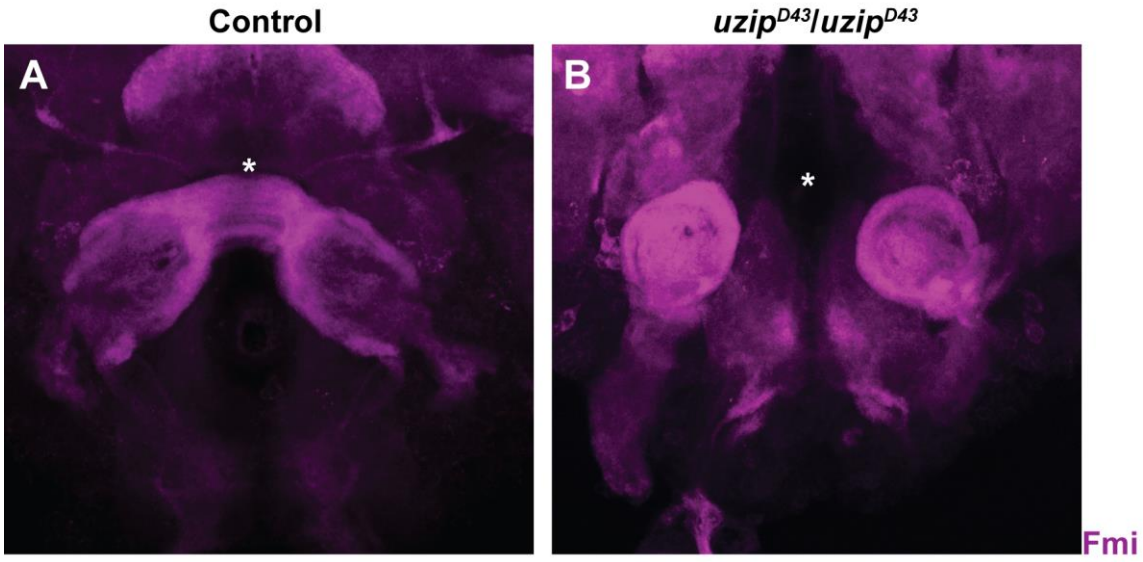

Figure 4.23. Analysis of commissure formation at 36h APF in wild type and *Uzip*^{D43}. (A) In wild type flies OSN neurons cross the midline and reach the contralateral antennal lobe. (B) In contrast, in *Uzip*^{D43} none of the OSNs can cross the midline and are stalled in the antennal lobes (n=7). Asterisk shows the midline region where OSNs form a commissure. Flamingo (Fmi) antibody (magenta) was used to visualize all OSNs.

Cell-type specific ablation of TIFR glia resulted in absence of commissure formation and axon stalling phenotypes in the ALs (Chen and Hing, 2008). Since Uzip is mainly expressed by glial cells, we suggested that Uzip might be expressed by TIFR glia

and might have a role in the formation of the TIFR structure. By using the *c442*-gal4 driver and the UAS-CD8::GFP reporter line, we visualized the TIFR structure at 36hAPF as shown by (Chen and Hing, 2008) (Figure 4.21).

In order to visualize TIFR from the side, optic lobes of pupal brains were removed and brains were mounted on one side. In Figure 4.21B, two developing antennal lobes visualized by Flamingo antibody are shown. OSNs can be seen to pass through the 3rd canal of the TIFR structure.

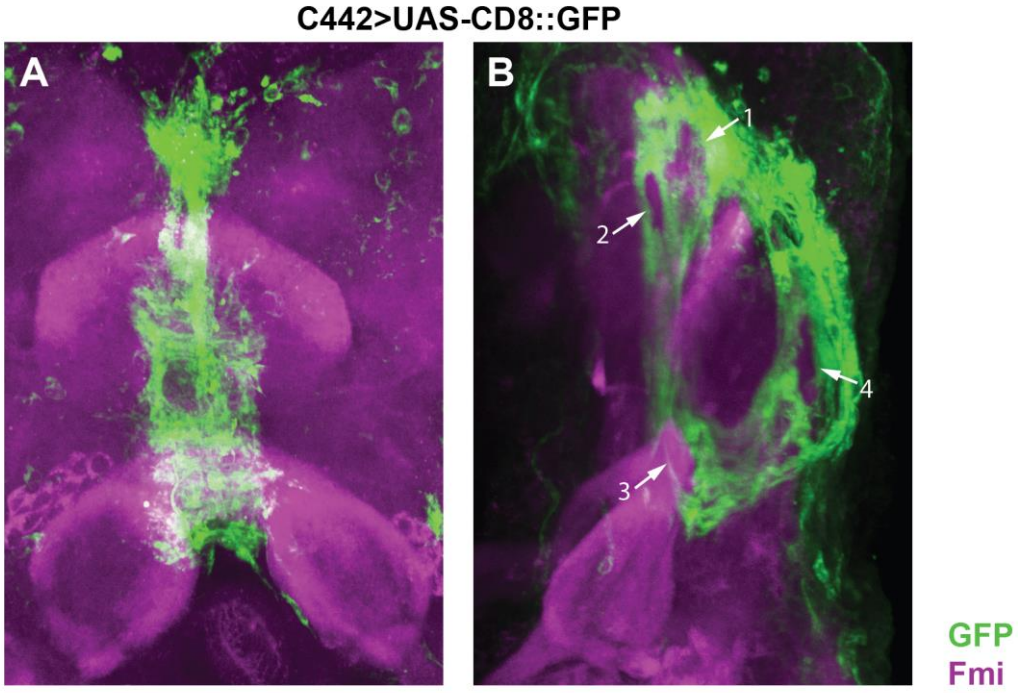

Figure 4.24. Structure of the TIFR glia at 36h APF and OSNs commissure. (A) Anterior, (B) sagittal view of the *Drosophila* pupal brain. *c442*-Gal4 driver was used to express membrane-bound GFP in TIFR glia. Flamingo is magenta, GFP is green. 4 Canals were formed by TIFR structure were shown with arrows. OSNs pass through 3rd canal.

We further investigated the structure of TIFR glia in Uzip null mutants. For this purpose, *Uzip*^{D43}/ CyO-GFP; *c442*-Gal4 > UAS-CD8::GFP stock was generated. From *Uzip*^{D43}/ CyO-GFP; *c442*-Gal4 > UAS-CD8::GFP stock, white pupae were selected under a fluorescent microscope. GFP-positive and GFP-negative pupae were individually grown at 25ºC until 36h APF. Flies displaying no GFP signal except in c442 cells, were selected

as these represent the homozygous mutant *Uzip*^{D43} population and 36h APF pupae were stained with GFP and Flamingo antibodies.

In Figure 4.22A, a heterozgous *Uzip*^{D43} pupal brain is shown, whereas Figure 4.22B and C demonstrate Uzip homozygous pupal brains. In *Uzip*^{D43} heterozygous flies, TIFR interacts with OSNs crossing the midline. In *Uzip*^{D43} null mutants, OSNs cannot form the commissure and TIFR does not interact with OSNs (Figure 4.25B.) Strikingly, one mutant brain has a strong phenotype in TIFR structure shown with an arrowhead in Figure 4.25C. In contrast to other brains examined, the arrow indicates a mistargeting effect of OSNs. These neurons neither stop at the AL as in the other Uzip mutants nor form a commissure as in wild type flies. Instead these axons were misguided to the dorsal side of the brain and might be interacting with TIFR glia.

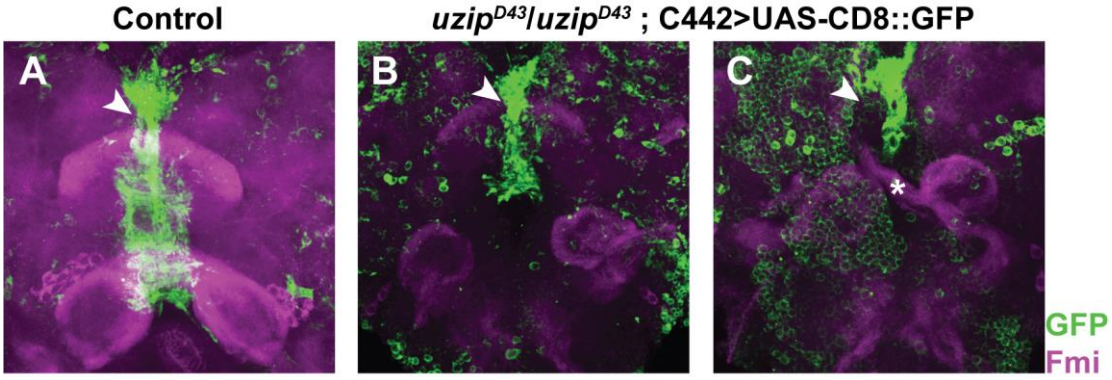

Figure 4.25. TIFR structure is disrupted in *Uzip*^{D43} mutant flies. The TIFR structure was examined both in heterozygous (A) and homozygous (B, C) *Uzip*^{D43} mutants. Additionally, the TIFR structure is disrupted compared with heterozygous *Uzip* mutants. (B) Arrowheads show axon stalling phenotypes at the ALs.

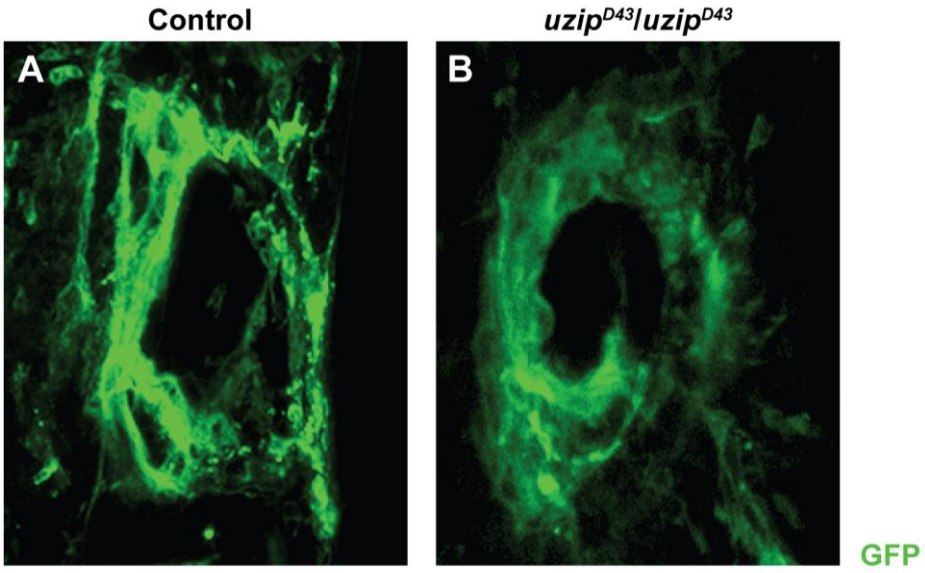

Figure 4.26. Canals do not form properly in Uzip null mutant flies (A) Heterozygous and (B) homozygous *Uzip* null mutant pupal brains are shown (sagittal view). (A) The 3rd canal through which OSNs pass to the contralateral side is clearly visible. (B) The 3rd canal of TIFR has not formed and in general, the TIFR structure appears disorganized compared to heterozygous flies.

In order to understand the role of Uzip in TIFR formation, the TIFR structure in Uzip heterozygous and homozygous mutants were compared. Pupal brains were mounted on the slides in upright position. Figure 4.26 displays TIFR in Uzip heterozygous and Uzip homozygous flies. In Uzip homozygous flies, the TIFR structure was destroyed and the 3rd canal of Uzip did not form. This data clearly indicate that Uzip is a cell surface protein that regulates olfactory sensory development by guiding TIFR glia to form properly.

4.5. Possible Interaction Partners of Uzip

Uzip is a cell adhesion molecule which genetically interacts with Wnt5 and Ncad in the embryonic stages (Ding *et al*., 2011). However, how these molecules are interacting remains unclear, Uzip levels are regulating the severity of axon guidance both in Ncad and Wnt5 mutants.

Here, we investigated to cell surface molecules which play a very similar role to Uzip in the olfactory system development. First of all, we investigated Nrg which has a

role in the formation of TIFR, thereby regulating OSN commissure formation between the two ALs. In Nrg mutants, olfactory sensory neurons show midline crossing and mistargeting defects.

Furthermore, we examined the interaction of Drl and Uzip, because Drl is the receptor of Wnt5 which has already shown to interact with Uzip (Ding *el al*., 2011). Secondly, Drl is expressed by TIFR glia and *Drl* null mutant show strong AL development and central complex phenotypes.

Therefore, in this study we checked the interaction of Uzip together with either Drl or Nrg.

4.5.1. Neuroglian

Nrg is cell adhesion molecule and homolog of vertebrate L1-type protein (Bieber *et al*., 1989) Nrg has two isoforms as Nrg167 and Nrg180 which are expressed by non-neuron cells and neurons, respectively (Hortsch *et al*., 1990) Nrg mutants show severe axonal defects in motor neuron and sensory neuron projectories in embryonic and larval development (Hall and Bieber, 1997; Martin *et al*., 2008; Garcia-Alonso *et al*., 2000).

Additionally, Nrg is involed in the regulation of mushroom body develeopment such as axon guidance, axonal branching and axonogenesis (Goessens *et al*., 2011). Furthermore, In Nrg^{849} mutants, TIFR structure was disrupted, OSNs cannot form a commissure and some OSNs are mistargeted in the AL (Chen and Hing, 2008) All of this defects were seen in Uzip mutants, thereby the genetic interaction between *Uzip* and *Nrg* was tested.

The genetic interaction of Uzip and Nrg mutants was previously shown by Çevrim (unpublished data) in terms of mushroom body development. In this study, we checked if this interaction is important for the projection and midline crossing of OSNs. So, transheterozygous flies having both mutation in heterozyous form were analyzed. In $Uzip^{D43}$ and Nrg^{849} transheterozygous mutants, missing lobe phenotypes were observed but

projection of OR47a neurons was normal. Additionally, both in heterozygous *Nrg*^{849} and Transheterozygous *Uzip*^{D43} and *Nrg*^{849} OR47a neurons were able to cross the midline and reach to contralateral AL.

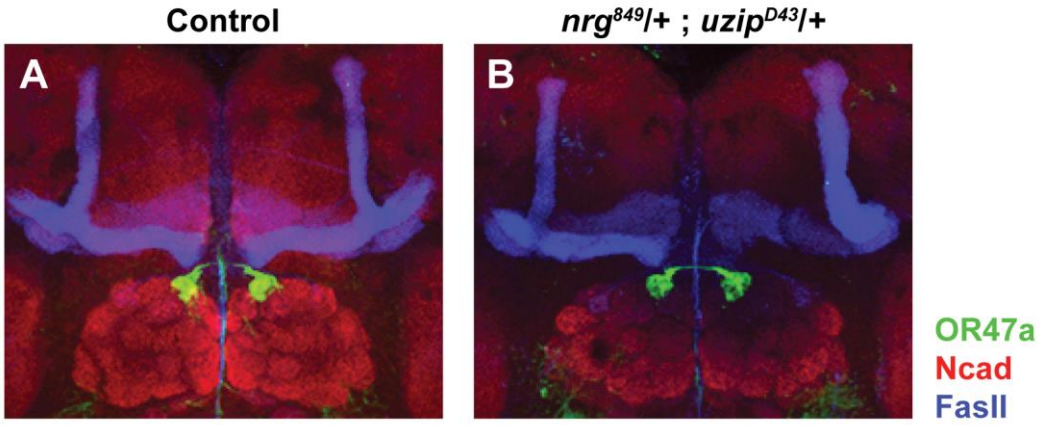

Figure 4.27. The genetic interaction between Nrg and Uzip^{D43} is demonstrated. On the left, *Nrg*^{849} heterozygous and on the right *Uzip* and *Nrg* transheterozygous mutants are shown. In transheterozygous mutants, missing lobe phenotype was observed in mushroom bodies but OR47a neurons cross the midline as in heterozygous *Nrg* mutants (n=8). OR47a-Gal4 driver was used to express membrane bound GFP in OR47a neurons for visualization.

Furthermore, Nrg-Uzip interaction was investigated by analyzing transheterozygous Uzip^{23} and Nrg^{849} mutants. The projections of OR59c neurons were analyze in transheterozygous mutants shown in Figure 4.28. Nrg^{849} heterozygous females adult brain were used as a control to Nrg^{849}–Uzip^{23} transheterozygous female flies. No axonal defects of OR59c neurons were seen, which indicates Uzip mutants are not genetically interacting with Nrg in the development of olfactory sensory system of *Drosophila*.

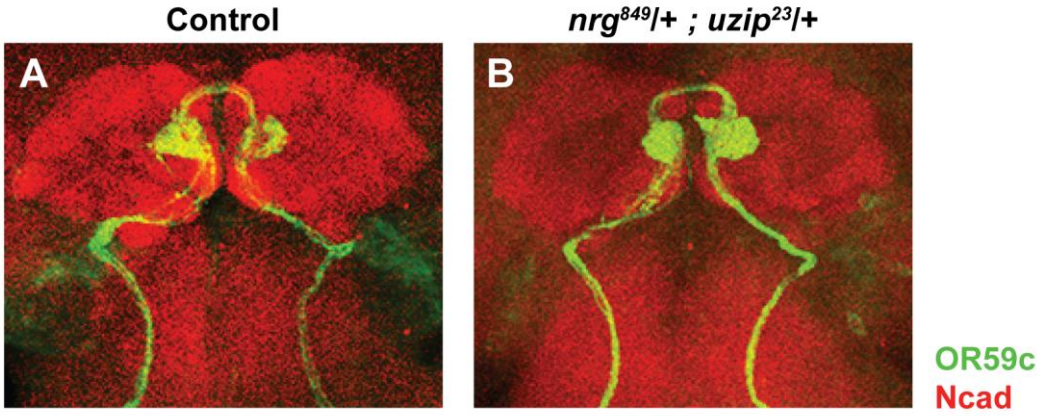

Figure 4.28. Transheterozygous mutants of *uzip*^{23} and nrg849 does not cause any defect of OSNs projections. (A) Heterozygous Nrg849 mutants were used as a control and the axonal projections of OR59c neurons were investigated. (B) In transheterozygous mutants of *nrg*^{849} and *uzip*^{23}, no axonal defects were detected (n=5). Anti-GFP was used to detect OR59c neurons' membrane and Ncad was used to label the ALs.

4.5.2. Derailed

Derailed is receptor tyrosine kinase and regulates Wnt5 signaling in the development of the olfactory system (Yao *et al*., 2007; Zhang *et al*., 2006). Drl mutants exhibit fan-shaped body, mushroom body and TIFR malformation phenotypes and was chosen as a candidate interaction partner of Uzip (Boquet *et al*., 2000b; Hitier *et al*., 2000).

We ordered null mutants of Drl (*Drl*$^{exc21)}$ to check whether transheterozygous form of Uzip and Drl null mutants cause axon guidance phenotypes as observed in null mutants of Uzip. Axons of OR47a neurons, which were labeled with membrane bound GFP (Or47a-Gal4 > UAS-CD8::GFP) were examined. In heterozygous from of both mutants, no phenotype was observed besides mushroom body beta lobe fused phenotype which was initially shown by Çevrim *et al*., (unpublished data).

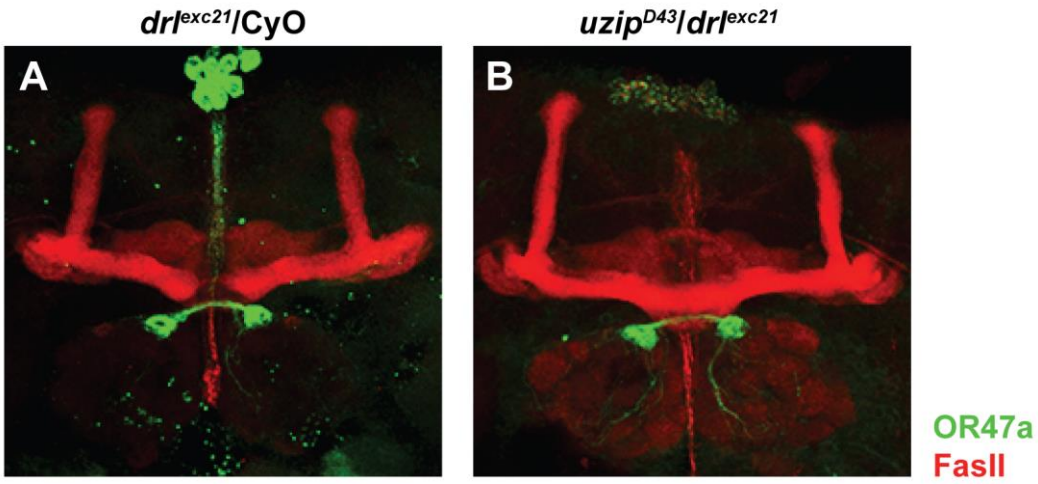

Figure 4.29. Transheterozygous mutants of *uzip*^{23} and *drl*^{exc21} does not cause any defect of OSNs projections. (A) Heterozygous drl null mutants and (B) transheterozygous Uzip, Drl null mutant adult brain were stained with FasII and GFP antibodies. FasII was used to show MB structure, GFP was used to detect membrane bound GFP expression of OR47a neurons.

4.6. Misexpression of Uzip

Uzip is known to be expressed both by glia and neurons in embryonic stages. In this study, expression pattern analysis done both with enhancer-trap line and Uzip::mCherry showed that Uzip is mainly expressed by glia. During olfactory system development, Uzip has a major role in axon guidance and Uzip mutants show strong axonal projection phenotypes.

In order to gain some insight into how the lack of Uzip is causing axon guidance phenotypes and in which cell types Uzip function is required cell-type specific loss of function and gain of function experiments have been performed. In all cases experiments were preformed at 29˚C to enhance Gal4 activity and UAS-Dicer to enhance the RNAi effect in neurons.

4.6.1. Downregulation

4.6.1.1. Ubiquitous downregulation of Uzip by RNAi. Initially, an UAS-UzipRi line was crossed with an driver that drives expression in all cells ubiquituously, *ubi*-Gal4, was used to assess if the RNAi line works efficiently. If this is the case we expect phenotypes similar to the Uzip null phenotypes. In Figure 4.30, 36h APF pupal brains of wildtype (Figure 4.30A), Uzip homozygous mutant (Figure 4.30B) and *ubi*-Gal4 > UAS-*uzipRi*, UAS-*Dcr* (Figure 4.30C) are shown. In wild type flies, OSNs form a thick commissural bundle between the two ALs (Figure 4.25A), whereas in homozygous null mutants of Uzip no commissure and a big gap between the two hemispheres was observed (Figure 4.30B). In addition, the fan-shaped body was divided into two parts in homozygous mutants (see thin arrows in Figure 4.30B). Downregulation of Uzip in all cells gave a very similar phenotype when compared to homozygous Uzip null mutants (See Figure 4.30C). The two ALs were separated and axons of OSNs could not cross the midline. Also, the fan-shaped body structure was disrupted.

Downregulation of Uzip in all cells gave a very similar phenotype when compared to homozygous Uzip null mutants (See Figure 4.30C). The two ALs were separated and axons of OSNs could not cross the midline. Also, the fan-shaped body structure was disrupted.

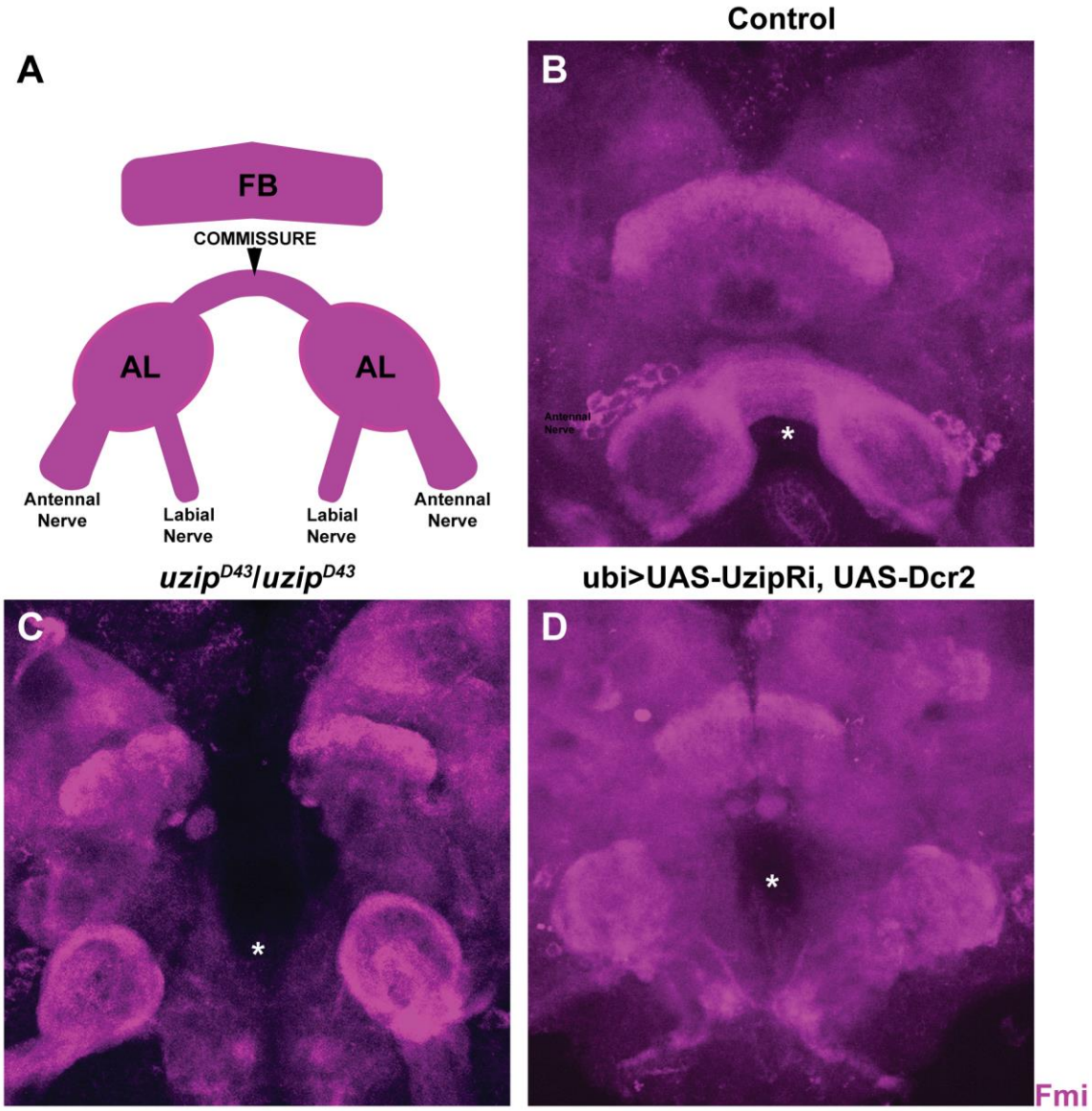

Figure 4.30. Ubiquitous downregulation of Uzip results in axon guidance phenotypes resembling Uzip null mutant phenotypes. (A) 36 h APF pupae brain is illustrated. Fan-shaped body (FB), ALs, antenna nerve and labial nerve are shown. A thick bundle between two AL were shown as commissure. 36h APF pupal brains of wild type (B), *Uzip*^{D43} homozygous (C) and ubiquitous downregulation of *Uzip* (D) was shown.

4.6.1.2. Uzip downregulation in glial cells. Uzip is mainly expressed by glial cells. To investigate if the observed phenotypes are caused by loss of Uzip function in glial cells Uzip was downregulated using a glial-specific driver. These experiments were expected to give similar results as in Uzip null mutant background (midline crossing, mistargeting, axon stalling phenotypes). However, glial-specific downregulation of Uzip did not cause

any detectable phenotypes in AL development or OSN commissure formation (Figure 4.31.).

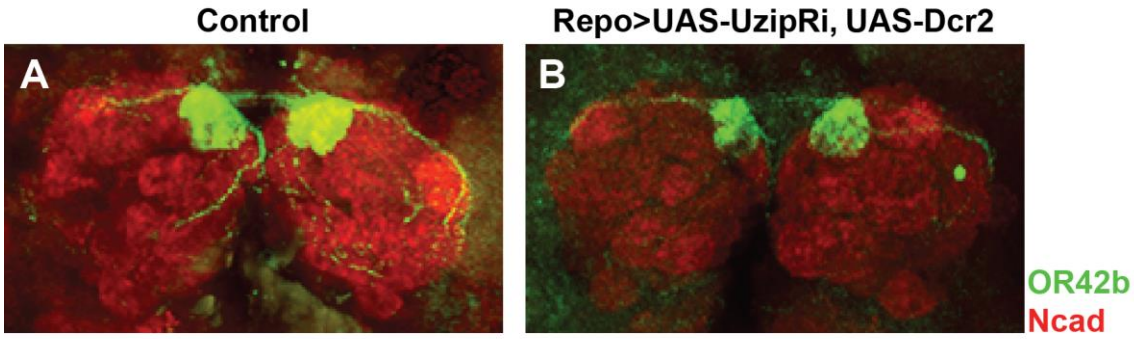

Figure 4.31. Glial-specific downregulation of Uzip does not cause a commissural phenotype. By using the glia-specific driver *repo*-Gal4, Uzip was downregulated specifically in glial cells. The effect of downregulation was enhanced by using UAS-Dicer and keeping flies at 29ºC.

4.6.1.3. Uzip downregulation in glia with double repo-gal4 driver. As shown in Figure 4.31 downregulation of Uzip in glia did not cause any obvious axon guidance phenotype. Since Uzip is mainly expressed by glia, this result was unexpected. To make sure that this result was not caused by insufficient downregulation of Uzip we tried to increase the efficiency of downregulation by doubling the number of repo drivers. As can be seen in Figure 4.32 in this configuration axon stalling phenotypes in the ALs can be observed that are similar to phenotypes in Uzip mutants. It should be noted that, Canton-S flies were used as a control. Sometimes P-element insertions can cause severe phenotypes without binding to an UAS sequence. Thus, this experiment should be repeated several times with more control experiments to make a clear statement.

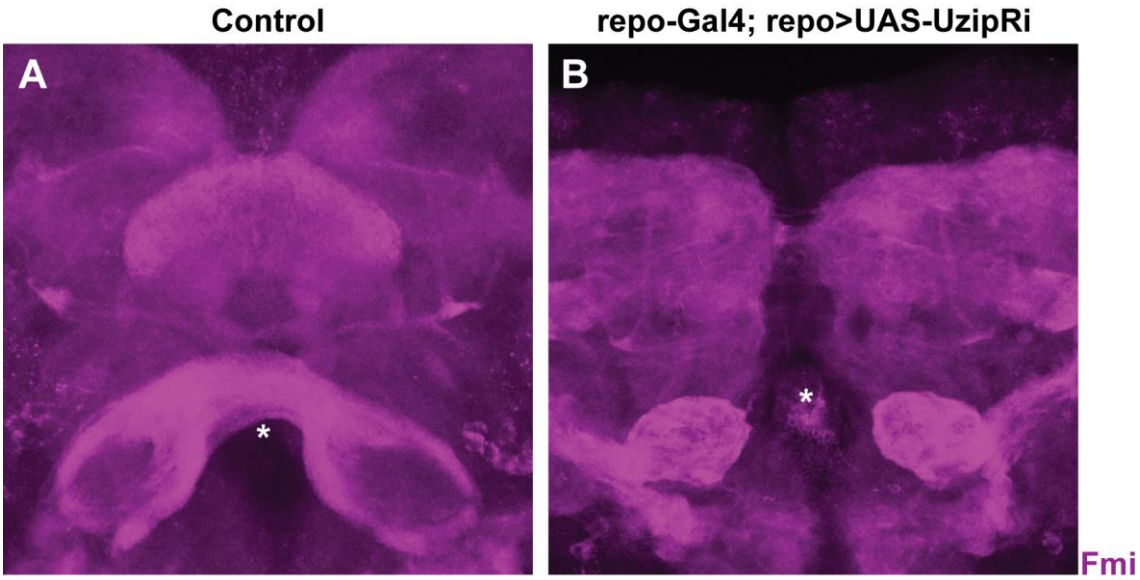

Figure 4.32. Uzip downregulation in glia using a double repo driver causes midline-crossing phenotypes. 36h APF pupal brains are shown. Flamingo was used to detect OSN commissure. Asterisks show the commissure. (A) In wild-type flies, commissure forms properly. (B) Downregulation of Uzip with the double repo driver, no commissure formation was observed (n=1/3).

4.6.1.4. Uzip downregulation in neurons. While Uzip did not appear to be expressed in neurons to evaluate a possible function of Uzip in neurons Uzip was downregulated specifically using the neuron-specific driver *elav*-Gal4. Formation of the commissure and possible axonal targeting phenotypes were evaluated using OR42b reporter line.

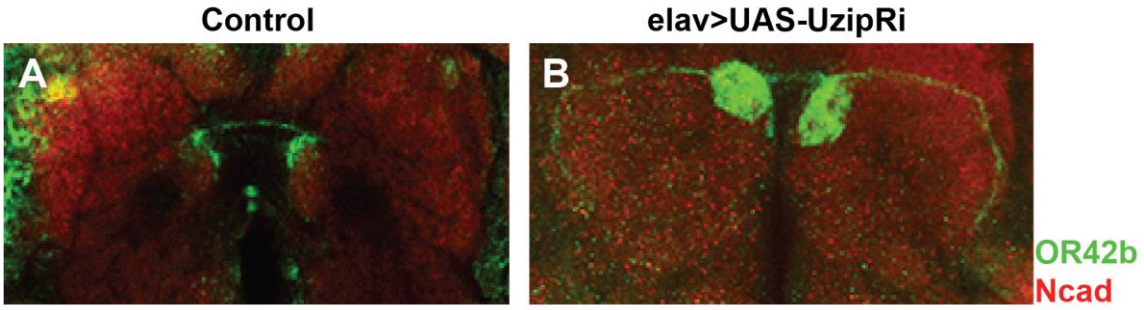

Figure 4.33. Downregulation of Uzip in neurons does not cause OSN targeting defects. *Elav*-Gal4 driver was used to downregulate Uzip expression specifically in neurons. Both in (A) Control and (B) Elav knockdown flies, OR42b neurons cross the midline. showAnti-GFP antibody (green) was used to visualize OR42b neuronal projections and Ncad (red) was used to label the ALs.

4.6.1.5. Uzip downregulation in TIFR glia. Uzip was shown to have a role in TIFR structure formation (Results section 4.5). Here we investigated, whether downregulation of Uzip in TIFR glia will effect the formation of OSN commissure or not.

For this purpose, a TIFR glia-specific driver was used to downregulate Uzip expression. *OR42b*-CD8::GFP construct was used in order to trace axonal projections of OR42b neurons. As shown in Figure 4.34 OSNs can cross the midline without a major defect, however the presence of minor defects cannot be excluded fully.

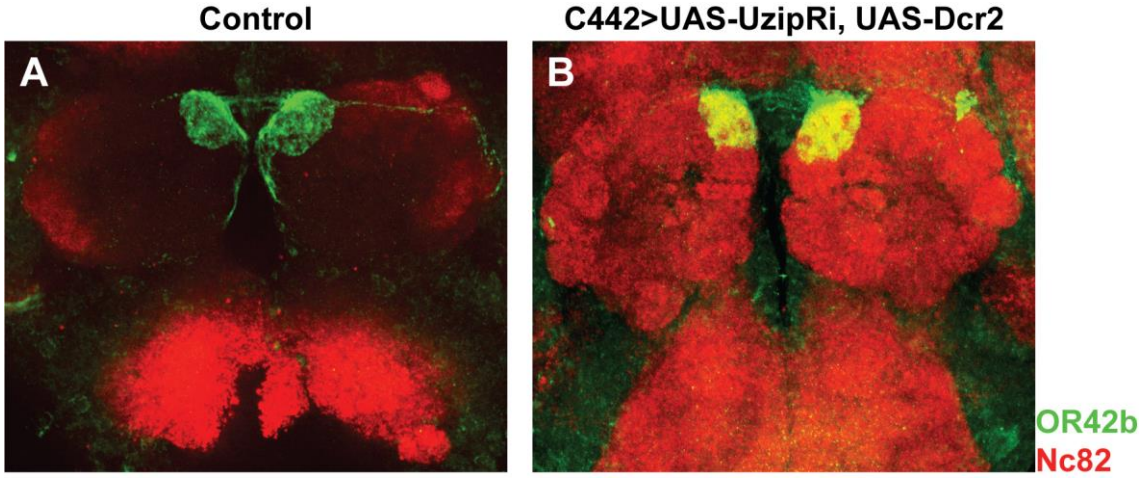

Figure 4.34: TIFR glia-specific downregulation of Uzip does not cause any axon guidance phenotypes in the AL. Both in (A) wildtype and (B) Uzip downregulation background, OSNs form a commissure (n=7). Minor axon guidance defects cannot be excluded. GFP was used to detect OR42b axons and Ncad was used to label the ALs.

4.6.2. Overexpression Experiments of Uzip

4.6.2.1. Ubiquitous overexpression of Uzip. According to Ding *et al.*, (2011), overexpression of Uzip in neurons results in clustering of neurons. In this study, we used the UAS-Uzip construct to overexpress Uzip using cell-type specific drivers.

First, overexpession of Uzip was performed with the ubiquitous driver *ubi*-Gal4 to see if a global increase in Uzip levels will cause any axonal defects. At 36h APF, pupal brains of WT and *ubi*-Gal4 > UAS-Uzip were stained with Flamingo antibody (Figure

4.35). OSNs were able to form a commissure between the two ALs. However, the thickness of the commissure appeared to be thinner in ubiquitious overexpression of Uzip. Additionally, some of the OSNs were stalled in the periphery of the ALs when Uzip was overexpressed. In order to make a clear statement however, a deeper analysis is required.

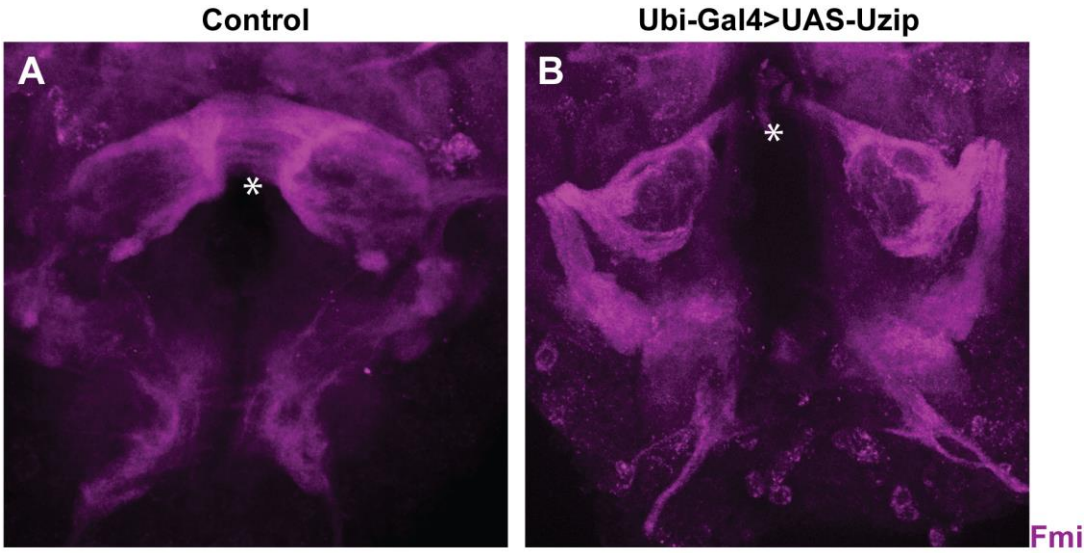

Figure 4.35. Ubiquitious overexpression of Uzip does not cause severe axon guidance phenotypes. (A) Control and (B) ubiquitous overexpression of Uzip are shown. Anti-Fmi antibody (magenta) was used to visualize the OSNs commissure shown with asterisk. At 36h APF, OSNs were able to cross the midline in transgenic flies overexpressing Uzip under *ubi*-Gal4 driver (n=4).

4.6.2.2. Uzip overexpression in glial cells. To understand the function of Uzip in glia, the glia-specific driver repo-Gal4 was used for overexpression. To enhance the overexpression effect two copies of the repo driver (double repo) was used to overexpress Uzip. *Repo*-Gal4 carrying flies were used as an experimental control. The OR42b-CD8GFP construct was used in this background to trace axonal projections of a single OR subtype in adult brains stained for GFP. Nc82 was used to visualize the whole glomerular pattern. Figure 4.36 shows that Uzip overexpression in glia does not have an detectable effect on OSNs commissure formation. In double repo > UAS-Uzip flies the commissure appears to be weaker as compared to the control. This observation needs to be validated further to make sure this is a real phenotype.

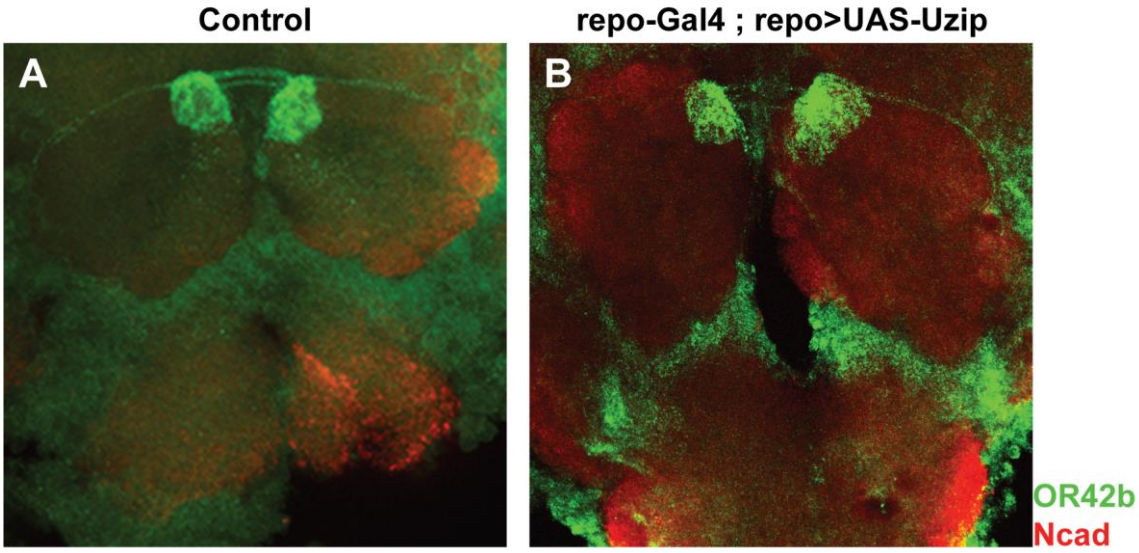

Figure 4.36. Overexpression of Uzip in glial cells using double *repo*-Gal4. Uzip was overexpressed in glial cells and axonal projections of OR42b neurons were investigated. GFP antibody (green) was used to show projections of OR42b neurons and Nc82 (red) labels the ALs. Both in the control and Uzip overexpression in glia, OSNs were able to form a commissure.

4.6.2.3. Uzip overexpression in TIFR glia. In the *Uzip* null mutants, TIFR was not formed properly, which indicated that Uzip expression is essential for TIFR formation. Here, we speculated if Uzip overexpression in TIFR glia will effect the structure of TIFR, thereby preventing OSNs to form commissure.

Uzip was overexpressed in TIFR glia by using the *c442*- Gal4 driver and the UAS-Uzip overexpression construct. At early pupal stages, wild type and *c442* > Uzip brains were stained with GFP and Flamingo. Figure 4.37 shows that the overexpression of Uzip in TIFR glia was not affecting commissure formation by OSNs (n=4). As flies were dissected earlier than 36 h APF, the commissure appears less thick than in earlier experiments. It seems like overexpression of Uzip in TIFR is not causing morphological defects which will effect OSN commissure.

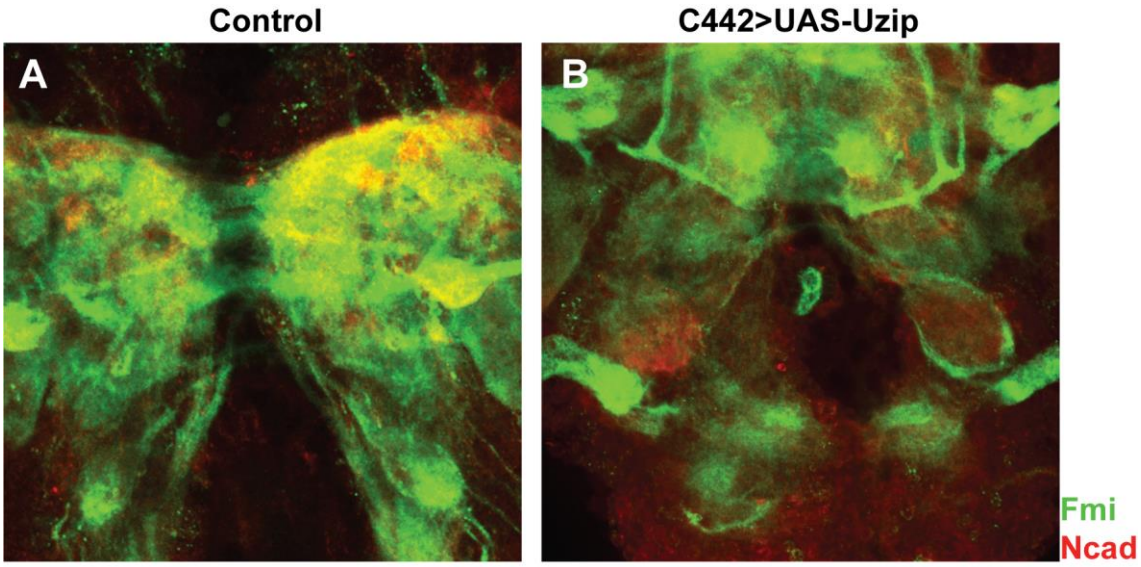

Figure 4.37. Overexpression of Uzip in TIFR glia does not cause defects in commissure formation. Pupal brains at 25-30h APF were stained with Flamingo to visualize all ORNs and Ncad to visualize all neuropil. (A) Wild type and (B) Uzip overexpression in TIFR glia was compared. In both cases the commissure can be observed (n=4). Arrows point to the commissure between the developing ALs.

4.6.3. Rescue Experiments

In the *Uzip* null mutants, where all coding sequence of Uzip was deleted, midline commissure formed by OSNs is missing. In order to be sure that this phenotype was caused by lack of Uzip expression, a copy of full uzip sequence was introduced into the genome of the null *Uzip* mutants. For this purpose, Uzip BAC construct and Uzip::mCherry constucts were introduced into the null *Uzip* mutant phenotype.

In order to identify the subtype of cells in which Uzip expression is necessary for midline crossing of OSNs, cell type specific molecular rescue experiments were conducted. In *Uzip* null mutant background, Uzip was overexpressed exclusively in subtype of cells by using cell-type specific Gal4 lines. We further investiaged the cell types, where Uzip expression recovers the commissure phenotype of *Uzip* null mutants.

4.6.3.1. Uzip mutants rescued with BAC construct. A transgenic fly line carrying a BAC construct with the genomic region of Uzip (with its upstream and downstream regulatory regions) was generated and used as a rescue construct (Section 4.2.). If the construct contains all the necessary regulatory sites we expect that Uzip will be expressed in its endogenous pattern and would be able to compensate for the loss of Uzip protein in Uzip mutants. In order to investigate if Uzip BAC expressing flies rescue the Uzip null mutant phenotype, a rescue experiment was performed by bringing the Uzip (BAC) construct into the Uzip mutant background. The OR47a-GFP line was used to evaluate if the axons can cross to the contralateral side after providing wt Uzip. Adult brains were co-stained with GFP and Nc82 antibodies (Figure 4.38). In Uzip mutants, no OSN commissure was formed between the two ALs as previously shown, but flies carrying one copy/two copies of the Uzip (BAC) construct rescues commissure phenotype. This indicates that Uzip (BAC) construct in the third chromosome is functional and has all necessary regulatory elements for Uzip expression. It shows also that the mutant phenotype is really only caused by the lack of Uzip as it is rescued by supplying back Uzip.

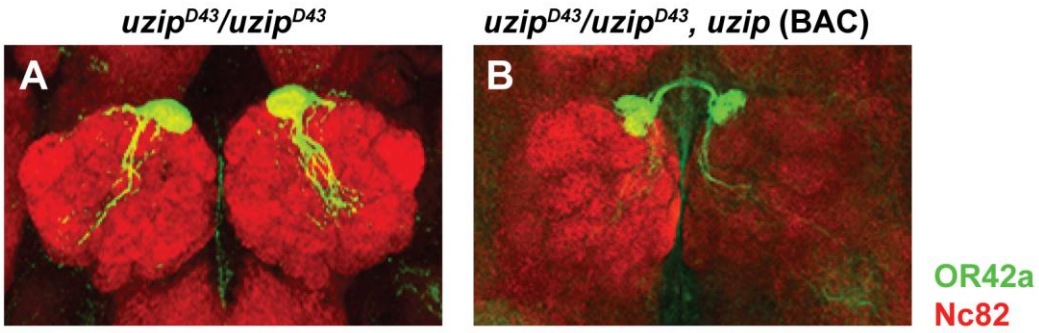

Figure 4.38. Uzip (BAC) expressing flies rescue the Uzip null mutant phenotypes. In Uzip null mutants without Uzip (BAC), OR47a neurons cannot cross the midline. Flies expressing Uzip (BAC) in Uzip null mutants rescued the midline crossing phenotype of OR47a neurons (n=4). GFP antibody (green) was used to visualize OR47a neurons and Nc82 antibody (red) shows the glomerular pattern.

4.6.3.2. Uzip mutant phenotypes can be rescued with Uzip::mCherry construct. In this study, a genomic Uzip::mCherry transgenic line was generated and used in determining endogenous expression of Uzip. This BAC transgenic line is a modified version of the

BAC construct used in results section 4.7.3.1. To validate that the fusion of the mCherry protein to the Uzip protein does not affect its functionality, this transgenic line was also used in rescue experiments. The projections of OR47b neurons were investigated in *Uzip* null mutant background in the presence of Uzip::mCherry. For the control experiment, OR47b neurons projections were examined in *Uzip* null mutant background without Uzip::mCherry. In $Uzip^{D43}$ homozygous mutants, OR47b neurons cannot cross the midline, however flies with one copy of Uzip::mCherry displayed commissure of OR47b neurons (Figure 4.39). This data proves that Uzip::mCherry line is functional and makes us also more confident about the localization studies performed under Results section 4.3.

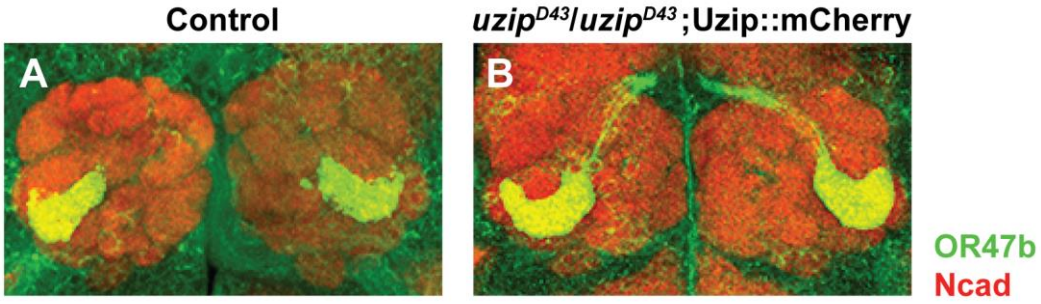

Figure 4.39. Uzip::mCherry is functional and rescues Uzip null mutant phenotypes. OR47b reporter line was used to evaluate the midline crossing phenotype. (A) $Uzip^{D43}$ homozygous mutant, (B) $Uzip^{D43}$ homozygous mutant with Uzip::mCherry expression adult brains were analyzed. (A) OR47b neurons cannot cross the midline. (B) OR47b neurons can project to contralateral glomerulus.

4.6.3.3. TIFR glia-specific rescue of Uzip. The broad expression of Uzip in many glial subtypes makes it difficult to pinpoint in which cells it is required and how its loss leads to the loss of commissure phenotype. Since the loss of other genes (Nrg and Drl) expressed in TIFR glia have been shown to give phenotypes to the phenotypes we are observing in Uzip mutants we hypothesized that Uzip functions in TIFR glia. To this end we have been trying to manipulate expression levels of Uzip in these glia to prove this hypothesis. In a further attempt we aimed at rescuing the Uzip mutant phenotype by providing back Uzip only in TIFR glia using a TIFR-specific driver and UAS-Uzip. A reporter line for OR46a was used to evaluate the resulting phenotypes.

In 2 out of 10 samples, OR46a neurons were able to cross the midline when Uzip was overexpressed in TIFR glia by one copy of UAS-Uzip. (Figure 4.40B and B'). On the other hand, OR46a neurons could not target properly to their glomeruli, which indicates that Uzip expression in TIFR glia is sufficient for midline crossing but not for axonal targeting.In the other 8 samples, OSNs could not cross the midline, which might be explanied by low levels of Uzip expression. In order to show this is the fact, two copies of UAS-Uzip might be used for the rescue experiments.

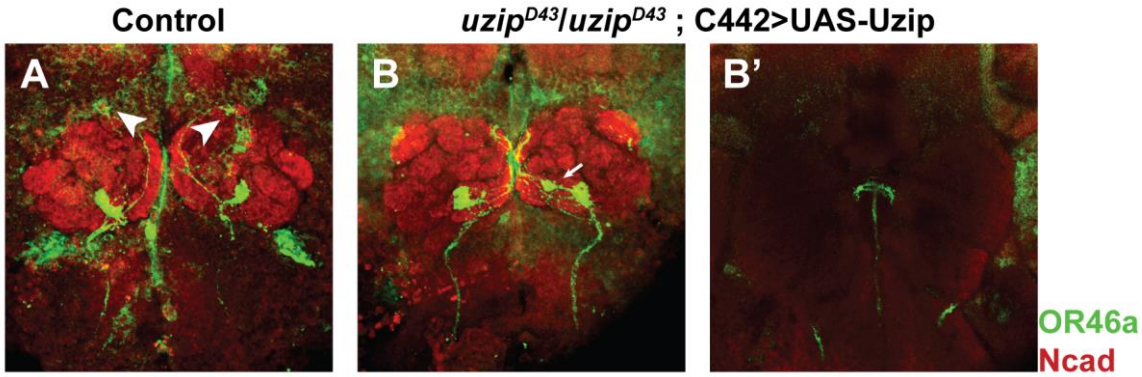

Figure 4.40. Overexpression of Uzip in TIFR glia rescues midline crossing of OR46a neurons in *Uzip*^{D43} homozygous background. (A) In *Uzip* null mutants, OR46a neurons cannot cross the midline and display misprojection defects (n=8/10). (B) Overexpression in TIFR glia do not rescue mistargeting phenotypes of OR46a neurons. (B') Overexpression of Uzip in TIFR glia rescues the commissure phenotype seen in *Uzip* null mutants.

4.6.3.4. Ubiquitous rescue without glia. By looking at the expression pattern analysis (Section 4.1 - 4.3) and glia specific Uzip downregulation experiments (Figure 4.32), it can be stated that Uzip is expressed in glia and this expression is necessary for neuronal midline crossing. The midline crossing phenotype of the *Uzip* null mutants is expected to be rescued by ubiquitous expression of Uzip. In order to show that Uzip expression in glia is enough and necessary for OSN commissure formation, a reverse experiment was set. We decided to try rescuing the *Uzip* null mutant phenotype by overexpressing Uzip in all cells but glia. To broadly overexpress Uzip, we used a Gal4 line in which the Gal4 expression is directed by promoter of *daughterless* (*da*), which is a ubiquitously expressed transcription

factor. Additionally, we supressed the Uzip expression in glia by using a *repo*-Gal80, which represses the GAL4 activity specifically in glia cells.

In Figure 4.36, Flamingo staining showed that in the *Uzip* null mutants overexpressing Uzip with da-Gal4 and suprressing Uzip overexpression specifically in glia cells rescued the commissure phenotype (n=2), whereas without UAS-Uzip OSN commissure was not formed (n=1). These results is unexpected since Uzip expression and function in *Drosophila* was shown before. One problem could be the suppression efficiency of repo-Gal80 line. In this experiment, only one copy of repo-Gal80 was used and Gal80 expression may be was not enough to repress Uzip expression in glia cells. This might explained to see a thinner commissure comparing with wild type flies. This experiement should be repeated by trying glia suppression with two copies of *repo*-Gal80. Moreover, overexpression in glia should be tried to have a more precise statement.

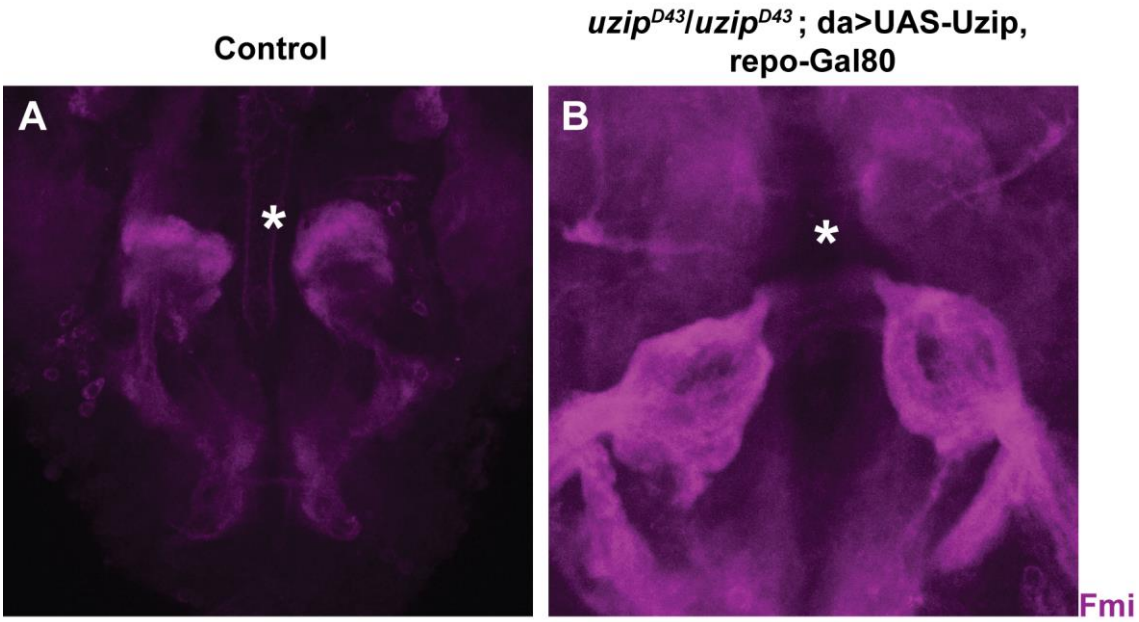

Figure 4.41. Overexpression of Uzip in all cells but glia, rescues commissure phenotype seen in Uzip mutants. 36h APF pupae brains were stained with Flamingo antibody. (A) OSNs cannot cross the midline although overexpression of Uzip in all cells but not glia (B) rescues midline crossing phenotype (n=2). Asterisks show the commissure.

4.6.4. Generation of Truncated Uzip Proteins

When Uzip was identified in our lab and we tried to identify homologous proteins and protein domains no matches were found in any of the databases. The recent publication by brought some insight into the possible function of Uzip as a cell adhesion molecule (Ding *et al.*, 2011). Similar to our own investigations they showed that Uzip is conserved among insects, but no vertebrate homologs exist. They identified a highly conserved region between amino acids 42 and 379 and show that deletion within this domain halts the cell adhesion ability of Uzip (homophilic binding ability), while deletion between amino acids 401 and 450 amino acids does not alter its cell adhesion property dramatically. Additionally, the sequence of amino acid 452 was predicted to have a GPI-anchor modification site and was shown to be essential for its cell adhesion ability (Ding *et al*., 2011).

To get more insight into the functional domains, we aimed to create different truncated versions of Uzip and test these *in vivo*. For this purpose, Swiss Model Protein Modeling Database was used to identify possible domains of Uzip and it predicted four different possible domains. These domains were separated at 130, 245 and 353 amino acids of Uzip. Moreover, three coding exons of Uzip are separated from 237 and 353 amino acids. We combined this information together and finally decided on creating 3 truncated Uzip protein constructs, which are shown in Figure 4.42.

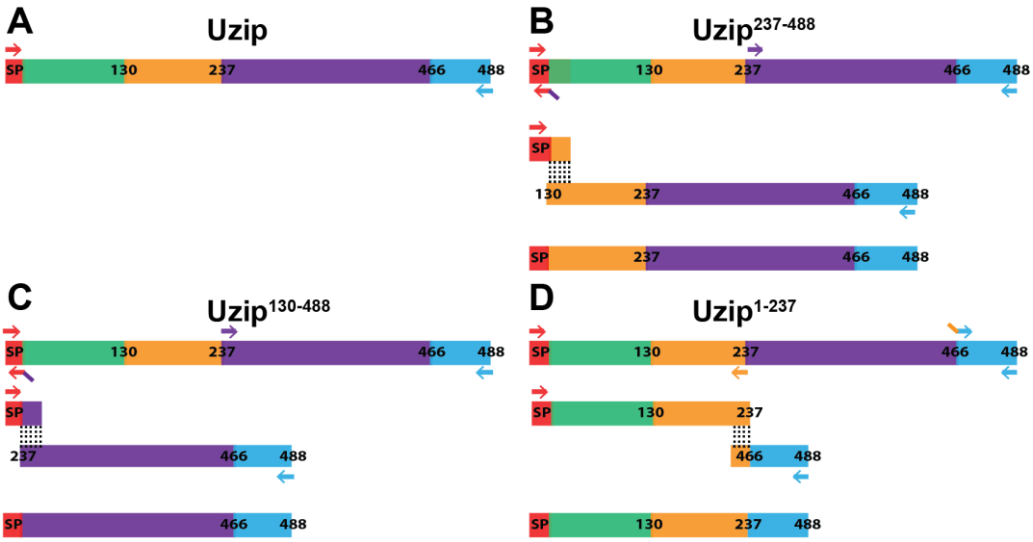

Figure 4.42. Generation of Uzip constructs are depicted. (SP) Signal peptide, amino acid numbers were shown inside the template. Arrows illustrate primer pairs and arrowtails showing the homology sequence of the primers. (A) Uzip fragment, (B) Uzip$^{237-488}$, (C) Uzip$^{130-488}$, and (D) Uzip$^{1-237}$ versions are shown. Uzip was created with a single PCR reaction by using Uzip F and UzipR primers.

SD09738 Expression Sequence Tag (EST) was used as a template to generate full length and also truncated Uzip constructs. The primers designed for the generation of truncated Uzip constructs are shown in section Material and Methods section 3.2.5, Uzip F and Uzip R primer were used to generate the full length Uzip fragment. In all constructs that were generated the signal peptide sequence was included.

For each truncated version one short and one long DNA fragment were amplified. The short fragments of Uzip$^{130-488}$, Uzip$^{237-488}$ and Uzip$^{1-237}$ were amplified with primers Uzip-F/SP-130-R, Uzip-SP-237/Uzip-F, and the TM-237-F/Uzip-R, and the PCR amplification results are shown in Figure 4.43A in lanes 1, 2, and 3, respectively.

The long fragments of Uzip$^{130-488}$, Uzip$^{237-488}$, and Uzip$^{1-237}$ were amplified with Uzip-130-F/Uzip-R, Uzip-237-F/Uzip-R, and Uzip-F/Uzip-237-R, and PCR amplification results are shown in Figure 4.43B in lanes 4, 5, and 6, respectively.

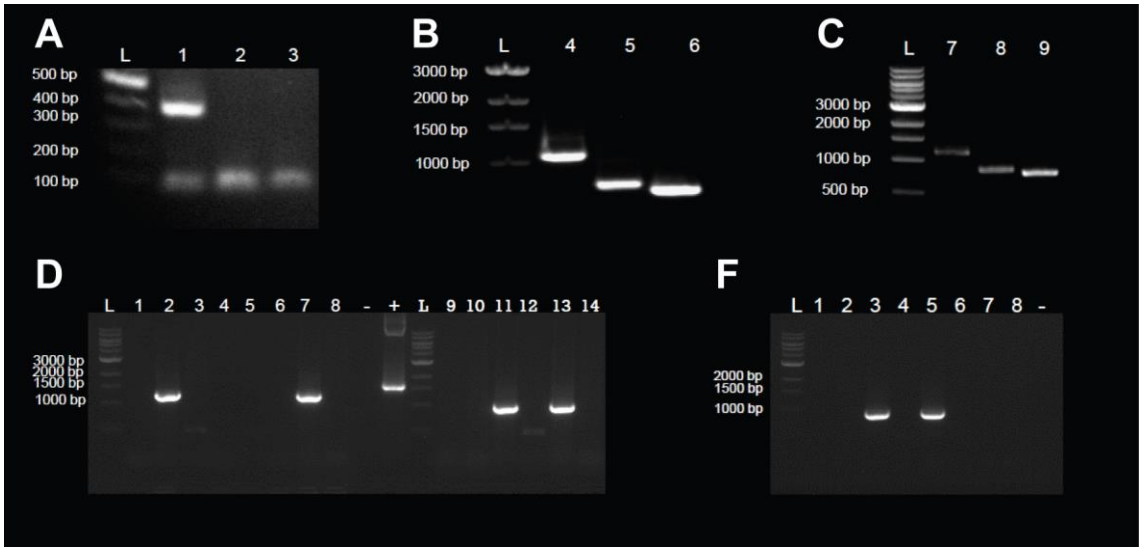

Figure 4.43. Generation of truncated Uzip constructs. (A) Short fragments of Uzip$^{130\text{-}488}$, Uzip$^{237\text{-}488}$, and Uzip$^{1\text{-}237}$ are shown in lanes 1, 2, and 3, respectively. (B) Long PCR fragments of Uzip$^{130\text{-}488}$, Uzip$^{237\text{-}488}$, and Uzip$^{1\text{-}237}$ are shown. (C) Short and long PCR amplicons to obtain the final Uzip$^{130\text{-}488}$, Uzip$^{237\text{-}488}$ and Uzip$^{1\text{-}237}$ fragments using primers Uzip F and Uzip R and the resulting PCR fragments are shown.

Finally, the short and the long fragments of each construct were amplified using Uzip-F and Uzip-R primer pair to generate the final constructs using the previous PCR products as templates (Figure 4.43C). Lanes 7, 8, and 9 lanes show the final PCR reaction products of Uzip$^{130\text{-}488}$, Uzip$^{237\text{-}488}$, and Uzip$^{1\text{-}237}$ fragments.

The amplified fragments were cloned into pGEM-T-Easy (Promega) and sequenced to select a mutation-free construct. Such colonies were further processed to generate the final construct by ligating the amplified DNA fragments into the P-element vector pUASt-*attB* vector. The correct ligation of the fragments into the vector was confirmed by colony PCR (Figure 4.43D, E). The vectors were injected into trangenic flies containing attP attachment site for site-specific integration and transgenic flies were generated.

The aim was to use these flies in specific rescue experiments and overexpression experiments. However, due to time restrictions we only used the ful length UAS construct.

4.7. Uzip Antibody

The expression and localization of Uzip have been studied in section 4.3. Obviously, the best was to show the localization of a protein is to generate a specific antibody. An antibody against Uzip was generated by Ece Terzioğlu-Kara (unpublished) in our group. Unfortunately, there was not enough time to perform localization studies using this antibody. Instead we used it in Western blotting experiments to visualize and quantitate expression levels of Uzip protein in various backgrounds.

Total protein extracts from adult flies were used in these experiments. To be able to compare the protein concentrations in different background these were measured using a Bradford Assay and the same amount of protein (60µg) was loaded for each sample.

Uzip has two isoforms, a membrane-bound form, which is 80kD and a secreted form, which is 65kD (Ding *et al.*, 2011), and thus these bands were expected on the blot. As shown in lane 1 in Figure 4.44 two bands corresponding to the expected bands can be observed. There are no bands in the lanes corresponding to the homozygous $Uzip^{D43}$ and $Uzip^{23}$ protein extract samples. Since the whole coding sequence of *uzip* is deleted in $Uzip^{D43}$, no bands were expected. However, $Uzip^{23}$ is a hypomorphic allele so it is expected to see weaker bands relative to the wild type.

The level of Uzip protein is highly elevated when the UAS-Uzip construct is driven by ubiquitously expressed Gal4. On the last lane Uzip:mCherry BAC line is observed. Those flies have there different Uzip proteins, two of which are endogenous forms transcribed from the original Uzip gene and one is the mCherry fusion protein. which is expected to be 108kD in size (See Figure 4.44).

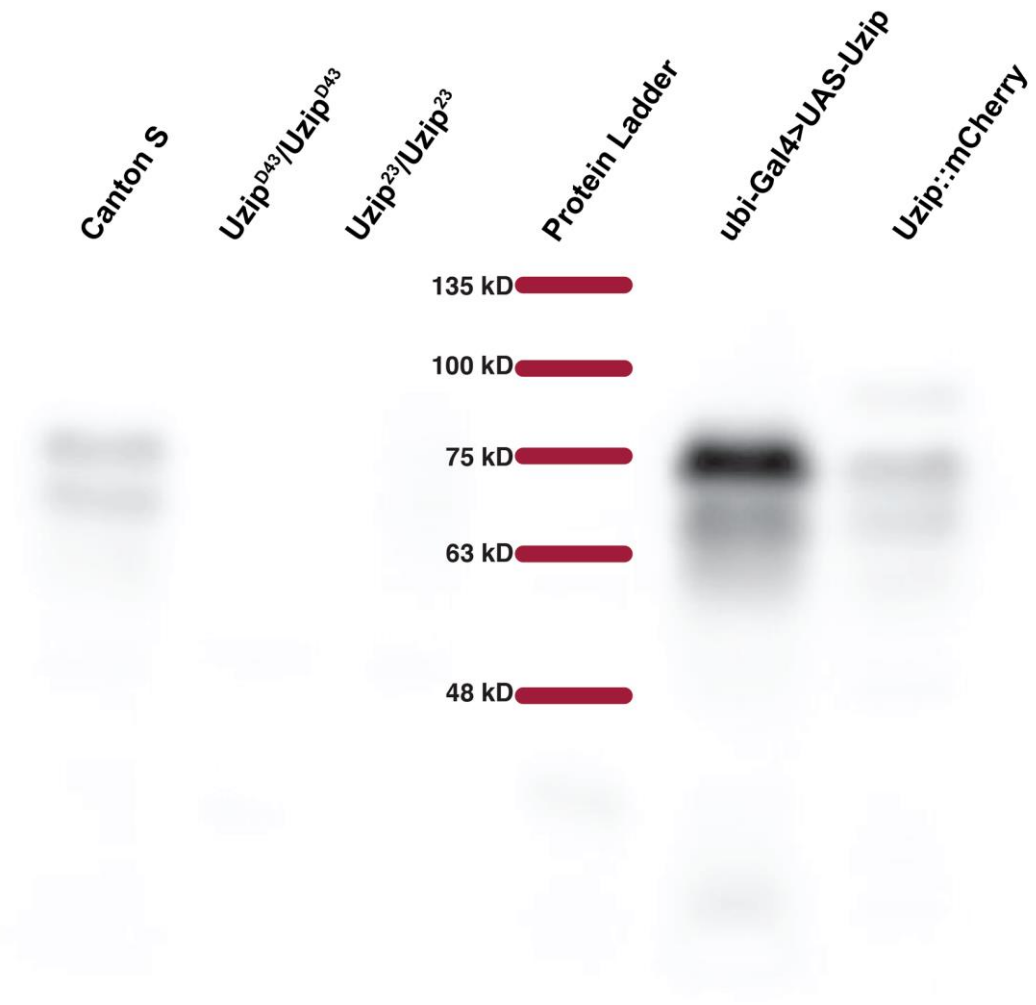

Figure 4.44. Western Blot analysis using Uzip antibody. Expression levels of Uzip protein were tested in flies with different genetic backgrounds. Two distinct bands were detected for Canton-S flies, whereas no band was observed for Uzip null and Uzip hypomorph mutants.

5. DISCUSSION

Perceiving and understanding chemical signals from the environment correctly are essential for an organism to find a carbon source, to mate, and to detect dangerous microorganisms. It is also essential for egg-laying. This depends on the proper detection of odorants in the periphery and the correct wiring of the OSNs that carry this information to higher order centers.

Olfactory cues in an environment are detected by OSNs in vertebrates and insects. In *Drosophila* two olfactory appendages, antenna and maxillary palp, represent the peripheral olfactory organs responsible for perceiving the signals. The surface of the antenna and maxillary palp are covered with sensilla that bear OSNs and supporting cells. Exclusively located on the 3rd segment of antenna, there are around 1200 OSNs, whereas the maxillary palp contains 120 OSNs.

OSNs project towards the brain to form proper connections. The olfactory system in general represents an exceptional specific wiring capacity, which is different from other sensory systems and thus the full logic is not understood yet. What is known is that each OSN expresses one of 60 OR genes encoding a single type of OR and together with other OSNs expressing the same OR projects its axons to a particular region in the AL called a glomerulus. The AL is composed of nearly 50 individual morphologically and also functionally subdivided units of these subunits (glomeruli). Within each glomerulus, one-to-one synaptic interactions between projection neuron dendrites and OSN axonal terminals occur. Additionally, GABAergic and cholinergic intrinsic local interneurons (LNs) are located around the AL to make specific synapses with OSNs, thereby regulating a cross-talk interaction between glomeruli (Sachse and Galizia, 2002; Ng *et al*., 2002). PNs transmit the olfactory signal to higher brain center such as MB and LH via 4 identified distinct tracts (Tanaka *et al*., 2008). In the calyx of the MB, PNs from different glomeruli make specific synapses with MB neurons (Kenyon cells) (Strausfeld *et al*., 2003). Furthermore, PNs from distinct glomeruli transmit the incoming signal to specific regions in the LH (Figure 5.1).

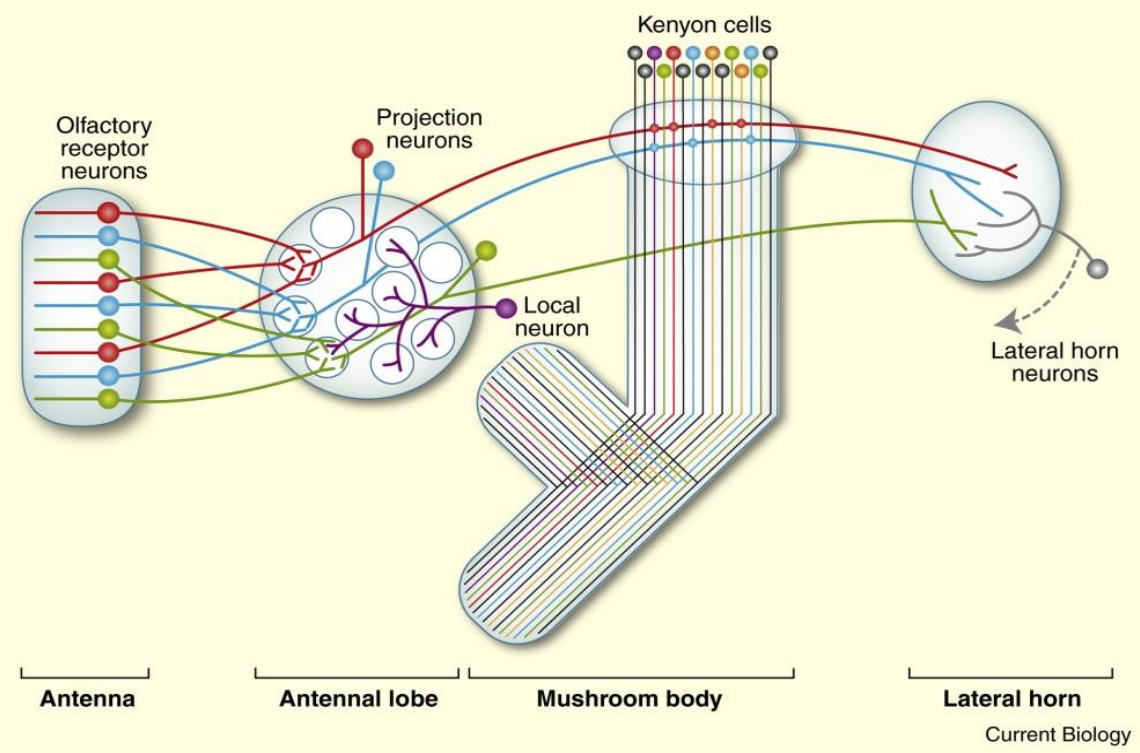

Figure 5.1. Wiring specificity in the *Drosophila* olfactory system is illustrated. Olfactory neurons expressing the same OR, project to a single glomerulus in the AL where they synapse with a single type of PN. Local neurons regulate the interaction among glomeruli by releasing neuropeptides such as GABA and acetycholine. PNs carry olfactory stimuli to higher brain centers, MB, and LH (taken from Masse *et al*., 2009)

It has been an intriguing subject for neuroscientist to identify the mechanisms that determine this complex neuronal wiring. While the ORs themselves have been implicated in being guidance receptors themselves in vertebrates this does not seem to be true for the *Drosophila* olfactory system. However, several transcription factors and cell surface molecules have been identified to play an essential role in proper guidance of OSNs in the olfactory system of *Drosophila*. Some of these molecules are highly conserved between vertebrates and insects.

Uzip is a cell adhesion molecule mainly expressed by longitudinal glia in embryonic stages (Ding *et al*., 2011). Uzip mutants together with either Wnt5 mutants or Ncad mutant displayed strong axon guidance phenotypes within the VNC. In our

laboratory, Uzip has been identified independently and investigated for its role in the assembly of the olfactory circuit and the mushroom body.

In a previous study in our laboratory Uzip expression was shown to have a glia-like expression pattern and Uzip is broadly expressed in the sensory appendages and the AL. In *uzip* null mutants, OSNs displayed axon guidance defects such as midline crossing, mistargeting, and axon stalling (Zülbahar, 2012).

In this study, the previous study by Zülbahar was extended, and I studied the expression pattern of Uzip using a novel tool I generated Uzip::mCherry). Moreover, we investigated the role of Uzip in axon guidance and proper targeting of OSNs within the AL by analyzing Uzip mutants in more detail. Additionally, I generated new tools to perform functional studies. I generated an overexpression line and truncated versions of Uzip and a BAC transgenic line that carries a rescue construct. Downregulation were done a new line generated at Janelia Farm and overexpression experiments were done using the line I have generated (UAS-Uzip). Additionally I performed genetic interaction experiments with a number of candidate interactors of Uzip.

5.1. Uzip is Mainly Expressed by Glial Cells and Non-Neuronal Cells

Enhancer trap line of Uzip (AC783-Gal4) was crossed with various reporter genes to identify the localization of Uzip-expressing cells. Formerly, glia-specific expression pattern of Uzip was observed in the adult brain (Zülbahar, 2012). Additionally, when the enhancer-trap line was crossed with a UAS-syt::GFP reporter line, a specific synaptic target was observed. Even though, a few candidates were tested, the glomerulus and the OSN subtype projecting there were not identified (Zülbahar, 2012).

In this study, we used the UAS-syt::RFP construct to analyze synaptic targeting of the Uzip enhancer-trap line. This allows the analysis of co-localization of the Uzip-positive glomerulus and OR neurons labeled with membrane-bound GFP. After a careful analysis of the glomerular pattern in the AL, OR2a was chosen as the best possible candidate. Analysis of adult brains showed that, Uzip-positive glomerulus was indeed DA4m, which

is targeted by OR2a neurons (see Figure 4.3). Suppressing the glial expression of syt::RFP using repo-Gal80 revelaed the presence of another previously unidentified glomerulus called VL1, which is the target of the Ionotropic Receptor 75d (IR75d) (Figure 4.3). The second glomerulus has not been observed before because of the high background caused by AL-associated glia that labelled the whole AL. Only the suppression of the signal coming from the glia allowed the uncovering of the second glomerulus. The significance of the specific labeling of these two glomeruli is not clear. It is also not known if this expression reflects the endogenous expression of Uzip. Nevertheless, this is a very interesting observation as there are, except for the ORs and IRs, no other genes that target glomeruli specifically. Thus, if the expression of Uzip in these glomeruli cannot be confirmed later the enhancer-trap line can be used as a tool to perform functional experiments in these glomeruli, if necessary.

Uzip expression was studied in the antenna and the maxillary palp by using the Uzip enhancer-trap line generated in our lab and a nuclear GFP reporter line (AC783-Gal4 > UAS-nGFP). Together with anti-GFP to detect the nucleus of Uzip expressing cells, anti-Repo and anti-Elav antibodies were used to identify uzip-expressing cells. Maxillary palp staining showed that most of the glial cells in the maxillary palp express Uzip. Also, Uzip expression was mainly seen in non-neuronal cells, which might be the supporting cells. These cells were not co-labeled, as no specific marker is known to label these cells. Moreover, the GFP signal was suppressed in glial cells, to determine if neurons express Uzip. Interestingly, Uzip expression was not detected in sensory neurons of the maxillary palp, which confirms a previous observation by Zülbahar (2012) (see Figure 4.5). Unfortunately, anti-Repo staining did not work for the antennal stainings, but anti-Elav showed a few co-localizations of Uzip-positive cells and neurons (Figure 4.6). Previously, it is shown that OR2a neurons project to same glomerulus with Uzip positive glomerulus. This result made us to check position of OR2a neurons in the antenna and compare with the location of Uzip positive neurons. OR2 neurons localize at the lateroventral region in the antenna, whereas Uzip positive neurons mostly localize at the dorsaventral side of the antenna. enhancer trap. While this experiment would need to be repeated and optimized a bit better, some co-localization with OR neurons is expected because of the staining of glomerular subsets in the AL.

An Uzip antibody was generated in a previous study (Ding *et al*., 2011). However, this antibody did not work in our hands. Thus, while trying to generate and Uzip antibody ourselves (Ece Terzioğlu-Kara, unpublished) we looked at alternative ways to observe endogenous Uzip expression and localization. An approach that has become popular in recent years is the generation of BAC transgenic lines, which contain the genomic region of the protein of interest with its regulatory regions and are genetically engineered and tagged with a label of interest. Previously, this technique was used in our lab to tag both versions of Uzip (secreted and GPI-anchored) by tagging from the N-terminal with Flag and HA tags. Unfortunately, the HA tag was not detected efficiently and caused high background when using anti-HA antibodies. Despite many optimization attempts this problem could not be solved (Zülbahar, 2012). Moreover, this construct was not able to rescue the mutant phenotype, which was a more serious problem (Zülbahar, 2012), which might have been caused because Uzip was tagged from the N-terminus.

Thus, in this study we used the BAC recombineering technique, to tag Uzip with mCherry from the C-terminal end in order to identify endogenous expression pattern. The mCherry protein was chosen for ease in using with follow-up experiments where OR genes are usually tagged by GFP. Unlike Flag and HA tagged of Uzip, tagging Uzip from its C terminal will avoid the detection of the secreted form of Uzip, which might by-the-way be another cause of the high background problem. Uzip::mCherry construct was made by inserting mCherry sequence before the last stop codon of Uzip via homologous recombination. Additionally, and the unmodified BAC clone was used to generate a transgenic rescue line in order to control that this construct contains the necessary regulatory regions and produces sufficient amounts of Uzip to rescue the mutant phenotype.

The Uzip::mCherry construct was used in immunohistochemisty experiments to determine the endogenous expression pattern of Uzip. Moreover, a rescue experiment was performed to prove the functionality of Uzip, since tagging proteins with reporters might disrupt the function the protein of interest. Both BAC and Uzip::mCherry constructs rescue midline crossing of OSNs observed in Uzip null mutant flies (see Figure 4.36 and 4.35).

These data also indicate that the BAC construct contains all necessary regulatory regions of Uzip.

The localization of Uzip::mCherry in adult brains demonstrates a pattern of expression that is reminiscent of ensheathing glia, which surround the ALs, MB, SOG, and antennal nerve, which carries the projections of antennal neurons. Additionally, high level of Uzip expression was detected in the compartments of the central complex, insulin-producing cells, and also in the optic lobe (see Figure 4.10). Furthermore, Uzip expression was examined both in the maxillary palp and the 3rd segment of antenna. Since the antenna and the maxillary palp contain a thick cuticle antibody penetration was a major problem in these stainings and were optimized as described in Section 3.3.1.3. Initially the maxillary palp and the antenna of 96h APF Uzip::mCherry transgenic lines were examined. Figure 4.11 and 4.12 show the expression pattern of Uzip in the maxillary palp and antenna. Uzip expression was observed in the main fascicles of the antenna and the maxillary palp, where glial nuclei are localized. Additionally, Uzip expression was detected around each neural nucleus and on the connections of each neuron to the main fascicles. These data indicate that Uzip might be expressed both by neurons and/or glia cells surrounding the axonal bundles. Furthermore, glial membranes in the antenna and the maxillary palp were visualized by expressing membrane-bound GFP under glia-specific driver (*repo*-Gal4) control. Figure 4.13 and Figure 4.14 show the expression pattern of Uzip in the maxillary palp and antenna, respectively. Uzip expression was detected in the region of glial protrusions and also around the glial nuclei, which might reflect the expression of Uzip in endoplasmic reticulum. This data suggested that glial cells in the sensory organs of *Drosophila* produced endogenous Uzip mainly.

Two main types of glia are known in the antenna of *Drosophila*, namely GH146 and Mz317 glia (Sen *et al*., 2005). GH146 glia directly wrap around OSN bundles, whereas Mz317 glia create a peripheral layer surrounding both GH146 glia and OSNs (Figure 5.2). In order to identify which glial subtype expresses Uzip in the sensory appendages of *Drosophila*, the Uzip::mCherry line was crossed with GH146 and Mz317 glia reporters, and maxillary palp and antenna staining was performed.

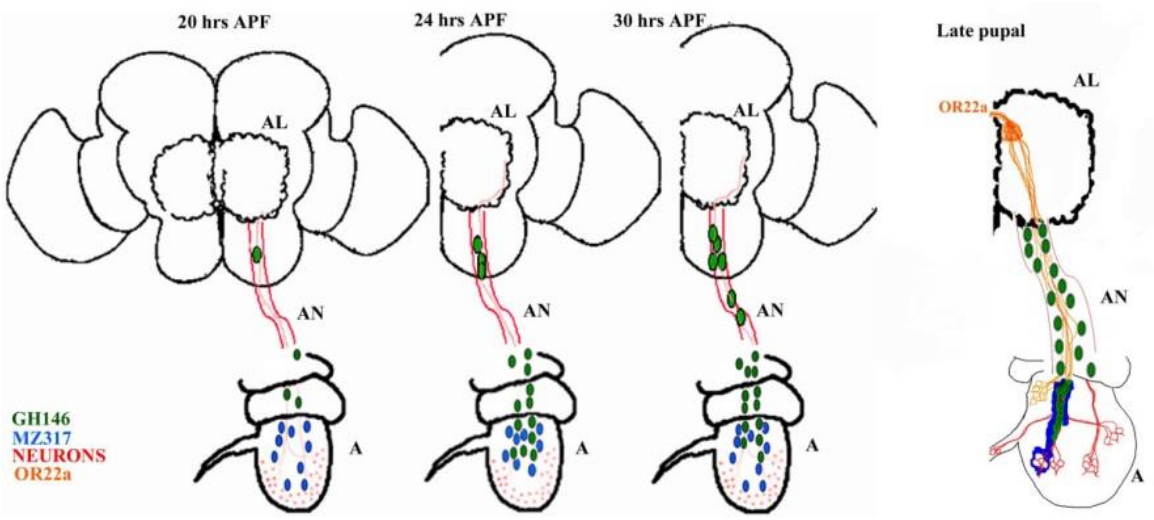

Figure 5.2. Antenna development in different pupal stages is illustrated. There are two types of glia in the antenna, namely GH146 and Mz317 glia. GH146 glia migrates from the AL to antenna throughout development and ensheaths the axon bundles of OSNs. Mz317 glia form a peripheral layer by wrapping the cell bodies of sensory cells and GH146 glia (taken from Sen *et al*., 2005).

Antenna stainings of GH146 glia did not work whereas the maxillary palp stainings showed some overlap of Uzip expression with the membrane of GH146 glia. A more detailed analysis needs to be performed to see if Uzip is really localizing on the membranes of GH146 glia. Confocal images with very short step size and 3D imaging could be used for this purpose. Additionally, investigation of antennae at earlier stages could show whether GH146 glia express Uzip or not, since before 20 h APF GH146 glia were not present in the 3rd segment of antenna. Additionally, investigating the expression pattern of Uzip in antennal nerve and labial nerve at different stages might provide a better understanding about the cell-type specific expression and function of Uzip in the development of olfactory sensory system.

Additionally, the maxillary palps and antennas of Mz317 > CD8::GFP, Uzip::mCherry expressing transgenic flies were examined. In order to overcome antibody penetration problem during antennal stainings, this time 0.14 µm sections through the antenna and maxillary palp were taken using a cryostat. These sections were stained with anti-Futsch, anti-GFP, and anti-Dsred antibodies. However, maxillary palp sections did not work properly due to the small size of the maxillary palp. In Figure 4.16 a very close

expression pattern between OSNs membranes and Uzip was observed. Moreover, membranes of Mz317 glia appear to surround the OSNs and the Uzip signal. Uzip expression was mainly observed between Mz317 and Futsch staining which labels the intracellular compartments of OSN membranes in the antenna. These data suggest that, Uzip might be expressed by sensory neurons of the antenna and GH146 glia.

5.2. Uzip Levels Determine Midline Crossing

In Uzip null mutants antennal and maxillary palp OSNs cannot cross the midline and maxillary palp OSNs have additional axon guidance phenotypes as axon stalling and mistargeting (Zülbahar, 2012).

In this study, we examined axons of both antennal OSNs and the maxillary palp OSNs in Uzip hypomorphic mutants. In the maxillary palp, axons of OR59c neurons were stalled in the SOG region whereas OR46a neurons were able to reach the AL, but always showed mistargeting phenotypes. Moreover, antennal OSNs were invesitaged in this study (OR47a and OR47b) showed only midline crossing phenotype in Uzip hypomorphic mutant background. In a few brains, a very thin commissure between the two ALs was observed suggesting that even low levels of Uzip might be enough for midline crossing of OSNs.

5.3. Uzip Has a Role in TIFR Formation

Glia cells play an important role in the organization of both the central and the peripheral nervous system by guiding neurons to their final targets. In *Drosophila* a distinct type of glial cell population was identified in the interhemispheric junction of 3rd instar larvae, called the TIFR glia (Simon *et al*., 1998). TIFR glia form a ring-like structure with four distinct canals between 25h and 48h APF. A transient role of this glia was shown to be essential for midline crossing, since cell-type specific ablation of TIFR glia using c442-Gal4 line resulted in OSNs to get stuck in the ALs without forming a commissure (Chen and Hing 2008), very similar to the phenotypes that were observed in Uzip mutants.

Moreover, Nrg, a L1-type cell adhesion molecule, was shown to affect the glial morphogenesis of TIFR glia. In Nrg^{849} mutants, the homophilic binding affinity of Nrg is lost and no midline commissure of OSNs was observed (Chen and Hing, 2008).

36h APF pupal brains were stained with anti-Flamingo antibody to visualize commissure formation in both *Uzip* null mutant background and to compare it to wild type. In the mutant background no commissure was observed and also we noticed that the structure of the central complex was disrupted as in Nrg^{849} mutants (see Figure 4.20). These data indicate a possible relation of Uzip and TIFR glia. In the present study, we questioned if *uzip* mutants cause similar morphological defects as observed in Nrg^{849} mutants in the formation of the TIFR structure. In order to investigate this hypothesis, the TIFR structure was examined in both $Uzip^{D43}$ homozygous and heterozygous mutant backgrounds. The *c442*-Gal4 line was crossed with UAS-CD8::GFP reporter line to visualize the TIFR structure. In Figure 4.21, anterior and sagittal views of the TIFR structure are shown. In *uzip* null mutans the TIFR morphology was clearly disrupted, indicating that Uzip is necessary to establish the proper morphology of the TIFR glia structure. Additionally, in one case, an interesting axon guidance phenotype was seen (Figure 4.22C). In *uzip* null mutant background OSNs projecting to the left antennal lobe were mistargeted to the interhemispheric space at the dorsal side of the pupal brain. Moreover, while the TIFR structure was totally disrupted in this case OSNs from one side of the brain appeared to interact with this disrupted TIFR. So, clearly a correctly developed TIFR structure is necessary for the contralateral targeting of OSNs.

In a more detailed analysis (Figure 4.23) we were able to show that the canals that are a hallmark of the TIFR glia cannot be identified in *uzip* null mutants and the structure is disorganized. Even though, these results indicate the certain role of Uzip in establishing TIFR morphology, further investigation should be done with a higher sample size. Obviously, the question how Uzip leads to a proper establishment of TIFR glia morphology remains an open question.

5.4. Uzip is Interacting Neither with Nrg Nor With Drl in The Olfactory System Development of *Drosophila*

Uzip was shown to genetically interact with Wnt5 and Ncad during embryonic development (Ding *et al*., 2011), but other interactions of Uzip remain to be elucidated. Çağrı Çevrim in our lab showed the genetic interaction of both Nrg and Derailed (Drl) with Uzip in the development of MB (unpublished data). Transheterozygous mutants of $Uzip^{D43}$ and Nrg^{849} cause missing lobe phenotypes and transheterozygous mutants of $Uzip^{D43}$ and Drl^{exc21} cause beta lobe fusion phenotypes in the MB (Çağrı Çevrim, unpublished data).

Derailed (Drl) is a receptor tyrosine kinase that regulates Wnt5 signaling during development of the AL (Yao *et al*., 2007). Moreover, Nrg is a cell adhesion molecule shown to be crucial for TIFR structure formation and OSN midline crossing. Both of these genes are important for formation of antennal lobe and they are expressed by both neurons and glia. Thus, these proteins were considered strong candidates as interacting partners for Uzip. Because of these specific reasons, the genetic interaction between Uzip and Drl as well as Uzip and Nrg were investigated. Different OSN subtypes were crossed into the transheterozygous mutant backgrounds of $Uzip^{D43}$ either with Nrg^{849} or Drl^{exc21} and the behaviour of the axons was analyzed. In contrast to phenotypes observed in the MB, no axonal defects were seen (see Figure 4.24, 4.26 and 4.25). These results indicate that Uzip and Nrg might act in parallel in the establishment of the TIFR structure and these two proteins although present in the same cells do not interact with each other.

5.5. Loss of Function Experiments

In order to investigate in which cells Uzip function is required Uzip was downregulated in a cell-type specific manner using specific drivers. Preliminary experiments performed by Selen Zülbahar in our lab showed that the UAS-UzipRNAi line generated by Ding *et al*., 2011 was not downregulating protein levels of Uzip sufficiently (Zülbahar, 2012). Recent studies performed by Çağrı Çevrim in our laboratory showed that MB phenotypes could be obtained using an UzipRNAi line generated by the Transgenic

RNAi Project (TRiP) at Janelia Farm (unpublished). Thus, this line was used in this study to repeat the experiments that have been started by Selen Zülbahar.

First of all, Uzip levels were ubiquitously downregulated by driving UAS-UzipRNAi with a ubiquitious (*ubi*-Gal4) driver. Flies were kept at 29ºC to increase the efficiency of the UAS/GAL4 system and UAS-Dicer was used to enhance the effect of the RNAi line. The results show that with this line in combination with a ubiquitous driver Uzip levels can be downregulated efficiently as *uzip* null phenotypes can be observed. The observed phenotypes are nearly as severe as in $Uzip^{D43}$ null mutants in that OSNs cannot form a commissure and the structure of the fan-shaped body was disrupted (Figure 4.27).

In the next step downregulation was performed in more specific cell types. A neuron-specific driver, *elav*-Gal4, and a glia-specific driver, *repo*-Gal4, were used separately to downregulate Uzip by the UAS-TRIP-UzipRNAi line. Since Uzip is mainly expressed by glia, the downregulation of Uzip in glia was expected to mimic $Uzip^{D43}$ phenotype. Downregulation in neurons was still important to show, in case any low expression of Uzip in these cells is contributing to the phenotype.

However, downregulation done by using the *repo*-Gal4 line (third chromosome) did not cause any detectable phenotype (Figure 4.28). Experiments were repeated by performing the downregulation using two copies of the *repo*-Gal4 driver (in the second and third chromosome) and in this case the *uzip* null mutant phenotype could be phenocopied (Figure 4.29). This is an intriguing result but has a caviard, as the correct control was not used (should be the two *repo*-Gal4 drivers together without an UAS-UzipRNAi construct). Whiel these lines are used by many researchers around the world it cannot be excluded that the Gal4 lines might cause phenotypes on their own in this particular setting. Nevertheless, if the results are true they show that Uzip function in glia is necessary and sufficient to cause Uzip null phenotypes. Furthermore, Uzip levels are important for its function, as even low levels are enough to rescue the pehnotype. In this case downregulation with one copy of *repo*-Gal4 did not give a phenotype, while downregulation with two copies phenocopied the mutant phenotype. In accordance with these results, neuron-specific downregulation of Uzip did not cause any commissural defects (Figure 4.30).

Repo-Gal4 is a driver that is expressed in most glia in the fly. In the next step we were curious to investigate if the downregulation of Uzip in TIFR glia using the TIFR-specific driver, *c422*-Gal4, would be sufficient to observe the Uzip mutant phenotype. In all of the examined adults brains, commissure-formation was observed and only minor defects were noticed at the commissure and glomerulus targeting (Figure 4.31). As has been determined in the downregulation experiments and mutant analyses little amounts of Uzip can rescue the phenotype. Thus, the experiments shown here should be repeated by increasing the copy number of *c422*-Gal4 to increase the downregulation effect, before excluding that Uzip function in TIFR is not sufficient for the Uzip mutant phenotype.

Taken together, we could show that ubiquitous and glial-specific downregulation of Uzip mimic $Uzip^{D43}$ homozygous phenotype indicating that, Uzip expression in glia is necessary and sufficient for proper projection of OSNs to the contralateral side of the AL.

5.6. Gain of Function Studies of Uzip

Uzip is a cell adhesion molecule and if this adhesive property is necessary for the establishment of a proper olfactory circuit, than changing the localization and levels of this molecule should have phenotypic effects that would give more insight into its function. For example, panneuronal overexpression of Uzip leads to neuronal clustering in the embryo (Ding *et al.*, 2011).

In the olfactory system development, overexpression of Uzip might cause clustering of OSNs as in VNC neurons of embryo. Additionally, we speculate increasing expression levels of Uzip in TIFR glia cells might change the morphology of TIFR structure, thereby might affect the commissure formation as well.

Overexpression of Uzip was assessed with using cell type specific drivers together with the UAS-Uzip overexpression line generated in our laboratory. Analysis of projections in a background where Uzip was ubiquitously overexpressed, no commissure defects were observed at 36 h APF. Only an increase in the density of Flamingo staining at

the antennal nerve where it connects to the AL was noticed. Additionally, the commissure appeared smaller compared to wild type flies (Figure 4.32). This phenotype might be the result of axonal stalling, which would be consistent with the function of Uzip as a cell adhesion molecule. However, these results could not be investigated further, because a more careful analysis requires the recombination of several alleles, which could not be done in the framework of this thesis.

Moreover, Uzip was overexpressed using the double repo driver and projections of OR42b neurons were examined. In all of the adult brains analyzed, OR42b neurons project properly and cross the midline (Figure 4.33). Some minor defasciculation defects were observed in the commissural axons and around the glomerulus structure of OR42b neurons. However, because of the high background problem, samples could not be compared thoroughly. More stainings should be performed after solving the background problem and give us some more information about of the specific function of Uzip in glia.

Finally, Uzip level was increased in TIFR glia using the *c442*-Gal4 driver. Early pupal brains show incomplete formation of the commissure, where most of the OSNs do not cross the midline. Still, since OSNs were able to cross the midline, this suggests that overexpression of Uzip in TIFR glia does not cause axon-stalling phenotypes (see Figure 4.34).

5.7. Rescue Experiments

Another way to assess the cell-type specific function is to rescue the function of Uzip selectively in the Uzip mutant background.

To do this first Uzip was overexpressed with the *c442*-Gal4 driver in Uzip mutant background. Figure 4.37 shows that overexpression of Uzip in TIFR glia partially rescues Uzip phenotypes. In rescued flies, OSNs are able to form a commissure, yet misprojection defects are still observed. This may explain that Uzip expression in TIFR is able to recover midline crossing phenotype but not other phenotypes of Uzip mutants. This experiment complements the previous experiment in which Uzip was downregulated in TIFR gli, but

downregulation was not achieved completely. Thus, taken together Uzip function in TIFR glia is necessary and sufficient for midline crossing of OSNs. Other cells, eg. projection neurons might contribute to the targeting phenotypes within the antennal lobe and have not been investigated at all yet.

Moreover, when Uzip was ubiquitously expressed but repressed in glia in Uzip null mutant background, which resulted the rescue of commissure formation. This data indicates that, Uzip expression in glia is not important for midline crossing. However, this result does not fit with our conclusions, since Uzip is mainly expressed in glia. We speculated that, repo-Gal80 is not fully suppressing the activity of Gal4 in the glia cells, which results overexpression of Uzip in all cells.

In order to validate this data, a rescue experiment should be carried by only overexpressing Uzip in glia.

5.8. Truncated Uzip Proteins

Uzip is a cell adhesion molecule with no common motifs to other cell adhesion molecules, which makes it dificult to speculate on its possible function. In a previous study (Ding *et al*., 2011) it was demonstrated that the region between 42-379 amino acids is conserved among insects and deletion of either half of this region causes Uzip to lose its homophilic binding ability. However, deletion of the region between 401 and 450 does not affect the binding ability of Uzip.

There are three coding exons; encoding 1-237 amino acids, 237-353 amino acids and 353-488 amino acids, respectively. In addition to this, the Swiss Model Protein Modeling Database predicts 4 domains separated from 130, 245 and 358. Putting all these data together, we created truncated Uzip constructs shown in Figure 4.39 and the corresponding transgenic fly lines to investigate the function of the putative domains *in vivo*. Due to time restrictions these lines could not be analyzed in the framework of this thesis but in future studies, these truncated versions will be used in rescue experiment

similar to those done with UAS-Uzip^{KM} and hopefully the functional domains of Uzip will be predicted.

6. CONCLUSION

In this study, a detailed analysis of Uzip expression was performed by using both an Uzip::mCherry transgenic line and the Uzip enhancer-trap line (AC783-Gal4). According to our expression pattern analysis in the adult brain, a glia-like pattern was seen, surrounding the antennal lobes, mushroom bodies, antennal nerves, and optic lobes. Additionally, Uzip expression was also observed around the central complex compartments.

Moreover, using the Uzip enhancer trap line Uzip expressing cells were identified as supporting cells and glia in the maxillary palp. Unfortunately, in the antenna stainings needs to be repeated to identify Uzip expresing cells. Uzip::mCherry transgenic line was used to identify glia subtypes expressing Uzip in the antenna and the maxillary palp. Our results indicate that membrane-attached Uzip expression might be on GH146 glia and the plasma membrane of sensory neurons. A further investigation is needed to specify glial subtypes expressing Uzip.

In $Uzip^{D43}$ homozygous and $Uzip^{D43}/Uzip^{23}$ mutants, none of the OSNs can cross the midline. Furthermore, homozygous $Uzip^{23}$ mutants were invesitaged both for antennal OSNs and maxillary palp OSNs. Intriguingly, in few of the antennal OSNs, a thin commissure can be formed. None of the maxillary palp OSNs can cross the midline. This data indicate that different mechanisms are used in the targeting and axon guidance of the maxillary palp and the antennal OSNs. Additionally, the commissure formation depends on Uzip levels in olfactory system development.

Rather than tracing axons of a single subtype of OSNs, all axonal projections of OSNs were visualized by anti-Flamingo staining at 36h APF. Interestingly, all OSN showed axon stalling phenotypes in the ALs. These results are similar to Nrg^{849} homozygous mutant where TIFR formation was disrupted. Analysis of TIFR in Uzip null mutants showed that Uzip indeed affects TIFR morphology dramatically. Additionally,

overexpression of Uzip in TIFR glia is enough to rescue midline-crossing phenotypes. These data cleary indicate the Uzip-TIFR glia relation.

Downregulation of Uzip with both double repo-Gal4 and ubi-Gal4 show $Uzip^{D43}$-like phenotypes. Taken together, this study shows that Uzip is expressed in glia and functions in the olfactory system development of *Drosophila*.

REFERENCES

Auld, V. J., R. D. Fetter, K. Broadie, and, C. S. Goodman, 1995, “Gliotactin, a Novel Transmembrane Protein on Peripheral Glia, is Required to Form the Blood-Nerve Barrier in Drosophila.”, *Cell*, Vol. 81, No. 5, pp. 757-767.

Barnea, G., S. O. Donnell, F. Mancia, X. Sun, A. Nemes, M. Mendelsohn, and R. Axel, 2004, "Odorant Receptors on Axon Termini in the Brain", *Science*, Vol. 304, No. 5676, p.1468.

Bate, C.M., 1976, “Pioneer Neurones in an Insect Embryo.” *Nature* Vol. 260, pp. 54-56.

Bieber, A. J., P. M. Snow, and M. Hortsch, 1989, "Drosophila Neuroglian : A Member of the Immunoglobulin Superfamily with Extensive Homology to the Vertebrate Neural Adhesion Molecule Ll", *Cell* Vol. 59, No. 3, pp. 447-460.

Boquet, I., R. Hitier, M. Dumas, M. Chaminade and T. Preat, 2000b, " Central Brain Postembryonic Development in Drosophila: Implication of Genes Expressed at the Interhemispheric Junction.", *Journal of Neurobiology*, Vol. 42, No. 1, pp. 33-48.

Brand, A. H., and N. Perrimon, 1993, "Targeted Gene Expression as a Means of Altering Cell Fates and Generating Dominant Phenotypes", *Development*, Vol. 118, No. 2, pp. 401-415.

Buck L. and R. Axel, 1991, "A Novel Multigene Family May Encode Odorant Receptors: a Molecular Basis for Odor Recognition.", *Cell*, Vol. 65, No. 1, pp. 175-187.

Chen, W., and H. Hing, 2008, "The L1-CAM, Neuroglian, Functions in Glial Cells for Drosophila Antennal Lobe Development.", *Developmental Neurobiology*, Vol. 68, No. 8, pp. 1029-1045.

Ding, Z.-Y., Y.-H. Wang, Z.-K. Luo, H.-F. Lee, J. Hwang, C.-T. Chien, and M.-L. Huang, 2011, "Glial Cell Adhesive Molecule Unzipped Mediates Axon Guidance in Drosophila.", *Developmental* Dynamics, Vol. 240, No. 1, pp. 122-134.

Dodd, J., and T. M. Jessell, 1998, "Axon Guidance and the Patterning of Neuronal Projections in Vertebrates", Science, Vol 242, No. 4879, pp. 692-699.

Endo, K., T. Aoki, Y. Yoda, K. Kimura, and C. Hama, 2007, "Notch Signal Organizes the Drosophila Olfactory Circuitry by Diversifying the Sensory Neuronal Lineages.", *Nature neuroscience*, Vol. 10, No. 2, pp. 153-160.

Estes, P. S., J. Roos, A. Van Der Bliek, R. B. Kelly, and K. S. Krishnan, 1996, "Traffic of Dynamin within Individual Drosophila Synaptic Boutons Relative to Compartment-Specific Markers", *The Journal of Neuroscience*, Vol. 16, No. 17, pp. 5443-5456.

Fishilevich, E., and L. B. Vosshall, 2005, "Genetic and Functional Subdivision of the Drosophila Antennal Lobe.", *Current biology*, Vol. 15, No. 17, pp. 1548-1553.

Freeman, M. R., and J. Doherty, 2006, "Glial Cell Biology in Drosophila and Vertebrates.", *Trends in Neurosciences*, Vol. 29, No. 2, pp. 82-90.

Garcı, L., F. Jime, I. De Neurociencias, and S. J. De Alicante, 2000, "The EGF and FGF Receptors Mediate Neuroglian Function to Control Growth Cone Decisions during Sensory Axon Guidance in Drosophila", *Neuron* Vol. 28, No. 3, pp. 741-752.

Goodman, C. S., 1990, "Drosophila Neurotactin , a Surface Glycoprotein with Homology to Serine Esterases , Is Dynamically Expressed during Embryogenesis", *Development*, Vol. 110, No. 4, pp. 1327-1340.

Goulding, S. E., P. zur Lage, and A. P. Jarman, 2000, "Amos, a Proneural Gene for Drosophila Olfactory Sense Organs That is Regulated by Lozenge.", *Neuron*, Vol. 25, No. 1, pp. 69-78.

Heimbeck, G., C. Ha, and R. F. Stocker, 1999, "Smell and Taste Perception in Drosophila Melanogaster Larva : Toxin Expression Studies in Chemosensory Neurons", *The Journal of Neuroscience*, Vol. 19, No. 15, pp. 6599-6609.

Hidalgo, A., and G. E. Booth, 2000, "Glia Dictate Pioneer Axon Trajectories in the Drosophila Embryonic CNS", *Development*, Vol. 127, No. 2, pp. 393-402.

Hitier, È., A. F. Simon, F. Savarit, and T. Pre, 2000, "No-Bridge and Linotte Act Jointly at the Interhemispheric Junction to Build up the Adult Central Brain of Drosophila Melanogaster", *Mechanisms of Development*, Vol. 99, No. 1-2, pp. 93-100.

Hong, W., and L. Luo, 2014, "Genetic Control of Wiring Specificity in the Fly Olfactory System.", *Genetics*, Vol. 196, No. 1, pp. 17-29.

Hummel, T., K. Krukkert, J. Roos, G. Davis, C. Kla, and D.- Mu, 2000, "Drosophila Futsch / 22C10 Is a MAP1B-like Protein Required for Dendritic and Axonal Development", *Neuron*, Vol. 26, No. 2, pp. 357-370.

Hummel, T., M. L. Vasconcelos, J. C. Clemens, Y. Fishilevich, L. B. Vosshall, S. L. Zipursky, and L. Angeles, 2003, "Axonal Targeting of Olfactory Receptor Neurons in Drosophila Is Controlled by Dscam", Neuron, Vol. 37,No. 2, pp. 221-231.

Imai, T. and H. Sakano, 2007, "Roles of Ddorant Receptors in Projecting Axons in the Mouse Olfactory System.", *Current Opinion in Neurobiology*, Vol. 17, No. 5, pp. 507-515.

Jefferis, G. S., E. C. Marin, R. F. Stocker, and L. Luo, 2001, "Target Neuron Prespecification in the Olfactory Map of Drosophila.", *Nature*, Vol. 414, No. 6860, pp. 204-208.

Jhaveri D. and V. Rodriguez, 2002, "Sensory Neurons of Atonal Lineage Pioneer the Formation of Glomeruli with in the Adult Drosophila Olfactory Lobe." *Development* 129, Vol. 129, No. 5, pp. 1251-1260.

Kliimbt, C., J. R. Jacobs, and C. S. Goodman, 1991, "The Midline of the Drosophila Central Nervous System : A Model for the Genetic Analysis of Cell Fate , Cell Migration , and Growth Cone Guidance", *Cell*, Vol. 64, No. 4, pp. 801-815.

Komiyama, T., W. A. Johnson, L. Luo, and G. S. X. E. Jefferis, 2003, "From Lineage to Wiring Specificity : POU Domain Transcription Factors Control Precise Connections of Drosophila Olfactory Projection Neurons", *Cell*, Vol. 112,No. 2, pp. 157-167.

Laissue, P. P., C. Reiter, P. R. Hiesinger, S. Halter, K. F. Fischbach, and R. F. Stocker, 1999, "Three-Dimensional Reconstruction of the Antennal Lobe in Drosophila Melanogaster", *The Journal of Comparative Neurology*, Vol. 405, No. 4, pp. 543-552.

Lee, T., and L. Luo, 1999, "Mosaic Analysis with a Repressible Neurotechnique Cell Marker for Studies of Gene Function in Neuronal Morphogenesis", *Neuron*, Vol. 22, No. 3, pp. 451-461.

Lue, N. F., D. I. Chasman, A. R. Buchman, and R. D. Kornberg, 1987, " Interaction of GAL4 and GAL80 Gene Regulatory Proteins in vitro.", *Molecular and Cellular Biology*, Vol. 7, No. 10, pp. 3446-3451.

Martin, V., E. Mrkusich, M. C. Steinel, J. Rice, D. J. Merritt, and P. M. Whitington, 2008, "The L1-Type Cell Adhesion Molecule Neuroglian Is Necessary for Maintenance of Sensory Axon Advance in the Drosophila Embryo.", *Neural Development*, Vol. 3, No. 10.

Masse, N. Y., G. C. Turner, and G. S. X. E. Jefferis, 2009, "Olfactory Information Processing in Drosophila.", *Current Biology*, Vol. 19, No. 16, pp. 700-713.

Mombaerts, P., F. Wang, C. Dulac, S. K. Chao, A. Nemes, M. Mendelsohn, J. Edmondson, and R. Axel, 1996, "Visualizing an Olfactory Sensory Map", *Cell*, Vol. 87, No.4, pp. 675-686.

Potter, C. J., B. Tasic, E. V Russler, and L. Liang, 2010, " The Q System: a Repressible Binary System for Transgene Expression, Lineage Tracing, and Mosaic Analysis.", *Cell*, Vol. 141, No. 3, pp. 536-548.

Python, F., and R. F. Stocker, 2002, "Adult-like Complexity of the Larval Antennal Lobe of D. Melanogaster despite Markedly Low Numbers of Odorant Receptor Neurons.", *The Journal of Comparative Neurology*, Vol. 445, No. 4, pp. 374-387.

Raper, J., and C. Mason, 2010, "Cellular Strategies of Axonal Pathfinding.", *Cold Spring Harbor Perspectives in Biology*, Vol. 2, No. 9.

Robertson, H. M., C. G. Warr, and J. R. Carlson, 2003, "Molecular Evolution of the Insect Chemoreceptor Gene Superfamily in Drosophila Melanogaster.", *Proceedings of the National Academy of Sciencesof the United States of America*, Vol. 100.

Sachse, S., and C. G. Galizia, 2014, "Role of Inhibition for Temporal and Spatial Odor Representation in Olfactory Output Neurons : A Calcium Imaging Study", *Journal of Neurophysiology*, Vol. 82, No. 2, pp. 1106-1117.

Sen, A., C. Shetty, D. Jhaveri, and V. Rodrigues, 2005, "Distinct Types of Glial Cells Populate the Drosophila Antenna.", *BMC Developmental Biology*, Vol. 5, No. 25.

Simon, A. F., I. Boquet, M. Syngue, and T. Pre, 1998, "The Drosophila Putative Kinase Linotte (Derailed) Prevents Central Brain Axons from Converging on a Newly Described Interhemispheric Ring", *Mechanisms of Development*, Vol. 76, No. 1-2, pp. 45-55.

Sepp, K. J., J. Schulte, and V. J. Auld, 2001, "Peripheral Glia Direct Axon Guidance Across the CNS/PNS Transition Zone.", *Developmental Biology*, Vol. 238, No.1, pp. 47-63.

Sweeney, L. B., A. Couto, Y.-H. Chou, D. Berdnik, B. J. Dickson, L. Luo, and T. Komiyama, 2007, "Temporal Target Restriction of Olfactory Receptor Neurons by Semaphorin-1a/PlexinA-Mediated Axon-Axon Interactions.", *Neuron*, Vol. 53, No. 2, pp. 185-200.

Vosshall, L. B., H. Amrein, P. S. Morozov, A. Rzhetsky, and R. Axel, 1999, "A Spatial Map of Olfactory Receptor Expression in the Drosophila Antenna", *Cell*, Vol. 96, No. 5, pp. 725-736.

Wicher, D., R. Schäfer, R. Bauernfeind, M. C. Stensmyr, R. Heller, S. H. Heinemann, and B. S. Hansson, 2008, "Drosophila Odorant Receptors Are Both Ligand-Gated and Cyclic-Nucleotide-Activated Cation Channels.", *Nature*, Vol. 452, No. 7190, pp. 1007-1011.

Yao, Y., Y. Wu, C. Yin, R. Ozawa, T. Aigaki, R. R. Wouda, J. N. Noordermeer, L. G. Fradkin, and H. Hing, 2007, "Antagonistic Roles of Wnt5 and the Drl Receptor in Patterning the Drosophila Antennal Lobe.", *Nature Neuroscience*, Vol.10, No. 11, pp. 1423-1432.

Zhang, T. J., B. G. Hoffman, T. Ruiz de Algara, and C. G. Helgason, 2006, " SAGE Reveals Expression of Wnt Signalling Pathway Members during Mouse Prostate Development.", *Gene Expression Patterns*, Vol. 6, No. 3, pp. 310-324.

Zhu, H. and L. Luo, 2004, " Diverse Functions of N-cadherin in Dendritic and Axonal Terminal Arborization of Olfactory Projection Neurons.", *Neuron*, Vol. 42, No. 1, pp. 63-75.

Zhu, H. , T. Hummel, J.C. Clemens, D. Berdnik, S. L. Zipursky, and, L. Luo, 2006, Dendritic Patterning by Dscam and Synaptic Partner Matching in the Drosophila Antennal Lobe.", *Nature Neuroscience*, Vol. 3, pp. 349-355.

Zülbahar S., 2012, *Identification of the Role of a Novel Cell Adhesion Molecule, Unzipped, in Mediating Neuron-Glia Interactions in Drosophila,* M.Sc. Thesis, Boğaziçi University.